Design of autonomous sustainable Unmanned Aerial Vehicle - A novel approach to its dynamic wireless power transfer

by

Kyaw Min Naing

A thesis submitted to the degree of

DOCTOR OF PHILOSOPHY

Major: Engineering

University of Wolverhampton

Telford, UK

2022

DECLARATION

The studies involved in this thesis were performed at the Telford Mechatronics Lab, in the Engineering Department at the University of Wolverhampton in the United Kingdom. This thesis has been written and submitted by only by me for the PHD final write up. I experimented and collected data all by myself.

Kyaw Min Naing 12/06/2022

---------- ----------

Kyaw Min Naing Date (Student)

Dr Ahmad Zakeri 12/06/2022

---------- ----------

Professor Dr Ahmad Zakeri Date (Director of Study)

TABLE OF CONTENTS

Page

LIST OF FIGURES

Page

LIST OF TABLES

Page

LIST OF EQUATIONS

NOMENCLATURE

WPT	Wireless Power Transfer
UAV	Unmanned Aerial Vehicle
DWPT	Dynamic Wireless Power Transfer
RDWPT	Rotational Dynamic Wireless Power Transfer
ROS	Robot Operating System
RL-POLICY	Reinforcement Learning Policy
RL	Reinforcement Learning
ML	Machine Learning
DL	Deep Learning
DL-RL	Deep Learning Based Reinforcement Learning
DRL	Deep Reinforcement Learning
KF	Kalman Filter
DKF	Deep Kalman Filter
INS	Inertial Navigation System
DDPG	Deep Deterministic Policy Gradient
DKF	Deep Kalman Filter
CNN	Convolutional Neural Network
VTOL	Vertical Take-off and Landing
PWM	Pulse Width Modulation
DSLKF	Deep Self-Learning Kalman Filter
IMU	Inertial Measurement Unit
IOT	Internet of Things

IPT	Information Processes and Technology
ESCs	Electronic Speed Controllers

ACKNOWLEDGMENTS

It is impossible to adequately express my gratitude to the numerous persons who assisted me throughout the four years of my PHD journey. From his personal advice, support, and patience during my PhD studies, I want to thank my supervisor Dr. Ahmad Zakeri. You have helped me so much with my engineering research and creativity. My success depends on your help. I would also want to thank Professor Keith Burnham and Research Department from my university for their efforts with me in my study. As the most basic effort in my research, their contributions are valued. I was also able to take a leave of absence for few months to prevent car accident sever injury during my studies with the help of my supervisor and Professor Keith. Thank you for all the wonderful memories I've made during my PHD years. My friends in University of Wolverhampton namely Navya, Ali Bushara, and everyone else deserve appreciation as well. My experience at PhD was improved thanks to the resources which have been provided for research students only. The final thing I'd want to do is thank my family. My Mom and Dad raised me and supported me mentally, physically and financially in every part of my life, and I appreciate that.

ABSTRACT

Electric UAVs are presently being used widely in civilian duties such as security, surveillance, and disaster relief. The use of Unmanned Aerial Vehicle (UAV) has increased dramatically over the past years in different areas/fields such as marines, mountains, wild environments. Nowadays, there are many electric UAVs development with fast computational speed and autonomous flying has been a reality by fusing many sensors such as camera tracking sensor, obstacle avoiding sensor, radar sensor, etc. But there is one main problem still not able to overcome which is power requirement for continuous autonomous operation. When the operation needs more power, but batteries can only give for 20 to 30 mins of flight time. These types of system are not reliable for long term civilian operation because we need to recharge or replace batteries by landing the craft every time when we want to continue the operation. The large batteries also take more loads on the UAV which is also not a reliable system. To eliminate these obstacles, there should a recharging wireless power station in ground which can transmit power to these small UAVs wirelessly for long term operation. There will be camera attached in the drone to detect and hover above the Wireless Power Transfer device which got receiving and transmitting station can be use with deep learning and sensor fusion techniques for more reliable flight operations. This thesis explores the use of dynamic wireless power to transfer energy using novel rotating WPT charging technique to the UAV with improved range, endurance, and average speed by giving extra hours in the air.

The hypothesis that was created has a broad application beyond UAVs. The drone autonomous charging was mostly done by detecting a rotating WPT receiver connected to main power outlet that served as a recharging platform using deep neural vision capabilities. It was the purpose of the thesis to provide an alternative to traditional self-charging systems that relies purely on static

WPT method and requires little distance between the vehicle and receiver. When the UAV camera detect the WPT receiving station, it will try to align and hover using onboard sensors for best power transfer efficiency. Since this strategy relied on traditional automatic drone landing technique, but the target is rotating all the time which needs smart approaches like deep learning and sensor fusion. The simulation environment was created and tested using robot operating system on a Linux operating system using a model of the custom-made drone. Experiments on the charging of the drone confirmed that the intelligent dynamic wireless power transfer (DWPT) method worked successfully while flying on air.

1 INTRODUCTION TO THE THESIS

- Chapter 1 shows Introduction, Motivation, Research questions, Methodology, Aims and Objectives, of the thesis topic.

Despite attempts from the UAV scientific community, autonomous WPT charging for unmanned surface vehicles remains a problem. A major drawback of aerial vehicles is the short amount of time they can spend in the air before their batteries die. This thesis's research and findings were driven by the need for autonomously charging Deep Learning and Reinforcement Learning (DL-RL) and Kalman filter-based Wireless Power Transfer (WPT) receivers for unmanned aerial vehicles (UAVs) that can handle dynamic rotating WPT transmitters. An unmanned aerial vehicle (UAV) flying over a rotating dynamic WPT transmitter can provide navigation and charging data for the control system using deep Kalman filter sensor fusion. It's worth noting that this is a complex issue that can't be solved with a single study, therefore any information gathered will serve a greater good.

According to the autonomous and flexible qualities of UAV networks, they are widely used in the design and execution of the next-generation WPT charging. Search-and-rescue operations that require high mobility and the deployment of base stations for wireless power transfer networks can be carried out by autonomous UAV systems using deep learning and deep reinforcement learning techniques, allowing for scalable, adaptable big data processing based on data collected by many UAVs.

1.1 Aim

It is the aim of this thesis to research, design and demonstrate in autonomous UAVs charging on air using deep reinforcement learning technique as an intelligence and With the Dynamic Wireless

Power Transfer (DWPT) charging technique, the distance between the wireless transmitter and receiver may be increased while simultaneously increasing the environment's safety and enabling autonomous charging.

1.2 Motivation

The motive for this research is to address international demand for ongoing scientific breakthrough in intelligent. Unmanned Aerial Vehicles (UAVs) charging while it's in operation. There is still development in dynamic WPT charging of UAV for domestic use. Current dynamic WPT research only discussed about moving vehicle or object while continuing wireless charging while improving the efficiency of the coil designs, shapes, materials for electromagnetic shielding and frequency of the energy transfer. Using machine and deep learning to enhance and speed up the process of UAV flying operation with automatic take off, hovering, trajectory flights, sensor fusion technique, landing and improving energy usage which can be used in DWPT with UAVs to charge on air.

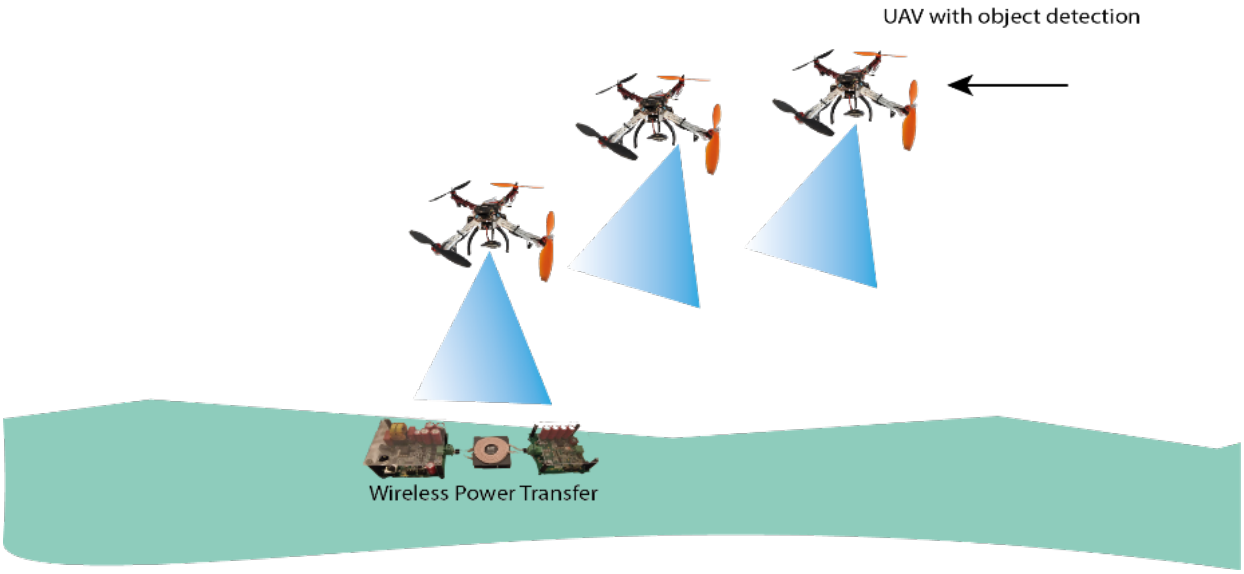

Figure 1.1 UAV equipped with WPT and object detection algorithm

From this thesis, the goal was to investigate and design the novel techniques of rotational dynamic

wireless power transfer of UAV charging by finding solution for the following:

1. Fusing Dynamic Wireless Power Transfer technique with drone's sensors using deep visual learning, Kalman filter and autonomous control system.

2. Current DWPT wireless powered UAVs which uses near range WPT energy transferring method to charge while the system is moving while RL-POLICY uses the same methodology but with the addition of rotating the transmitter and receiver for the purpose of increasing the distance of the power transfer operation.

3. Using deep learning and Robot Operating System (ROS) to simulate the virtual simulation for autonomous UAV charging before testing on an actual device.

1.3 Contribution

Unmanned aerial vehicles (UAVs) and other electronic equipment have never been charged using a method that uses an established way to rotational dynamic wireless power transmission Reinforcement Learning Policy (RL-POLICY). The RL-POLICY charging process of a UAV may be automated using a unique Deep Learning and Reinforcement Learning based Kalman Filter model, which was examined in this study. RL-POLICY UAVs may be charged autonomously using the RL model, which is a self-learning system that does not depend on the system's usual dynamics. The deep learning method is used to predict the charging position of the RL-POLICY system utilizing numerical data from a vision-based object identification research. Multi-agent deep reinforcement learning for intelligent charging of UAVs designs were also created, and the results show that RL approach provides better trajectory optimization and energy consumption compared to other designs. For electric UAV, boat, and automobile designers to analyze potential design alterations to improve the operating time in this research can be used in future.

1.4 Research Questions

1. What impact does rotational dynamic wireless power transfer (RDWPT) method have on UAV's flight time?
2. How do the design of an autonomous deep reinforcement based Kalman filter approach can be able to train to fly, hover and charge itself the UAVs autonomously?
3. What are the most effective design of Vision-based Object detection use of Deep Learning be reliable navigation for autonomous charging of UAVs?
4. What effect does multiagent deep reinforcement learning have on the autonomous charging of UAVs?

1.5 Methodology

1. **Investigation in autonomous UAV charging using deep learning and sensor fusion**

   An investigation on the use of artificial neural networks to recognize objects, Kalman filter and WPT techniques are essential for long operation time of UAVs. It is also necessary to increase the distance of charging of wireless powered UAVs.

2. **Design and demonstration of an autonomous UAV charging technology for extending the charging range in UAV's WPT architecture**

   The design of WPT system by using UAVs in a wider area comparing with the traditional designs. When the desired attributes have been identified they should be demonstrated into practice through an appropriate drone's architecture.

3. **Automatic charging of a rotational dynamic wireless powered UAV**

The main task of this research is concerned with the study of different kinds of path planning in an taking off and landing environment, path planning using sensor systems. The methods by which a rotational dynamic wireless powered UAV can locate itself within its environment self-charging should be covered using deep learning approach.

4. **Simulation and Control**

This involves a study of the control systems, control algorithms, including Deep Kalman filter control approach, and a comparison of results for different control algorithms obtained by simulation.

1.6 Research Outline

The thesis consists of the following nine chapters in the following order:

- Chapter 1 shows Introduction, Motivation, Research questions, Methodology, Aims and Objectives, of the thesis topic.
- Chapter 2 focus on a literature review and investigation of the autonomous charging of UAV and reinforcement learning which related to this thesis. Then, more in depth details about the concept of deep learning and sensor fusion with UAVs. Also discuss the literature review of static and dynamic WPT of UAVs.
- Chapter 3 focuses on the Hardware and Implementation of the autonomous charging of UAVs which consists of Navigation, control system and sensor fusion and reinforcement learning.
- In Chapter 4, a wireless power transfer system with rotating dynamic behavior is described using significant study.
- Chapter 5 continues with implementing the design of Reinforcement Learning Policy (RL-POLICY) system into the autonomous UAV.

- Chapter 6 introduces the method of Deep Kalman Filter and Dynamic Wireless Power transfer approach for UAVs charging based reinforcement learning techniques.
- Chapter 7 presents vision-based object detection using deep learning for reliable autonomous charging of UAVs
- Chapter 8 brings together with using Reinforcement Learning (RL) techniques to train and test multi agent self-learning system to automate collaborate flying and charging process.
- Chapter 9 brings the overall discussion of all results and concludes this research with a contribution to the science community, limitation, and future research possibilities.

1.7 Publication by the Author

- 1. Naing, K.M. (2020). Wireless Energy transfer to long distance flying Intelligent Unmanned Aerial Vehicles (UAVs) using reactive power transfer techniques.
- 2. Naing, K., Zakeri, A., Iliev, O. and Venkateshaiah, N., 2018. Application of Deep Learning Technique in UAV's Search and Rescue Operations. Advances in Intelligent Systems and Computing, pp.893-901.
- 3. Naing, K., Zakeri 2020. Deep Kalman Filter and Sensor fusion approach to the estimation of UAV's Attitude. Book of Abstracts: 1st Faculty of Science and Engineering (FSE) Research Conference. Theme: United Nations sustainable development goals (SDGs) (: University of Wolverhampton)
- 4. Robust Interaction-based reinforcement learning of an Autonomous Driving Agent for the Real World with Position Control, Naing Kyaw, University of Wolverhampton - Powertrain Modelling and Control, Testing, Mapping and Calibration 2022 – Conference Programme

- 5. Accelerated Real-World Deep Reinforcement Learning for Collision Avoidance of an autonomous vehicle in crowded traffic Environments, Naing Kyaw, University of Wolverhampton - Powertrain Modelling and Control, Testing, Mapping and Calibration 2022 – Conference Programme

2 Literature Reviews

- Chapter 2 focus on a literature review and investigation of the autonomous charging of UAV and reinforcement learning which related to this thesis. Then, more in depth details about the concept of deep learning and sensor fusion with UAVs. Also discuss the literature review of static and dynamic WPT of UAVs.

2.1 Introductions

Inspections, distribution, agriculture, surveillance, and many more which uses unmanned aerial vehicles (UAVs) for their operations are climbing exponentially (A. Gupta et al., 2021). It is predicted that by the year 2040, UAVs/drones would become the primary delivery method for parcels to meet the rising demand (Doole et al., 2020). Concerns and unresolved research questions about the future of UAV charging remain despite their growing interest in civil applications (Nex et al., 2022). It will be difficult and time-consuming to deal with many drones and their batteries in the case of mail delivery (Cokyasar, 2021). UAVs can operate more efficiently if they can avoid multiple landing to charge or replace battery (Boukoberine et al., 2019a).

Using Wireless Power Transfer for UAV not only can improve the battery charging capabilities but also useful for autonomous multi-drone control in remote areas (Junaid et al., 2017). There have been just a few studies on wireless charging for UAVs in the past decade. There was multiple concern on drone weight limitation, WPT dynamic charging methods and autonomous flight operations has been discussed (Chittoor et al., 2021). Long term flight time of UAV sparked the author to write this review autonomous charging of UAVs. It also gives an in-depth look at how well different research institutions, universities and businesses have studied the technical elements of wireless charging. For a more secure operation, the study also covers the history of drones, WPT technology, Reinforcement Machine Learning.

When discussing Unmanned Aerial Vehicles, commercial ones are usually referred to as "drones" Due to its high maneuverability, compact design, and light weight, many researchers have focused on the advancement of UAVs more than ground vehicles (Ahmed et al., 2022). This means that the UAV tech has limitless range of applications, including inspections, agriculture, 3D mapping-modeling, damage assessment.

A radio controller or pre-programmed flight routes can be used to remotely operate a drone (Aibin et al., 2021). Using semi-autonomous UAVs for photography and recreational flight is becoming increasingly common in modern times (Hall & Wahab, 2021). Electric Drones, on the other hand, can use the onboard battery within few minutes because of the usage of maximum energy from the propeller motors (X. Yang & Pei, 2022). This type of inefficient UAV is unable to cover a large region of interest in a single charge. Drones may be recharged by switching out their depleted batteries with fully charged ones, which is a frequent method of doing so. Remote or difficult-to-reach locations cannot use autonomous drones since the manual battery switch procedure necessitates the presence of human staff. To enhance the flying time in air of unmanned aerial vehicles (UAVs), a few non-electrical magnetic fields (EMF) charging methods have been developed in recent years. According to the diagram shown in Figure 2 below, an intelligent control system architecture.

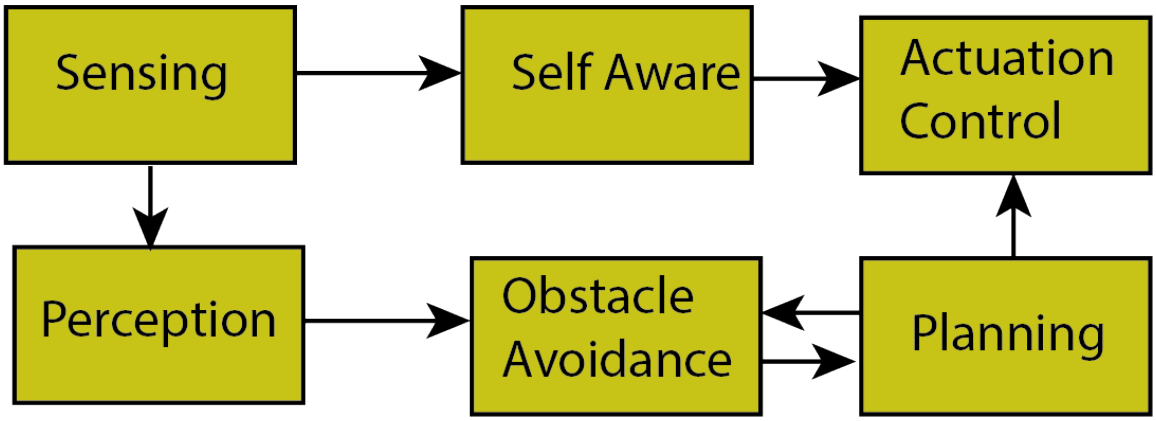

Figure 2.1 Architecture of an intelligent control system

There will soon be a slew of drones being used for anything from delivery to surveillance and monitoring units (Yaacoub et al., 2020). With so many units, managing them and charging them through airgap will become a time-consuming chore. For extended flight periods, a drone must minimize its weight because it is an aerial vehicle. Drones are being developed for a variety of uses, but there is only a handful of research being done on autonomous drone charging (Grlj et al., 2022). A lack of exponential progress in wireless charging for drones in the past decade will make it difficult to charge the rapidly increasing number of devices. Real-time case studies from leading research institutes and industry will be used to examine the drone wireless charging idea. The future of drone wireless charging technology is also discussed in this thesis, as are the problems and opportunities that lie ahead.

2.2 Background Information on Electro-magnetic Field based charging method

The use of Electro-Magnetic Field Based charging systems for small electric items and electric vehicles has grown in popularity in recent decades (Sanguesa et al., 2021). For autonomous drone charging, the same method may be used. Capacitance charging method is more suited for use across small distances, such as a few millimeters, than others. Several scientific investigations show that inductive charging is an efficient power transmission method for transmitting electricity

to a few centimeters, which is ideal for charging drones (Simic et al., 2015).

The current review papers on UAVs are mostly focused on their applications in the UAV and Internet of Things (IOT) industry (Alsamhi et al., 2021). Few studies have been done on the internal structure of UAVs, wireless circuit modelling and the difficulties and future trends of UAVs (Elmeseiry et al., 2021). Drones with combustion engines are more efficient, according to the authors (Townsend et al., 2020), but they also pollute more. Additionally, solar charging provides an environmentally favorable charging circuit that demands a substantial investment and ongoing maintenance. UAV categorization, structure, features, and applications were studied by (Tahir et al., 2019). The author of this study set out to find out how much the public knew about drones and the necessary usage for them. Subjective research was carried out in two nations by 187 experts from various fields. Among the topics covered in the survey are the use of UAVs, their applications, surveillance, and concerns. The authors (Siddiqi et al., 2022) found that 95% of the population is aware of unmanned aerial vehicles (UAVs), 23% had used UAVs for various reasons, and 60% felt that UAVs are superior surveillance tools. Construction, engineering, and architecture researchers (Sulaiman et al., 2023)conducted a comprehensive assessment of the literature on unmanned aerial vehicles (UAVs), including a categorization system and examples of UAVs in the field. Drones are integrated with a variety of onboard sensors and transducers to keep it in the air and serve their purposes, according to the authors (Lagkas et al., 2018). In addition, new technologies for UAVs were examined to improve performance and mitigate other technical and environmental issues.

To construct flying cellular networks, (de Silva et al., 2022) investigated the properties of UAVs and charging mechanisms. The authors discussed the advantages and disadvantages of current charging methods but concluded that further in-depth research is needed to extend flying time.

According to (Ucgun et al., 2021)UAVs may be recharged near the ground using a wide variety of methods.

It was concluded that mid-range charging approaches like Information Processes and Technology (IPT) might enhance the range of unmanned aerial vehicles (UAVs) by summarizing obstacles and possibilities in near-field transmission (NFT). The wireless power transmission method can be reliable to extend flying time of UAVs, according to the researchers (Le et al., 2020a). studied the market for unmanned aerial vehicles, their structure, classifications, charging methods, and uses. They also discussed UAV energy management tactics and concluded that further research is needed before it is possible to propose UAV energy consumption predictions based on regular flying schedules. There was an extensive literature review conducted by (Zhao et al., 2020)that included information on market opportunities, classifications, applications, and predictions for the future. Issues described by the author are a threat to the future of UAVs, according to the author. The WPT for the UAVs has not been adequately studied in any of the studies that have examined the UAVs. Uses, market potential, classifications and structures were all discussed in this overview study of the multiple features of drones. WPT methodologies, mathematical modelling, charging standards, and future research plans for WPT for UAVs are all covered in this thesis.

2.3 A summary of UAV History

The term "UAV" has been used from the beginning of the 20th century, according to the author (Giordan et al., 2020). In 1910s, the military in US began mass manufacture of Charles Kettering's aerial torpedo (Aerial Bug) flying bombs, which were hurled and operated using radio controls (García Carrillo et al., 2013). It was invented the name "drone" to refer to these autonomous aerial vehicles. Remotely Piloted Vehicle (RPV) was the name given to the drones of the late 1960s and early 1970s. There was a lot of focus on drones being used for military purposes such as gathering

intelligence, scouting, and dropping bombs. It was possible for unmanned aerial vehicles (drones) to fly deep into enemy territory and collect information without putting their operators in risk. The propulsion system was heavily reliant on jet propulsion due to the immature nature of the power converter technology (B. Zhang et al., 2022). It was able to fly missions over a considerable distance, though. Electric components have been reduced in size while power converter technology has improved over the previous decade. The technology's price has dropped down as well, making it more accessible to the general people. Recently, the technology is used in a variety of ways, from seed planting to airport security from birds to disaster control to disinfectant spraying for contagious pandemics. UAVs that are autonomous have been developed because of advances in drone technology; some of these UAVs employ biomimicry for navigation (Ahmed et al., 2022). GPS signals were not necessary because it relied on inertial navigation systems.

2.4 Type of UAVs

Aeronautics advances have led to the development of several flying robot categories. Drones have major role in a wide variety of capabilities depending on their intended use (Ducard & Allenspach, 2021). Gravity (the downward force), lift (the upper force), thrust (the forward force), drag (the backward force), and all have a role in the construction of a UAV. There are many types of unmanned aerial vehicles (UAVs) include those with fixed-wings aircrafts (wings which won’t move), rotary-wings drones (rotor-wings rotate by forcing air pressure downward), Hybrid-VTOL (which uses both fixed and rotary wings), Gas-powered airships, and those with birds like flapping-wings crafts.

Aerodynamic lift beneath the wing is generated by a stiff construction of the UAV body, thus the name "fixed-wings." The tilt control on the wings lifts the UAV into the desired position when

subjected to forward airspeed.

Aerodynamic lift is generated by the revolving propellers of rotary-wing unmanned aerial vehicles (UAVs). Conventional fixed-wing UAVs are far heavier than these. These unmanned aerial vehicles, on the other hand, have proven helpful for short-range tasks because to their quick maneuverability.

Gas powered airships operate by their large surface area with less weight makes them able to achieve flight using various lifting gas.

Hybrid VTOLs utilize rotary and fixed capabilities for extended flight time. The VTOL propulsion start flight operation by taking off vertically using rotary wing, and the fixed wing method can keep them in the air for longer periods of time.

An ornithopter, or flapping wing, imitates the nature of efficient flight method found in flying animals. They usually use their wings flap to achieve airborne.

2.5 UAV Internal Structure

As a result of its capacity to lift and land precisely vertically and move easily in small places, rotary-wing UAVs are the primary focus of this study. Single-rotor and multi-rotor rotary wing unmanned aerial vehicles (UAVs) fall under this category. For example, there are four different types of quadcopters: tricopter, quadcopter with four blades, and quadcopter with four blades (hexacopter), as well as an octocopter with eight blades (having eight rotors). A wireless charging system for quadcopters and hexacopters is the focus of this study because of their nature of stability and reliability which can be huge advantageous while charging battery midair flights. Hexacopters and quadcopters shall be referred to collectively as "drones" for the purposes of this guide.

The Proportional Integral Derivative (PID) loop control in filters and processes information from the radio receiver finding the trajectory of the drone which was experimented briefly from

(Kangunde et al., 2021). There are scaling factors for each of the three blocks of flight control: Proportional, Integral, and Differential. For the drone to move, the updated signal is supplied to the Electronic Speed Controllers (ESCs). However, this is subject to change. While 5.8 GHz offers a large coverage area, it is constrained in terms of data transfer speed.

If a sufficient power supply is available, Brushless DC electric motor (BLDC) motors are small, powerful, and can run at high RPM. The flight controller sends control signals to the ESCs, which then give the appropriate power to the motor. Drone operators can benefit from these when flying outside of their line of sight.

Lithium-polymer batteries are smaller, lighter, and more flexible in their design. The high power-to-weight ratio of lithium batteries makes them ideal for use in unmanned aerial vehicles, according to a study published (Townsend et al., 2020). There is a comparative examination of popular batteries in Table. For lithium batteries, weight is closely correlated with capacity, as demonstrated by an investigation conducted by researchers. Increasing UAV weight reduces flying duration since the battery drains more quickly. It is demonstrated in Figure that the best battery utilization characteristics. When it comes to electric vehicle batteries, manufacturers must choose between delivering electricity and storing it. The expended battery of a drone, in contrast to an EV, must be physically removed and replaced. The implementation of autonomous applications in UAV is constrained because of this action. In the next part, we'll go through the many ways a drone may be charged.

2.6 History of WPT

History of WPT technology start from 18th century when a Danish physicist named Hans Christian Oersted breakthrough that electricity can influence magnetic compass direction which led to the creation of groundwork of electricity and magnetism by famous scientist Michael Faraday and Andre Marie Ampere (Shinohara, 2014a). From 1831 to 1879, James Clerk Maxwell presented his

popular equation named electromagnetic theory which transform world because he connected the bridge between light and electromagnetism. In Germany, a physicist named Heinrick Rudolf Hertz who experimented and verified the existence of Electro Magnetic (EM) waves in the year 1888. These discoveries help Serbian American scientist Nikola Tesla to patent and experiment the first ever wireless power transfer (WPT) using low and high frequencies from 1890s. Tesla aim was to distribute power wirelessly through globe for everyone, but he lacks investment to finish his project. He discovered that by coupling transmitter and receiver coil of WPT device by using resonance magnetic field and electric field.

1890, Tesla first experimented with vacuum bulb to transfer power wirelessly which is known today as tesla coils (Shinohara, 2014b). He also patented many applications of wireless power transfer technique such as long-distance resonant energy transfer, inductive coupling, capacitive coupling, etc. Two French scientists named Maurice Hutlin and Maurice Leblanc who successfully patented WPT method to be able to use in Railway stations using wireless inductive resonant coupling method in 1892. After researching into wireless electricity using high frequency, tesla gave presentation about high frequency current and voltage to many institutes in America, England from 1891-1893. An Indian physicist named Jagadish Chandra Bose has conducted research and experimented successfully in EM wave to wirelessly send power to a bell less than 100 fts in 1895. Dr Tesla's inventions led to the experimentation of long-distance wireless energy transfer in Wardenclyffe tower which "The New York Sun" also reported that there is mysterious plasma like electric lightning coming from the tower to unknown land in 1903. The main coil (TX) and secondary coil (RX) of tesla's inductive wireless power transfer (WPT) were employed as primary and secondary coils, respectively, in the same manner as an electrical transformer, but the RX and TX were not physically connected. This method is one of the first type of WPT technique that

transfer energy wirelessly between two separate inductors is called WPT inductive coupling.

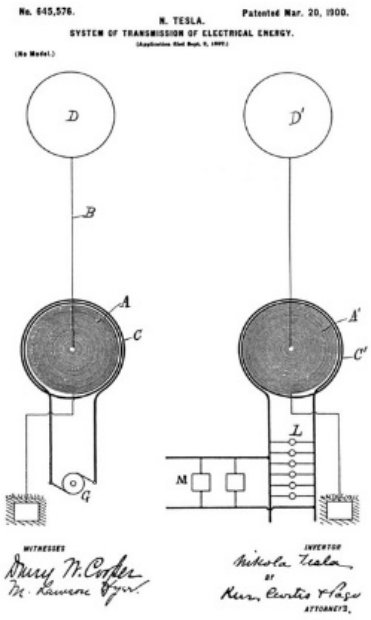

Figure 2.2 Tesla's WPT patent showing wireless transmitter and receiver (*System of Transmission of Electrical Energy.*, 1897)

Dr. Nikola Tesla patented several applications related to long distance WPT techniques and applications. He submitted first WPT application "System of transmission of Electrical Energy" on September 1897 and approved on March 1900 and serial number is US.645,576 in figure 2.2. He also discovered WPT capacitive coupling is to exchange power from one capacitor to another, WPT resonant coupling which tune the same frequency between TX and RX to move power efficiently. In 1896, Marconi experimented with electromagnetic radio signals from one place to another and proved that by transmitting signals when Nikola Tesla was performing wireless power transfer experiments in figure 2.2.

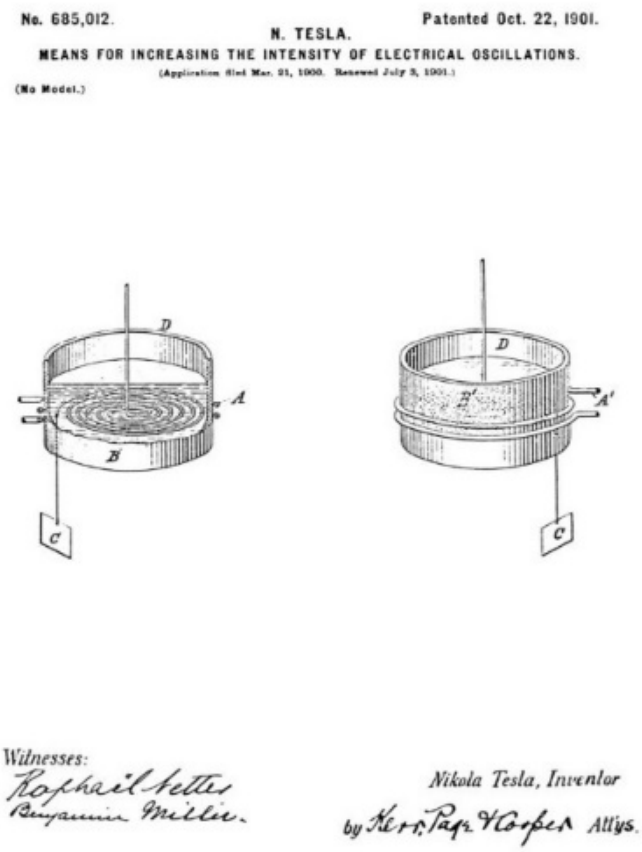

Figure 2.3 Means for increasing oscillation between WPT transmitter and receiver (*Means for Increasing the Intensity of Electrical Oscillations.*, 1900)

There is a British patent (No.685 012) which was approved in Oct 1901 “Mean for increasing intensity of electrical oscillations” in figure 2.3 showing the possibilities of sending signals between TX and RX with the conjunction of wireless power transfer.

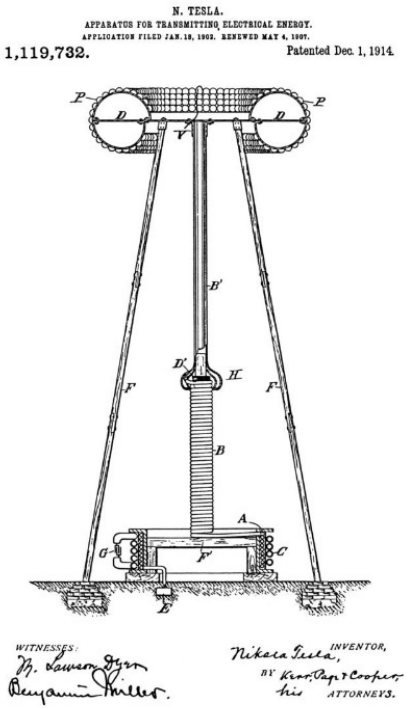

Figure 2.4 WPT Transmitter Apparatus (*Apparatus for Transmitting Electrical Energy.*, 1907)

On Dec 1914, Tesla hold United States patented in figure 2.4 which represents "Art of Transmitting Electrical Energy Through the Natural medium". This design is further improvement of long-distance wireless energy transmission producing and using stationary waves as tesla mentioned in this patent which is also possible to have multiple receiving stations. It seems that these devices can convert traditional alternating current into stationary waves to transfer power efficiently.

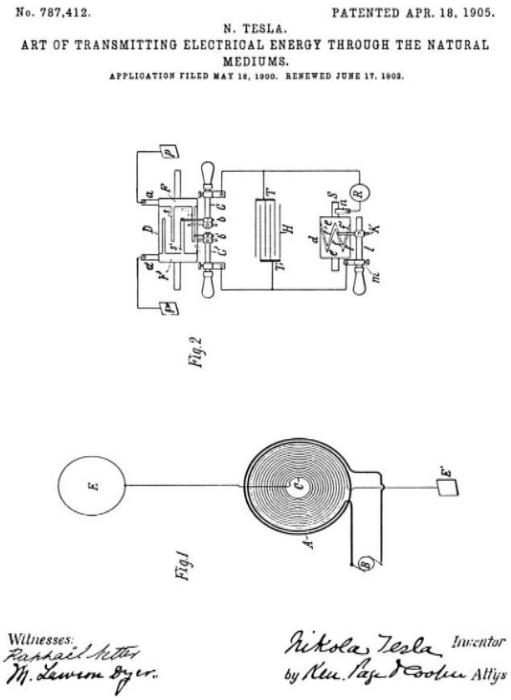

No. 787,412. PATENTED APR. 18, 1905.

N. TESLA.

ART OF TRANSMITTING ELECTRICAL ENERGY THROUGH THE NATURAL MEDIUMS.

APPLICATION FILED MAY 16, 1900. RENEWED JUNE 17, 1902.

Fig. 2

Fig. 1

Witnesses: Randall Potter, M. Lewis Dyer.

Nikola Tesla Inventor

by Kerr, Page & Cooper Attys

Figure 2.5 WPT Transmitting through natural medium patent (*Art of Transmitting Electrical Energy through the Natural Mediums.*, 1900)

Tesla's last patent "Apparatus for transmitting electrical energy" of WPT was patented in figure 2.5. He claimed in this invention that the design can avoid high voltage current spark discharge leakage because of large round external conducting layer. This breakthrough of tesla also claimed that elevated terminal capacitor and ground connected with earth also play a vital role transmitting power efficiently. The circuit oscillate with Resonant frequency to increase pressure and voltage in the secondary coil of transmitter to transmit power wirelessly.

Japanese inventor Shintaro Uda and Hidetsugu Yagi further developed and patented electromagnetic wave antenna with variable directions in 1926 (Ishiguro et al., 2012). After 26 years, an American scientist named William C. Brown first proposed the method of transmitting power using microwave energy using magnetron. He submitted a paper which was successfully published under the name "Microwave Energy for Power Transmission" in 1961 and later proved

this method by transferring power directly to the flying electric helicopter using microwave energy. Within 7 years after William demonstrated the Microware Wireless Energy Transfer, Dr Peter Glaser who first proposed the method of using sun's solar microwave energy for powering electric devices and space shuttles. Peter Glaser also works as a private consultant for space missions in 1960s. In 1973, a new way to transmit power to the Radio Frequency Identification (RFID) devices small distances for the purpose of monitoring nuclear energies by Los Alamos National Laboratory. This project also acts like a security device to track and lock dangerous materials storage facilities. A project named "WiTricity" was developed by Massachusetts Institute of technology (MIT) physics research team who were transmitted wireless power to a light bulb which placed less than three meters successfully using resonant coupling method for inductors. This method opened the possibilities of powering mobile phones, laptops and UAVs using indictive resonant wireless charging techniques when transmitter and receiver placed nearer will coupled by magnetic field produced from TX. Dr Chun Taek Rim demonstrated innovative type of wireless diploe antenna coil for Inductive Wireless range reached 5 meters in 2015 ("WiTricity - The Wireless Power Transfer," 2007). In January 2016, a group of scientists patented "Method and apparatus for adaptive tuning of wireless power transfer" which shows how a wireless transfer and receiver resonant power can be tuned with desirable frequencies to receive energy efficiently. In May 2016, a US patent (*Chargers and Methods for Wireless Power Transfer*, 2013) was published for the inventor Afshin Partovi under the title "Chargers and method of wireless power transfer" which shows the systematic approach to design and develop a near-field WPT charging batteries for the use of mobile phones and other electric appliances to support with WPT. US patent number 9831920B2 presents ultrasonic power amplifier can be transformed to wireless power to the receiving station using customized signal generator was published in 28th

November 2017. In July 2019, inventor (Sengupta, 2013) proposed and patented the method of radio frequency lensing effect to power mobile WPT device efficiently which works in a same way as glass lens creates heat from sun's heat. A US patent "Encloses for high power wireless power transfer systems" was published to transfer high energy to vehicles using different types of magnetic surfaces by a customized resonant transmitter in 25th of February 2020.

2.7 WPT Technology

Wireless Power Transfer (WPT) is defined as the techniques of charging or powering electrical devices without wires. Traditional wired energy transfer (WET) method is expensive, takes up space, when comparing with WPT (Zhu et al., 2022). For example, consumer using power from WET lead to disruption if the wire broken or damaged while WPT user don't need to worry about it. WPT charging technique can also be applied to any electronic devices such as mobile phones, unmanned aerial vehicles (UAVs), ground vehicles, electric toothbrush, etc (Huda et al., 2022). This technology is emerging in the field of autonomous UAVs because of intelligent charging without need for human to connect with plugged chargers. So, UAV can continue its operation autonomously in remote areas where human interaction is impossible or dangerous. Although this technology is promising to solve many problems, still there are many research areas needed to accomplish. The main obstacle is that current consumer WPT device transfer distance is short enough to charge continuously to the UAV for long term flight operations (Nguyen et al., 2020b). To be able to figure out the limited distance between WPT transmitter (TX) and receiver (RX), a new approach should be needed to integrate with current scientific knowledge of WPT with UAV. The principle of WPT is that power can be taken from main alternating current (AC) power to the TX to the RX module which the energy can be use as direct current (DC) or AC in the output device such as UAV. There is also other form of WPT transmission which can be used to transport

power long distance but it's not safe for the environment because of radiation problems. Theoretically, if autonomous UAV can power wirelessly without interruption from main AC, it will fly and continue its operation perpetually. This will be great advancement for the area of sustainable intelligent UAVs and other similar electronic devices.

WPT's charging method is currently extensively used for objects such as mobile phones, headphones, small gadgets. This technology, however, is not being commonly and commercially used for charging of the unmanned aerial vehicles (UAVs) or electric vehicles because of the huge loss of power involved when the energy is wirelessly transferred from WPT's device to the UAV's batteries. But since the WPT charging allows the energy can send directly from the ground station to a UAV, through the natural air medium, without wires, there should not be any need for the UAVs to carry heavy weight batteries anymore. As such the use of WPT systems for Wireless Transfer of power to UAVs could create a mass market opportunity. The first WPT system was discovered by famous scientist named Nikola Tesla (David Wunsch, 2018) in 1890. He also patented many wireless power transmission applications at that time, making him the true founder of wireless electricity, but that technology never became a commercially available technology because of the lack of sufficient financial support he needed in his time. The use of WPT in UAV research is already established for some extent but, due to some technical limitations reported by the research, the technology has not yet been proved economically feasible or technically efficient for embedding in the Design of intelligent long distance flying UAVs, especially in cases where the UAVs required to fly longer that demanded by applications. The various methods of wireless power transfer being reported in literature can be categorized based on particular techniques they have used, five well known techniques are; (David Wunsch, 2018) Electromagnetic Induction (Kerr et al., 2017), (Miller et al., 2015),(Reed & Jr., 2013), (G. Zhang et al., 2013), (Campi et al.,

2018a) Electromagnetic Resonance (Bécherrawy, 2012), (D. W. Kim et al., 2012), (Toh, n.d.), (Huan-Huan et al., 2013), (Griffin & Detweiler, 2012)Electrostatic Induction (W. Han & Kunieda, 2017), (Jenn, n.d.) Use of Microwave technology (P. Lu et al., 2017), and (Xu et al., 2018a) use of laser wave technology. Some of these used long wave transmission and some covered short-wave transmission which also provides detailed discussion of the use of Electrostatic Induction (category 3), and the combined use of the categories; (1) Electromagnetic Induction, (2) Electromagnetic Resonance, and (3) Electrostatic Induction.

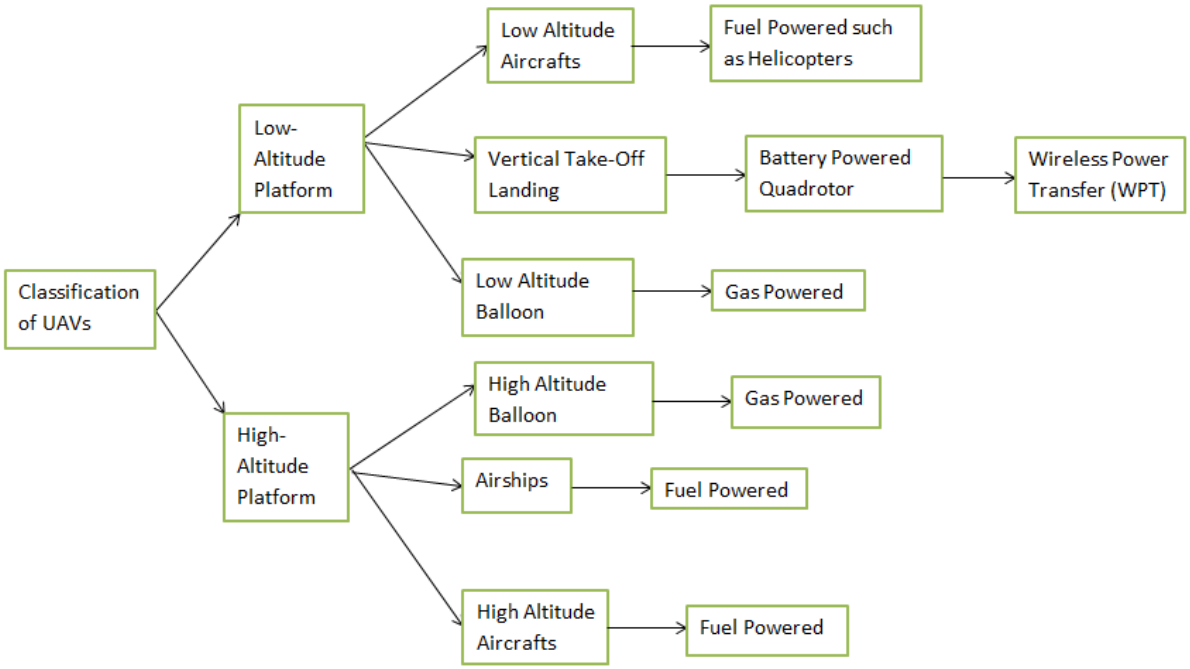

Figure 2.6 UAV Altitude platform classification

Jenn, D (Jenn, n.d.), extensively researched and experimented with short distance wireless power transfer for UAVs using electromagnetic induction method with over 90 % efficiency. His work established that the near field, short distance wireless power transfer technology has already been applied to UAVs successfully but for long distance flying drones this has not been so, and the technology is not safe and reliable because the microwave and laser wave transmissions have poor

efficiency in extreme weather conditions (Ma et al., 2016), hence dangerous to human beings (Dickinson & Grey, 1999). This chapter is focused mainly on VTOL (vertical takes-off and landing) type of UAV in figure 2.6 because this craft is currently using battery to operate in Low Altitude Platform (LAP) and can easily be integrated with WPT system. LAP category UAVs fly below 15km height whereas the High-Altitude Platform (HAP) category UAVs fly 15 km above sea levels.

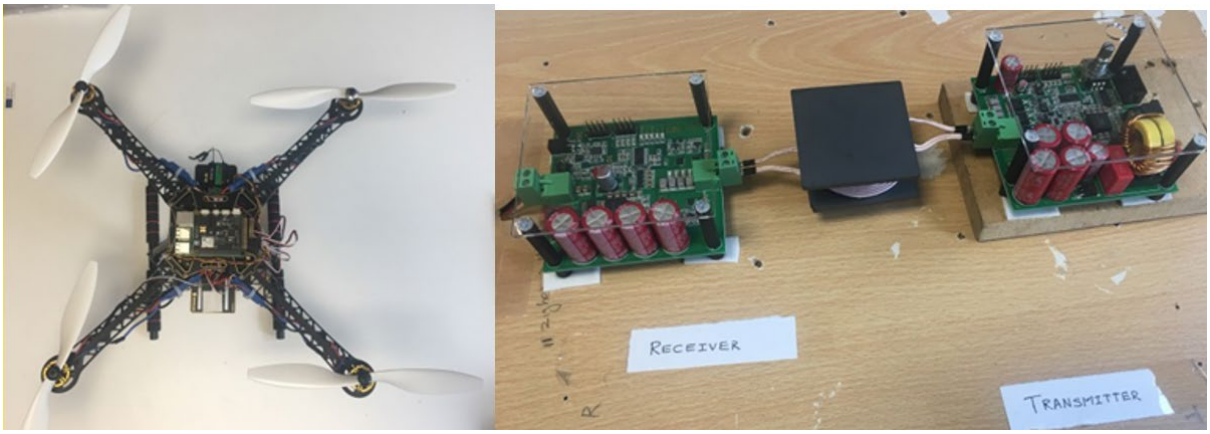

Figure 2.7 Quadcopter with Raspberry Pi 3b and Navio 2 Flight Controller Module used to test with (b) a 200 W Wireless Power Transfer Module

Furthermore, WPT techniques can enable faster communication with UAV, avoiding using inefficient radio communication. The project also investigates application of sensor fusion and deep learning algorithm on UAVs aiming to fuse WPT sensor with IMU (inertial measurement Unit) sensors and deep learning algorithms for long distance flying UAVs, which is an innovative novel approach. For our research experiments we use a quadcopter that developed and a 200 watts Wireless Power Transfer (WPT) kit (shown in figure 2.7).

2.8 Wireless Powered UAVs

Some of the batteries powered commercially available aircrafts in industry uses the wireless powered UAV and links to charge UAV's battery each time by landing the aircraft to the transmitter (TX) coil (Campi et al., 2018b). In some battery powered WPT aircrafts running todays, they are still using electromagnetic resonance method for cost effectiveness but the transmission power and the location between the TX and the RX are extremely low. (Hua et al., 2018). The WPT of the aircraft needs with the long-distance wireless power transfer to fly without landing for each charge. The microwave and laser powered wireless aerial vehicle which would harm humans or birds to fly in air against radiation caused by these extreme frequencies wave transfer methods (Junaid et al., 2016). These types of wireless power transfer technology require efficient solution of the cost-effectiveness and safety of the environment.

The primary UAV wireless power transfer system consists of the following.

- Electromagnetic Resonance wireless battery charging of UAVs (J. Jiang et al., 2018).
- Microwave Power Transmission of electricity using high frequency antennas to transmit power to aerial vehicles (Wang et al., 2022).
- Laser power transmission of electricity to UAV receiver in the same method solar panels method (Carrasco-Casado et al., 2011).

2.8.1 Short Distance Electromagnetic Resonance Wireless Powered UAVs

Electromagnetic resonance coupling method works at a tuned resonant frequency between TX and RX inductive coils which attached to the load (UAV) (Naimushin et al., 2005). Whenever UAV battery become low, the UAV which already has installed the receiver coil connected to the battery that going down to the exact place where the transmitter resonance coil is located and lands over

it to recharge itself. When the full power is taken, the UAV continue its operation by taking off from the transmitter coil (Tullu et al., 2018).

2.8.2 Long Distance Microwave Powered Wireless UAVs

Since all wireless powered aircraft uses same method to power the entire circuit, sensors, and actuators of the UAV (Duggal et al., 2009), that is the motors are powered by energy storage and controlled by speed controller devices and micro-controllers. For long distance and space UAV operation, microwave wireless power transfer method is can reach longest range because of electromagnetic wave transfer which travel at light speed in vacuum (K. Li et al., 2019).

The principle of microwave WPT UAV technology is that electricity is first converted into high frequency using tradition microwave magnetron transformer. Using same antenna design as radio techniques to transfer microwaves to the receiver antenna located in UAV with same resonance microwave frequency. Figure-3 is a block diagram illustration of the basic microwave electric powered UAV propulsion system. The UAV system starts by powering the motor and throttling the motor speed by controlling voltage input of the motor which make the propeller rotate and cause thrust and airspeed using energy from microwave wireless power. Although system looks simply but there are several different power configurations mode and safety issues (K. R. Li et al., 2017) according to the application and difficulty in flying in extreme weather conditions (Ludeno et al., 2018).

2.8.3 Long Distance Laser Powered UAVs

The working principle of laser powered WPT system for UAV is that high power laser pointer acts as the transmitter which surface which receive laser power as heat energy which can be converted into electric current (Cui et al., 2017) transmitted into load which itself is UAV. Figure shows that

multiple UAV is powered using laser WPT transfer which discussed in paper (Boukoberine et al., 2019b). Advantage of using this method is high power can be transmitted using laser power which is lower than microwave UAV wireless power transmission system (Ouyang et al., 2018). Drawbacks are laser radiation is highly dangerous living beings and transmitter and receiver should be always in sight for efficient power operations (J. Yang et al., 2011).

2.8.4 Autonomous UAV charging

The one of the most difficult aspects to operate. As a starting point for comparison, a brief history of previously employed methodologies is provided. There are three things to keep in mind before landing: control, position assessment, and navigation. Keeping a vehicle's speed and position within a predetermined range is the primary function of the lower layer of control (GPS, Inertial Measurement Unit (IMU), altimeter, etc.). Using sensors and visual feedback, the posture estimation is used to determine the UAV's location. Once the vehicle's position has been determined, it's time to build and adapt a route to the destination location. This section focuses primarily on the literature on posture estimation and navigation for this thesis.

Sensor-fusion, device-assisted, and vision-based approaches are grouped. A popular method for improving performance is to combine data from many sensors. Sensor-fusion systems typically employ this approach. IMU and camera sensor were used to create a three-dimensional reconstruction of the ground in a recent study (Aliakbarpour et al., 2011). Vision and differential GPS were used by (Kumar & Moore, 2002) to estimate the UAV's relative posture in relation to the heli-pad. Geometric invariant extraction is employed in this study to locate a landing pad with a H shape. Kalman Filter is an technique used to combine multiple sensor output into one to simplify the process of UAV navigations. Kalman filtering was used to land the UAV on a moving target in a subsequent study (Saripalli & Sukhatme, 2006). Optical flow, gyroscopes, and

accelerometer readings were coupled in (Bassolillo et al., 2022) to improve the resilience of a vision system for hovering and landing a drone.

It has been proposed by (Zhou et al., 2010) that a ground-based multisensory fusion system be implemented. Sensor Fusion is another term for Kalman Filtering which was mentioned above paragraph. Sensor-fusion techniques have two key issues. Noise from sensors in an unstructured environment can be exceedingly high. Second, the lack of access to navigational data or inaccurate sensor readings. For example, if you're at a remote location, you can't change the trajectory with GPS.

The use of on-board and ground-based equipment to improve marker recognition has been widely used. Infrared lights have been employed in a system in (T. Yang et al., 2016). Infrared lights set in a runway in a succession were used by the writers. Optically filtered infrared light was captured by the vehicle's camera, which was then sent to a control system for pose assessment. For ground stereo-vision detection(D. Tang et al., 2016) developed a technique complemented by an extended Kalman filter. Omni-directional cameras were utilized in (J. Kim et al., 2014) to increase the UAV's field of vision and recognize a red marker. On-board infrared cameras were utilized in (Kubota et al., 2021). Another tool utilized to aid in the marker's discovery is infrared ground spots. There is a plethora of ways in which these techniques fall short. Second, some of these gadgets are too costly and cannot be justified in commercial goods.

Pose estimation and planning are generally accomplished using camera pictures in vision-based systems. They recognize the ground marker and extract characteristics that can be used to determine the vehicle's position. To go closer to the pad, this data is sent into a control loop. Lange et al. proposed a system that relies solely on a monocular camera (X. Liu et al., 2019). Using a well-defined pattern of targets, the system was able to distinguish itself from a variety of distances.

The landmark could be located even when partially obscured thanks to a system of concentric rings. Lin et al. employed a reworked version of the standard international landing pattern. Feasibility studies on the usage Quick Response (QR) markers have been conducted by (Fiala, 2005). An onboard camera was all that was used in both situations to get an accurate pose assessment. For example, in (Kälin et al., 2021), on vision-based control system. It is proposed that the vision problem can be approached as an estimation of ego-motion, in which the vehicle's height in reference to a fixed planar surface is estimated. As a result, the landing controller may employ vision as a state observer in the feedback loop. Control and planning for commercial vehicles can be simplified by relying on vision-based systems, which employ little technology. When the pad is far away, partially obscured, or fuzzy, these ways might be problematic.

The limits of the methodologies that have been outlined thus far being addressed. Sensors fusion approaches focus on costly sensors that can’t always exist on cheap UAVs, making them difficult to implement. The position of the UAV may be accurately determined using device-aided techniques. The industry-based sensors aren't ideal for many situations. Finally, vision-based techniques rely on pictures taken by onboard sensors, such as cameras, to operate the vehicle. This has a distinct benefit over other methods, although it may not be able to detect low-level details in distorted pictures. The issues raised above are addressed in this chapter.

2.9 Deep Learning Approach

2.9.1 Artificial Intelligence

As a cutting-edge technology, artificial intelligence (AI) is described here as a method of simulating/reverse engineering and enhancing biological intelligence to develop intelligent systems and processes that can operate autonomously in a variety of situations (Cockburn et al., 2018). Cognitive reasoning, knowledge representation, machine learning, big data analysis, and problem solving are just a few of the numerous subfields that make up artificial intelligence. This cutting-edge technology has its origins in ancient philosophers' attempts to explain human thinking as a set of symbols that resulted in "association" as a cognitive process. There are two methods to artificial intelligence: a top-down approach and a bottom-up approach. A bottom-up deductive method is used by traditional AI approaches to formulate broad, abstract assumptions about the world based on pre-existing knowledge and a small number of instances. According to their hypotheses, they construct predictions about what the data should look like if those hypotheses are correct, then change those hypotheses based on the findings of these forecasts. Computational intelligence and current artificial intelligence (AI) approaches are described as bottom-up methods that work with numerical data to infer symbols and seek to discover patterns from the raw data they are fed into the system. Many businesses and services have been enabled by these cutting-edge AI technologies, which allow them to identify patterns, trends, and data anomalies in archived, streaming, or live data. Learning from examples and observations at various levels of abstraction is used to predict future values and states. Several novel features, including as mapping, intelligent control, autonomous driving, active safety, and forecasts, have been developed using sophisticated statistical machine learning approaches. Every part of a vehicle's lifetime, from design to production to operation, may be influenced by AI.

2.9.2 Machine Learning (ML)

In ML, computers can learn without being explicitly instructed in this field of artificial intelligence. A bottom-up inductive reasoning approach is used in modern statistical machine learning algorithms to uncover patterns from a large quantity of data (Woolf, 2009). Simple models trained on a big data set outperform complicated models learned on smaller data sets based on empirical evidence. In statistical machine learning, general principles are inferred from a collection of instances, which is an inductive reasoning process that uncovers rules that are valid for most samples in the given data set. Traditionally, ML system have been divided into 3 types: reinforced, unsupervised, and supervised. Data and labels/categories may be approximated using supervised learning, which employs inductive reasoning. The training data used to learn this mapping has already been categorized. In supervised learning, it is typical to perform classification and regression tasks. The rating, for example, is looking for the scoring function:

Equation 2.1 Supervised Learning Classifications

$$f:\mathbf{X}\times\mathbf{C}\rightarrow\mathbf{R} \quad (1)$$

Training data space (X) and label/class space (C) are defined above. This basic equation was necessary to be use in my research for deep learning with UAVs.

2.9.3 Deep Learning

When it comes to machine learning, one of the most often used techniques is deep learning (DL) (Najafabadi et al., 2015). The term "representation learning" may also be used to describe DL (RL). There will continue to be new research in the disciplines of deep and distributed learning if data collection methods, such as High-Performance Computing, can increase as rapidly as they have (HPC). Deep learning, even though it is based on the standard neural network, is much

superior. In addition, DL employs transformations and graph technologies to simultaneously construct multi-layer learning models. Natural language processing, audio and speech processing, and visual data processing have all been greatly improved by the most recent DL algorithms (NLP). The performance of an ML algorithm is typically dependent on the quality of the input data. An adequate data representation has been shown to boost performance when compared to a poor one. This has resulted in a long history of feature engineering as a significant ML research area. Create features from raw data is the purpose of this method. Due of its specificity, it's a one-size-fits-all solution and typically requires a lot of physical effort. When a new feature is deployed and shown to be beneficial, it establishes a new research route that will be explored for many decades to come. An algorithmic approach is used to extract features from the data. The least amount of human effort and field knowledge possible may be used to identify distinguishing traits. It is possible to extract the low-level properties of a data structure first, and then the high-level ones in successive layers. It's worth noting that this design was initially inspired by AI, which simulates the process that occurs in the brain's major sensory centers. Data representations may be automatically generated by the human brain from a wide range of visual settings. Scene data is the input for this technique, while the classified items are the output. This approach is based on how the human brain functions. As a result, DL's primary benefit is brought to light.

While unsupervised learning reignited interest in deep learning, exclusively supervised learning has now overtaken it. Even though we didn't give it much emphasis in our evaluation, it's feasible that unsupervised learning may become more important in the future. People, unlike animals, learn most of their abilities via observation rather than by being taught the names of items. Humans and the majority of animals. A high-resolution fovea surrounded by a low-resolution, task-independent peripheral vision is used in active, task-specific vision. In the future, vision research will benefit

greatly from systems that are taught end-to-end using a combination of ConvNets and RNNs that use reinforcement learning to select where to look. When it comes to video game categorization, systems that mix deep learning with reinforcement learning beat passive vision systems by a considerable margin. Future developments in deep learning will have a substantial impact on the area of natural language processing. As a result, we predict that RNNs will become considerably more accurate if they are taught to concentrate on a single part of either a phrase or the whole text. In the field of artificial intelligence, systems that combine representation learning with complex reasoning will be the ones that develop the field. We need new approaches for speech and handwriting recognition that don't rely on rules-based manipulations of symbolic expressions, which have been around for a long time.

2.10 Deep Learning Based Reinforcement Learning

Deep Learning based Reinforcement (DL-RL) is first step of human evolution to create thinking robot within many areas of research including drones. DL-RL is growing more powerful because of the current use of Deep Learning (DL) which uses neural network to train the multi-dimensional inputs. By using vision DL method, DL-RL robot can learn environment more reliably due to the development of advance polices and customized algorithms. The literature also mainly targeted on the agent, state, action, environment, reward system of the DL-RL. Later, we discuss about what are the advantages and disadvantages of current DL-RL and how to improve them. In conclusion, why DL-RL has been chosen for the research of autonomous UAVs.

Value functions and dynamic programming, as well as animal psychology, were the driving forces behind the development of RL. Controlling a dynamical system in such a way as to minimize the loss function over time was initially described as an optimum control problem (Busoniu et al., 2020). During the mid-1950s, Richard Bellman proposed a method to solving the optimum control

issue based on studies by (Chow et al., 2017). Therefore, as outcome of the existing status of the system's data, a value function is used to optimize the input trajectory (Walter, 1976). A discount factor is included in the Bellman equation to account for uncertainty in future rewards.

RL uses an Adaptive Dynamic Programming (ADP) technique to find the best offline policy. If the agent has certain goals, the ADP can be designed to meet those goals in any number of ways. When it comes to difficulties involving process control. First, the agent uses self-error learning to identify which actions produce the best results, and then it only repeats those actions that yielded positive results.

Reward learning for UAV control is still in its infancy, though. (Tovarnov & Bykov, 2022) employed the policy search approach to control the heli-copter, for example. Another comparable example is (Z. Jiang & Lynch, 2021), who demonstrated the ability to fly in reverse by teaching a tiny aircraft how to do so. (Cimurs et al., 2020) integrate model predictive control with reinforcement learning to develop an obstacle avoidance strategy that only has access to sensor data and not the complete system state. Rather than a high-level navigator, the policy in each of these circumstances.

Reinforcement learning was able to be applied to a new set of issues thanks to the usage of DNNs as Q-function approximators. For activities like tightening a cap on a bottle that need close synchronization between vision and control, (Buşoniu et al., 2018) employed a guided policy search technique. The author also employed a deep network to teach a robotic manipulator's gripping hand-eye coordination. Using an asynchronous variation of the actor critic system, (Mnih et al., 2016) developed a novel task for navigating random 3D mazes, which was the best-scoring job in the Atari domain.

The reason for using DL-RL is to eliminate the use of traditional complicated theories and dynamics by using self-learning approach to create environment for the agent (for example: UAVs) which learn from previous actions and reward itself to create autonomous robots. The main obstacle with this DL-RL method is that the algorithm needs modification for each new environment or agent to work better. There is heavy research going with the use of one algorithm to work all types of environments and robot's requirements (Zeng et al., 2019). Traditional approaches use conventional physics dynamic of the pre-programmed equation to solve the real-world problems, but the DL-RL create its own equation from the event-driven technique. Although DL-RL breakthrough many areas such as the science and technology but it's still need so much computational power and newer algorithms due to the requirement of multiple dimensions which leads to limitation. The other issue is that the lack of inadequate samples of the environment and the agent of the robot because complex DL and DL-RL method demand numerous data to work efficiently. The recent development of DL such as function approximation create more opportunities for DL-RL.

There is a significant improvement of DL in the areas such as object-recognition, natural language processing (NLP), sensor error predictions which open the door for much other research such as deep reinforcement learning (Fink et al., 2020). The working principle of DL is that it can train using minute pixels of the data such as image, sound, or text to detect them in bigger scale. Neural Networks (NN) are the base foundation of the successful DL that uses weight and biases to control the output of the system. This method will become more and more complicated when there are multiple dimensions of data. For making a successful autonomous robot, the raw sensors data need to be trained by multiple NN from DL which enhance the operation of DL-RL method. The objective of this review is to research of deep reinforcement recent developments and the use of

DL with it which in terms making the intelligent robots or UAVs. The extensive survey of deep reinforcement learning applications breakthroughs such as RL agent outperforming best game player which is presented in the paper.

The use of DL in Reinforcement Learning solves the problem the multi-dimensional of the parameters of action and state in environment by predicting or combining numerous data into single output. There are several advances in DL-RL which will be discussed in the followings.

Both theoretical and practical advances in the field of reinforcement learning have been achieved recently. Reinforcement learning, on the other hand, has several challenges when applied to a real-world system. Most real-world systems are massive and riddled with a slew of thorny issues. Matrix focuses on the behavior-based multirobot models and discusses the method of learning behavior policies using behavior space (Dulac-Arnold et al., 2019); Recent years have seen an explosion of interest in the application of reinforcement learning as a foundation for the construction of numerous intelligent models, including artificial intelligence and robots. Reward-based learning can adapt to its surroundings. With its ability to tackle a variety of complicated optimization problems, many different tasks can be achieved with it. RL algorithms have emerged and are being used to enhance the development of artificial intelligence.

Reinforcement learning is defined by (Andreae & Cashin, 1969) as the study of how to get the most out of a reward signal by mapping situations to actions. Reinforcement learning is best described by the aspects listed below: Agents move and interact with other entities in the world, which has laws that are either visible to or invisible to the agent.

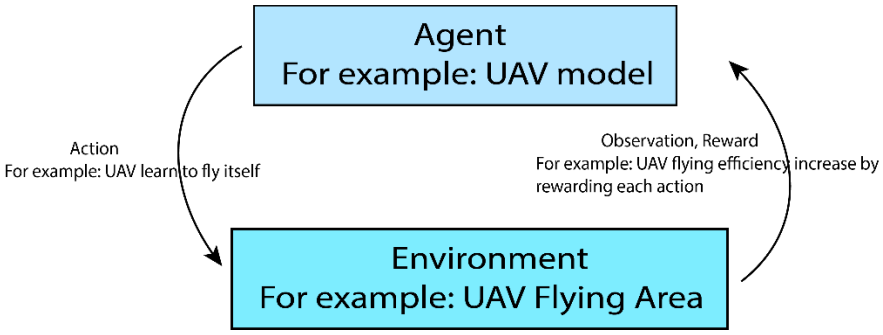

Figure 2.8

Status is a representation of the current state of an environment at a specific point in time.

movement or interaction in the world is defined by the action taken by the agent.

• Policy: the function that the agent learns to translate state to action is called policy.

input from the world that the agent receives

It's common for agents to get the current state at each time step t, execute an action from the action space A sampled at that time step t, and receive a reward at that time step supplied by a R function (st, at). T (st+1|st, at) is the environmental transition model for st+1, and the action gets the agent to this new state. An action performed in state st+1 moves the agent to the next state. Model-based algorithms are those in which the transition model is provided.

Equation 2.2

$$E\left(\sum_{t=0}^{h} r_t\right)$$

$$E\left(\sum_{t=0}^{\infty} \gamma^t r_t\right)$$

$$\lim_{h\to\infty} E\left(\frac{1}{h}\sum_{t=0}^{h} r_t\right)$$

The proposed agent in RDWPT UAV research considers the future while deciding how to act in the here and now. Most of the research in this area has focused on three specific models. At every given time, an agent should focus on optimizing. This is the simplest model to understand.

Received t steps into the future, the vector reward is referred to as rt in this and following formulations. This model may be utilized in two different ways: non-stationary policies are those that change with time, and this is what the agent will have in the beginning. It will do an h-step optimum action as its first step. This is considered the ideal course of action because it has just h actions left to do and earn support. Step optimum action will be taken on the following step and so on until it reaches the end of the process. Using receding-horizon control, the agent always does the h-step optimum action, is the second option. As long as the value of h is equal to or greater than zero, the agent will always operate in accordance with its stated policy. The nite-horizon concept is not always applicable. Many times, we have no idea how long an agent will last.

Discount reward strategy is known as a improve optimum policy (Bertsekas, 1995). This criterion has the drawback of making it impossible to tell the difference between two policies, one of which reaps huge rewards early on while the other does not. The long-term average performance of the agent overshadows any reward received on the early pre x. Taking into consideration the long-term average as well as the quantity of early reward is conceivable in this approach. Bias-optimal policies are those that maximize the long-run average while also breaking ties in the short term. When comparing various models of optimality, we can see that the optimal policy differs depending on which one is used. In this illustration, the environment is represented by circles, and the arrows show the changes from one condition to another. Only one option is available in every condition except the start state, which is represented with an oncoming arrow in the top left. Except where noted, all awards are zero. According to this model, we should do action number two since it's better than action number one. However, if we modify it to 1000 and 0.2 it's better than action number one because it's better than any other option. It is critical to pick the optimality model and parameters carefully in every application since they have such a large impact. This model is useful

when we know the agent's expected lifespan. This is the best technique to represent a system with a strict deadline. Even today, experts disagree on the relative merits of bias-optimal versus in nite-horizon discounted models. A discount parameter is not necessary for bias-optimal policies.

2.10.1 Rewards

Real-world settings with huge state-action spaces are being examined for use in Reinforcement Learning (RL), but even in the presence of accurate simulators, knowing how best to explore the environment remains a significant difficulty. In many cases, the problem is so complex that the obvious reward functions are few and few between (van Seijen et al., 2017). These kinds of incentives are often tied to the completion of a specific objective, such as a robot reaching specific waypoints, and provide no feedback on the actions taken along the route to accomplish these goals. Existing reinforcement learning (RL) systems generally fail to learn viable policies unless they are supplied with finely calibrated reward feedback by a domain expert who is knowledgeable in the subject matter(Rengarajan et al., 2022).

2.10.2 Challenges in DL-RL

Vehicle edge computing (i.e., machine learning on MEC-enabled networks) is still in its infancy, though. Some researchers are using deep learning and convolutional neural networks to forecast traffic patterns. It is unusual, however, for DL-RL to be considered (Sánchez et al., 2022). There are three key hurdles to building an intelligent offloading system for vehicle edge computing that works well:

Despite its effectiveness in Atari games and Go, the use of DL-RL in vehicular networks is almost nonexistent. Unlike chess, the constraints of offloading systems are more implicit, adaptable, and diversified than chess's explicit rules.

A series of captured photos is used to examine both DL-RL and regular vehicular networks. However, our intelligent offloading system does not have any sequential photos. DL-RL to vehicle networks without visuals is a difficult task.

When playing chess or Atari games, there is always one "agent" in a DL-RL model, regardless of the type of game. For intelligent offloading systems, constructing a suitable environment and building the matching DL-RL model is quite tough which was mentioned in (Ning et al., 2019).

2.10.3 Value Based RL

Reinforcement learning based on the maximization of value functions optimizes strategy. Estimation may be used to determine the value function for each robot state. Q-learning is the most extensively utilized of these algorithms. A technique called Q-learning constantly improves a robot's approach based on data it gathers while exploring its surroundings (Sun et al., 2021). Gracious approach is one of the most successful ways to pick actions for reinforcement learning, and it can assure algorithm convergence even if the model isn't known up front.

Equation 2.3

$$Q^*(s_t, a_t) = Q(s_t, a_t) + \alpha\left(r_t + \gamma \max_a Q(s_{t+1}, a) - Q(s_t, a)\right)$$

The equation 2.3 is used to evaluate actions and states and the -greedy approach to pick actions. The algorithm's convergence can be assured even if the model isn't.

To get the correct Q value, the neural network uses a dynamic wave expansion. Integrating existing knowledge into a learning system helps students learn faster and more effectively.

2.10.4 Multi-Agent RL

Real-world interactions with the environment are conducted through a process of trial and error, in which they are rewarded (reinforced) for their behaviors. Direct application of single-agent real-time optimization (SAEO) to many agents has not been demonstrated in empirical studies since the environment no longer remains fixed from each agent's point of view. However, depending on other agents' behaviors, a single agent's acts might generate different rewards. To design an effective multi-agent RL (MARL) method (Canese et al., 2021), the non-stationarity of the environment must be addressed.

The quality of the policies generated and the pace at which convergence is achieved can only be maintained if only a small number of agents are involved, even if convergence is achieved. When formulating algorithms for use in the real world, it is critical to keep in mind that they must be able to handle many agents.

Multi-agent reinforcement learning (MARL) is introduced in this survey. Our research focuses on the framework environment and how to use suitable single-agent reinforcement learning techniques in multi-agent contexts.

MARL algorithms that handle non-stationarity and scalability that, we focus on environments that are just partially visible. Partially seen events are more prevalent than in single-agent systems, hence they are critical to the development of real-world algorithms. An examination of the most frequent benchmarking settings for evaluating RL algorithm performance concludes this section. This study is meant to serve as an introduction to multi-agent reinforcement learning, highlighting the key challenges and solutions that have been implemented in the literature. Finally, we'll go

through some of the more common uses for MARL. Even though MARL research is still in its infancy, it has showed promising development in terms of its practical use. Systems capable of aiding humans in complicated activities, such as working in dangerous areas, and exhibiting general artificial intelligence might be deemed a revolutionary method.

2.11 Chapter Summary

This chapter presents a review on the design of UAV, wireless power transfer and deep learning-based reinforcement learning, which may be found. According to the research that was conducted, even though utilizing the dynamic WPT technique is a very common but by using RL can improve the performance. There are still several challenges to re-design them for the purpose of improving the UAV dynamic WPT efficiency and reliability.

There isn't enough study to determine the reliability of these novel designs, thus the market hasn't used them in new DWPT devices. Therefore, the UAV electric market hasn't used them commercial purposes. Before applying these novel ideas on a large scale, it is important to examine their reliability and investigate their failure.

In conclusion, the research on dynamic wireless power transfer system for UAV revealed that there are several significant voids and problems that need to be researched and solved using deep learning and reinforcement learning. Next chapter will be focus on hardware and implementation of the proposed RL-POLICY UAV system in this thesis.

3 HARDWAR AND IMPLEMENTATION

- Chapter 3 focuses on the Hardware and Implementation of the autonomous charging of UAVs which consists of Navigation, control system and sensor fusion and reinforcement learning.

3.1 UNMANNED AERIAL VEHICLE

Using a Custom-made quadcopter, this research uses a variety of sensors, including cameras, an onboard processor, gyroscopes, accelerometers, magnetometers, altimeters, and pressure sensors. Here are the details of the drone:

• Dimensions: 62cm x 43cm.

• Weight in grams: 530g; • IMUs including gyroscopes, accelerometers, magnetometers, altimeters, and pressure sensors.

To accurately measure horizontal velocity, the quadcopter's height and ground texture must be taken into consideration. It is only possible to broadcast one of the one video at a time. Data from sensors is generated at a rate of 180 Hz. To regulate the platform's roll and pitch, yaw, and altitude, the onboard controller (closed source) is employed (z). Quadcopter directives u = [-1,1] are given to the quadcopter at the rate of 60Hz to control it.

3.2 NAVIGATION SYSTEM

An angle sequence known as the Euler angle sequence or quaternion can be used to characterize a person's attitude. To represent three sequential rotations about the z, y, and x axes of a body, and Euler angle sequence includes three angles: yaw (ψ), pitch (θ), and roll(φ). Even though it has a physical interpretation, this depiction is unique at 90^{o}. The following relationship may be used to link the roll, pitch, and yaw angles to a quaternion.

Equation 3.1

$$\phi = \arctan\left(\frac{2q_2q_3 + 2q_0q_1}{2q_0^2 + 2q_3^2 - 1}\right)$$
$$\theta = \arcsin\left(-2q_1q_3 + 2q_0q_2\right)$$
$$\psi = \arctan\left(\frac{2q_2q_3 + 2q_0q_1}{2q_0^2 + 2q_3^2 - 1}\right)$$

Transformation from local one location to another is represented by [q0 q1 q2 q3]. Despite its lack of singularity, it might be difficult to visualize the aircraft's orientation in its entirety. Equation below presents alternatively for cases where only trajectory navigation moves are expected.

Equation 3.2

$$\begin{bmatrix}\phi[s+1]\\ \theta[s+1]\\ \psi[s+1]\end{bmatrix} = \begin{bmatrix}1 & \sin(\phi[s])\tan(\theta[s]) & \cos(\phi[s])\tan(\theta[s])\\ 0 & \cos(\phi[s]) & -\sin(\phi[s])\\ 0 & \sin(\phi[k])\sec(\theta[s]) & \cos(\phi[k])\sec(\theta[s])\end{bmatrix}\begin{bmatrix}\omega_x^B[s]\Delta t\\ \omega_y^B[s]\Delta t\\ \omega_z^B[s]\Delta t\end{bmatrix}$$

With the use of gyro output, one may determine one's position by integrating one's angular velocity into one's current position. Because of this, they may be ignored for the most part in practice. Equations for Euler angle and quaternion attitude representations can be used to calculate attitude at the IMU sample rate:

Equation 3.3

$$\mathbf{q}[s+1] = \mathbf{q}[s] \otimes \begin{bmatrix}1 & \frac{1}{2}\omega_x[s]^B\Delta t & \frac{1}{2}\omega_y[s]^B\Delta t & \frac{1}{2}\omega_z[s]^B\Delta t\end{bmatrix}$$

The quaternion multiplication operator is referred to as the operator in this context.

3.3 CONTROL SYSTEM OF RDWPT OF THE UAV

The UAV hovering platform likewise follows the same concept, with the landing platform's frame centered in the middle of the traditional UAVs. The landing system's coordinate frame. When it comes to the UAV and USV, their positions are represented by Xlv (the local frame) and Xls (the global frame). Down-facing camera Xc1v and frontal camera Xc2v are the two conversions between the vehicle's body frame and these cameras.

A PID controller, such as the one included in the tum ardrone package (Open-Source UAV control library), can be used to guide the drone. A proportional, integral, and derivate term are all included in the adjustment. The following is a mathematical representation of the overall control function: In a global coordinate system, p = (x, y, z,) – R4 is a desirable objective location for the quadcopter. At 100Hz, the UAV receives a robotic-centric coordinate frame containing the created commands.

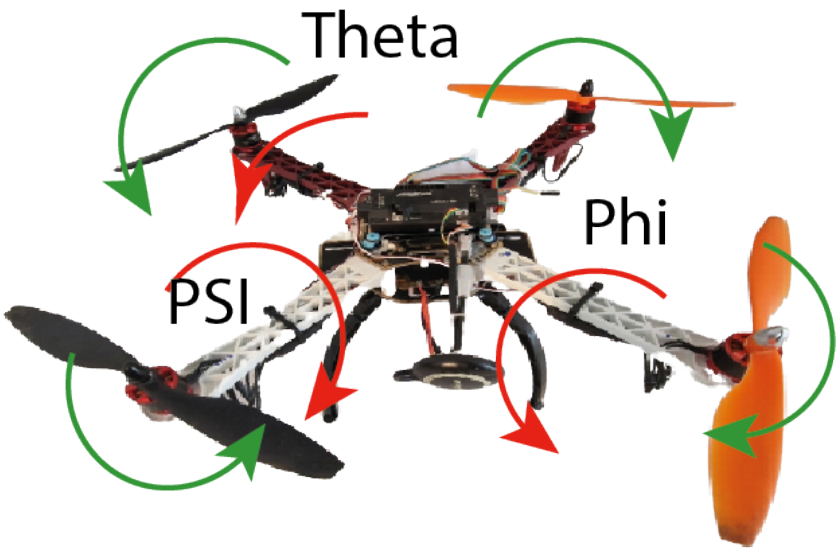

Figure 3.1 UAV pitch, roll and yaw movement

Quadrotors feature four fixed-pitch propellers in a cross arrangement with no tail rotor. If two propellers on either side of each other are rotating in the same direction, the other two propellers should be rotating in the opposite direction. Four propellers at the same time increase or decrease

the body's speed, and it may go in any direction by retaining the rotation of one pair of propellers at a constant speed and creating angular speed differences between the other opposing propellers. Thus, the pitch movement (theta direction in figure 3.1 is achieved by raising or lowering a gradual increase or decrease in speed of either of the two motors, shown below. To roll, you must increase (decrease) the rear motor's speed while reducing (raising) the speed of the front motor.

Equation 3.4

$$X = [\varphi\ \dot{\varphi}\ \theta\ \dot{\theta}\ \psi\ \dot{\psi}\ z\ \dot{z}\ x\ \dot{x}\ y\ \dot{y}]^T$$
$$B = [\mathrm{B}_1\mathrm{B}_2\mathrm{B}_3\mathrm{B}_4]^T$$
$$\mathrm{B}_1 = b(\mathrm{omega}_1^2 + \mathrm{omega}_2^2 + \mathrm{omega}_3^2 + \mathrm{omega}_4^2)$$
$$\mathrm{B}_2 = b(-\mathrm{omega}_2^2 + \mathrm{omega})$$
$$\mathrm{B}_3 = b(\mathrm{omega}_1^2 - \mathrm{omega}_3^2)$$
$$\mathrm{B}_4 = d(-\mathrm{omega}_1^2 + \mathrm{omega}_2^2 - \mathrm{omega}_3^2 + \mathrm{omega}_4^2)$$
$$\dot{X} = f(X, U)$$

$$\dot{Where}^2$$
$$\dot{x_1} = x_2 = \dot{\varphi}$$
$$\dot{x_2} = a_1\dot{\theta}\dot{\psi} + a_2\dot{\theta}\mathrm{omega}_r + b_1\mathrm{B}_2$$
$$\dot{x_3} = x_4 = \dot{\theta}$$
$$x_4 = a_3\dot{\varphi}\dot{\theta} - a_4\dot{\varphi}\mathrm{omega}_r + b_2\mathrm{B}_3$$
$$\dot{x_5} = x_6 = \dot{\psi}$$
$$\dot{x_6} = a_5\dot{\varphi}\dot{\theta} + b_3\mathrm{B}_4$$
$$\dot{x_7} = x_8 = \dot{z}$$
$$\dot{x_8} = g - \frac{B_1}{m}\cos\ \varphi\cos\ \theta$$
$$\dot{x_9} = x_{10} = \dot{x}$$
$$\dot{x_{10}} = \frac{u_x}{m}B_1$$
$$\dot{x_{11}} = x_{12} = \dot{y}$$
$$\dot{x_{12}} = \frac{u_y}{m}B_1$$

Increase (decrease) the speed of the front and rear motors together while simultaneously reducing (raising) the speed of lateral motors from equation 3.4. Keeping the overall thrust constant is the only way to do everything. Despite having four actuators, Quadrotor is a dynamically unstable and

under-actuated machine. When Newton-Euler formalism is used to represent a system, equations of motion can be obtained. A state-space form allows us to construct twelve state variables and four inputs, each of which is mapped by the angular rate (i=1,2,3,4) of the four propellers, as well as the thrust (b) and drag (d) components (i=1,2,3,4). Finally, the complete system is summarized by the following description:

Equation 3.5 The total residual angular speed of the propeller formula

$$\text{omega}_r = \text{omega}_1 - \text{omega}_2 + \text{omega}_3 - \text{omega}_4$$
$$a_1 = \left(I_{yy} - I_{zz}\right)/I_{xx}$$
$$a_2 = J_r/I_{xx}$$
$$a_3 = (I_{zz} - I_{xx})/I_{yy}$$
$$a_4 = J_r/I_{yy}$$
$$a_5 = \left(I_{xx} - I_{yy}\right)/I_{zz}$$
$$b_1 = l/I_{xx}$$
$$b_2 = l/I_{yy}$$
$$b_3 = l/I_{zz}$$
$$u_x = \cos(phi)\sin\left(theta\right)\cos\left(phi\right) + \sin\left(phi\right)\sin\left(phi\right)$$
$$u_y = \cos\left(phi\right)\sin\left(theta\right)\sin\left(phi\right) - \sin\left(phi\right)\cos\left(phi\right)$$

Equation 3.5 explain it's the horizontal distance from the propeller's center to its center of gravity that's being measured here. A two-section model may be derived from angle section is used to assess the first six state variables because their evaluation is independent of the other variables. The findings of the first part are utilized to establish the coordinates of the UAV in the second portion, which is a translation section.

3.4 STATE ESTIMATE FILTERING BASED ON DATA FUSION

State estimate filtering-based sensor fusion is defined for estimating unknown variables, the Kalman filter (Yuan et al., 2021) employs a collection of imprecise measurements made during a certain time. The combined probability distribution of the variables at each time step is used to get this outcome. As a result of this attribute, it is frequently employed to ascertain the internal state of systems with linear dynamic behavior.

For most algorithms, prediction and update are considered separate functions. Predictions are based on the KF's best guesses of the present situation, together with their associated levels of uncertainty. The estimations are updated using a weighted average whenever a new measurement is observed. According to the sensor measurements, the following equations are satisfied:

According to Gene et al. (2000), the random process that has to be approximated using the Kalman filter (KF) has the following structure:

Equation 3.5

$$\dot{x} = Fx + Bu + Gw$$

White noise with known covariance is used as an example of a state value. At discrete points in time, measurements of the process occur in accordance with this relationship:

Equation 3.6

$$z = Hx + Du + v$$

This equation expresses what happens when you have a noisy sample, an ideal (noise-free) link between the measurement and the state, as well as an inaccuracy in your measurements. Assuming no system control inputs u, the discrete model for this process looks like this:

Equation 3.7

$$x_{K+1} = \Phi_K x_K + w_K$$
$$z_K = H_K x_K + v_K$$

There are several components to this model, each representing a discrete point in time.

3.5 DISCUSSIONS

In the upcoming introduction to this chapter, a comparison of several sensors used to gather data about the environment was offered. Sophisticated UAV sensors have been tested to see how effectively they can detect stationary and moving objects. These sensors have also been put to land vehicles, such as GPS, IMU and cameras. They have been studied and their pros and disadvantages have been documented. When trying to detect things at close range, the radar has a poor degree of accuracy, even though it was the most employed sensor for this purpose in the past. Cameras that use infrared light can partially solve the issues, although they have been used in just a few of projects. However, despite progress in resolving calibration concerns for on board sensors from autonomous aerial vehicles, the same challenges with vision sensors persist.

There have been several path planners, both global and local, documented. The so-called 'intelligent' approaches, which are based on soft computing principles, have been given their own area. Because of its non-linear mapping, learning capabilities, and parallel processing, deep reinforcement learning has been used to solve this problem. Instead, knowledge-based conditional rules in RL-policy can mimic human reasoning. There is a great deal of complexity in handling situations that demand human-like expertise to pick the appropriate course of action.

One of the biggest issues with most of the proposed solutions is that they have only been evaluated in a computer simulation; they have yet to be proven true in the real world. The results are also restricted in their dependability since they may be incomplete because only a small number of

situations were investigated.

The UAV's actuators may be damaged by a trajectory that features excessive turn rates when wrong path planning algorithms used. A cost function that incorporates the dynamics of the vessel. There must be intelligent behavior in all sorts of drones for them to learn and follow the normal laws of search and rescue (SAR) navigation. There is no widely accepted approach. There are a few instances in which this is the case.

Their inclusion in the solution space does not imply that they are optimum. That's why it has been agreed that an autonomous vessel always must give up when it meets a manned vehicle, to simplify the decision-making process.

Future work must deal with environmental disruptions and uncertainty. Heavy wind currents are critical to drone course design, whereas wind and wave effects on bigger boats may be ignored. The vehicle may be deviated off its intended direction by high-speed currents. An increase in computing complexity for optimum path planners comes from the addition of such environmental factors into planning processes. Real-time vision-based perception is still hampered by changeable ambient circumstances (e.g., fog; illumination; rain; wave occlusions; complex backdrop).

This thesis can play a significant function in this regard. Researchers from around the world are growing increasingly interested in UAVs as they become more affordable. Because of UAV's ability to view far ahead, impediments that are moving away from the drone may be spotted and a new course can be plotted a second or many times while the drone is still in motion.

To put it simply if the drone is incapable to complete its operation. Additionally, the data collected by these sensors isn't just a backup plan; it's also used during all phases of navigation, including in foggy situations. However, these flaws present exciting problems that must be solved in the future. When flying a UAV in the Search And Rescue (SAR) environment is more challenging than flying

it on land. The use of unmanned aerial vehicles (UAVs) presents several additional difficulties aside from those listed above. For example, the magnetometers are influenced by electro-magnetic radiation created by the drone actuators and are affected by the error of cheap GPS devices fitted with UAVs. Due to natural disruptions, it is impossible to estimate the movement of the USV. An unmanned aerial vehicle may have a tough time landing on a moving maritime vessel because of the low quality of its posture data.

The multi-agent system described above will benefit greatly from this thesis. Two new approaches to autonomous UAV landing, will be discussed in the following chapters. It is suggested that the use of fiducial markings on the ship's deck will enhance the accuracy of future estimates.

3.6 Chapter Summary

Hardware and implementation of the proposed customized UAV design and dependability, wireless power transmission, and deep learning-based reinforcement learning are all discussed in this chapter's section. Examine their dependability and study their failure before using these new concepts on a broad basis.

In conclusion, we'll go into the specifics of building the design of rotational wireless power transfer system in this thesis's next chapter.

4 DESIGN OF ROTATIONAL DYNAMIC WIRELESS POWER TRANSFER SYSTEM RDWPT

- In Chapter 4, a wireless power transfer system with rotating dynamic behavior is described using significant study.

4.1 ABSTRACT

Making electric vehicles (EVs) widely available requires a solution to the problem of low range and long charging times. Solving the limitation of commercially available short wireless charging distance is indispensable in making battery powered UAVs. One of the most efficient alternatives is a dynamic wireless power transfer (WPT) system, which can supply electric power to moving electric vehicles. In this chapter, multiple motor powered (primary) coils and a moving load (secondary) coil are proposed for a rotational dynamic WPT system. The common load coil is used in both dynamic and stationary WPT scenarios in the traditional system, but this chapter focus on the rotational dynamic WPT platform proposed. According to theoretical study, the dynamic WPT system that results from a stationary WPT system is identical to the stationary system in equivalent circuit but in this chapter, the use of novel approach of RDWPT can increase the distance of the charging of UAVs gradually.

4.2 Introductions

Since pollution increases all over the world, Electric Unmanned Aerial Vehicles (EUAVs) have attracted interest across a wide range of industries due to the promise they hold for environmental conservation and the eventual replacement of conventional gasoline-powered drones (Stolaroff et al., 2018). WPT has been explored extensively to enhance pricing and address the issues outlined in this article. It has been recommended that DWPT be used as an example of

WPT to accomplish continuous charging in EUAVs to increase their flying range and reduce the weight of their heavy batteries.

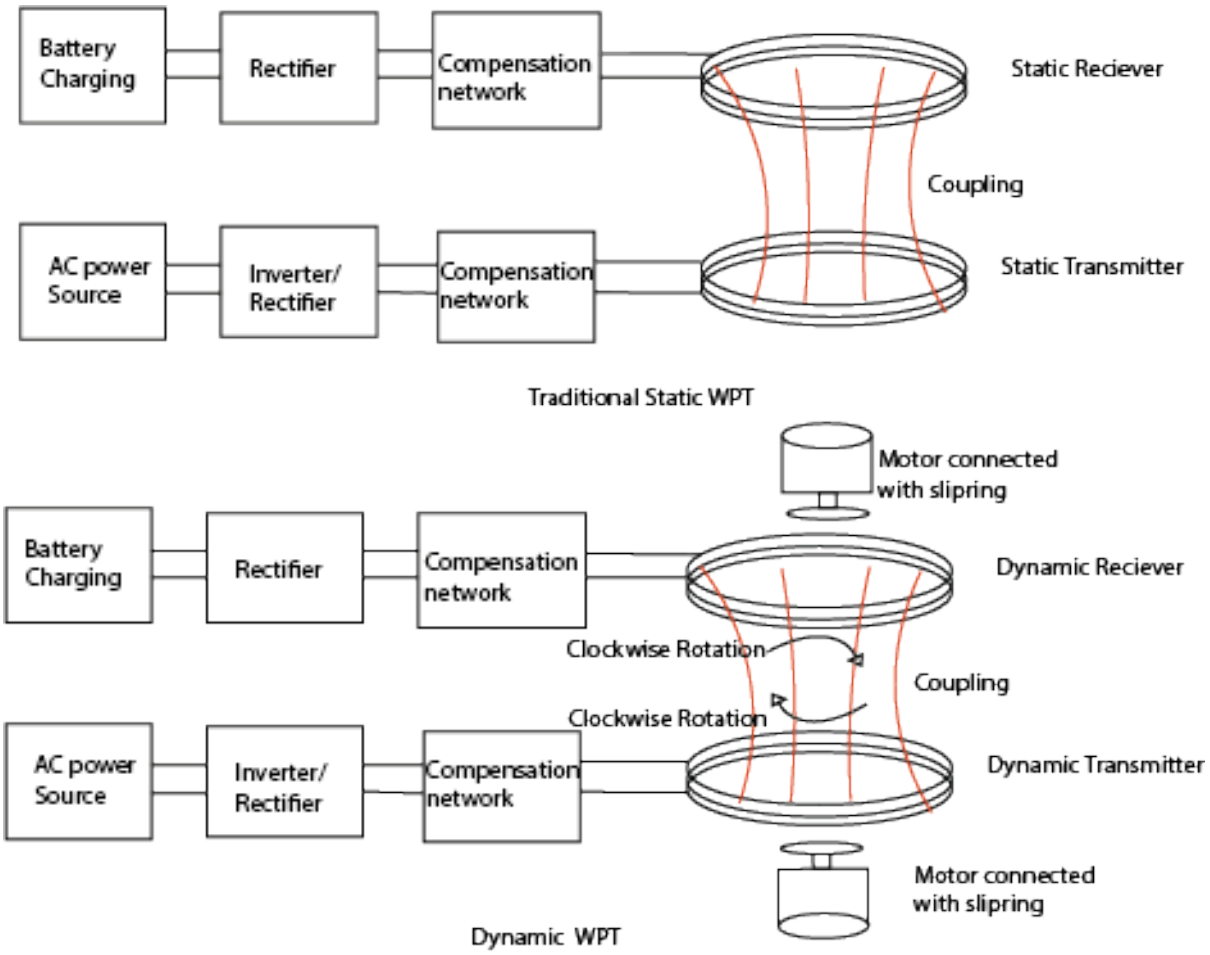

Figure 4.1 Comparison between static and rotational dynamic WPT

In this study, a rotational dynamic WPT system is described in figure 4.1. First, the dynamic system's configuration is explained in depth. On the input side, a slew of solenoid coils is linked in series. The parallel series (PS) serves as the foundation for the topology. Another comparison was made between the results of a theoretical model based on PS topology and those of a practical model based on an analogous transformer. On the robotic lab, the experimentation was set up with

200 watts WPT modified by adding motors and sliprings to the primary and secondary coil, which was used to show how the system works with an actual EUAVs in the next chapter. Finally, based on the results of the trials described here, a set of performance indices was provided for comparing dynamic DWPT systems (Toshiyuki et al., 2019).

4.3 Wireless Power Transfer

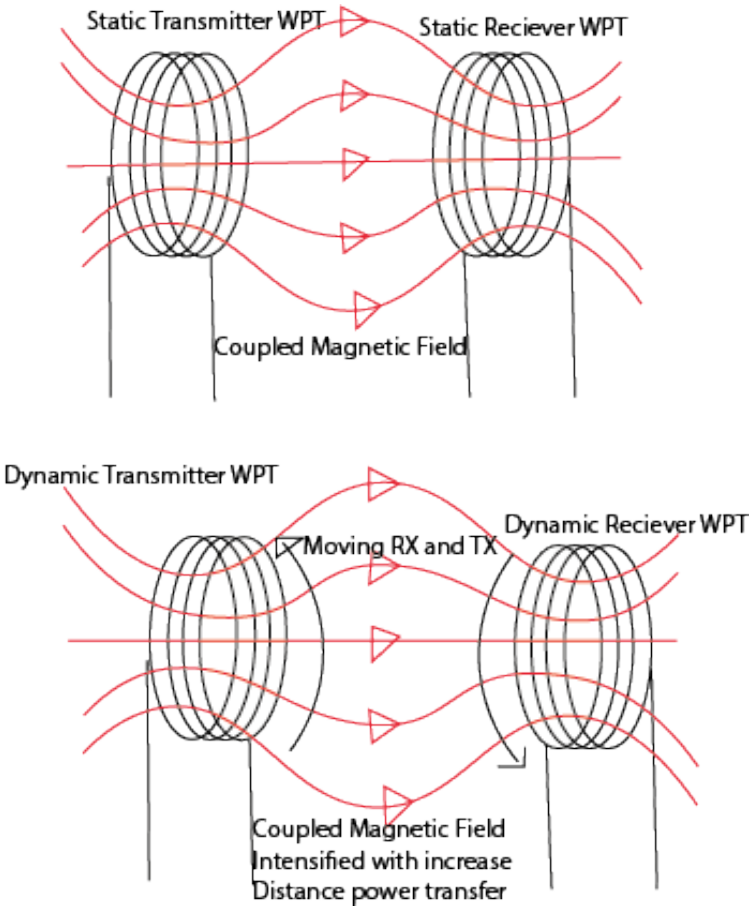

Figure 4.2 Coupled Magnetic between static and dynamic WPT

Figure 4.2 shows a rotational intensified magnetic field pulsating at a predetermined frequency powers the entire operation. A transmitter coil is attached to each (receiver coil). As soon as a reception coil is positioned near the transmitter coil supplied by AC, a voltage is induced in the receiver coil, resulting in an AC in figure 8. Then Raspberry Pi controlled motor is activated to move the transmitter and receiver coil. The sensor device is powered by a steady DC supply that

is generated by power supply. The power converter's internal circuitry loses some power when there is energy transform from alternating current to direct current.

4.4 Related Work

WPT has been discussed in the chapter to help power Internet of Things (IoT) devices. Wireless harvesting approaches, for example, have been demonstrated to significantly improve the longevity (Kamalinejad et al., 2015). Technology and methods to allow DWPT for IoT systems were discussed in this paper. A DWPT approach was utilized to develop the energy management policies. Using a dynamic WPT system, the author came up with a method that is in the form of transferring energy while moving. The behavior of the system was examined considering the current condition of the system. IoT devices may request power on demand from an energy transmitter capable of delivering power through guided RF signals, according to the author (Lhazmir et al., 2020). An energy harvesting in figure 9 and queuing model for the nodes was constructed using a discrete time Markov chain. Packet loss probability, average packet latency and network performance were all included in the design assessment. IoT devices with energy collecting capability have their offloading policies optimized. As an Markov-Decision Process (MDP), the author developed strategies for reinforcement learning to arrive at the best offloading strategy.

The author (Johnson et al., 2013) studied two charging methodologies and evaluated the energy consumption of UAVs. Remaining stationary, the UAV charges sensors in its area of coverage. Each sensor node may be recharged by a UAV that flies above it, replenishing the sensors' depleted energy. The unmanned aerial vehicle (UAV) has been employed as a transportable power source. A regression approach was used to improve the energy efficiency of the flying path. A weighed

harvest and transmit technique were also devised to maximize the combined throughput of all nodes.

However, unmanned aerial vehicles (UAVs) have been employed for data gathering as well as WPT. Among other things, the authors (X. Lu et al., 2021) looked at the trade-off between power transfer time and data gathering time. The scheduling approach of low battery first is proved to provide better advantages. Additional to this, the author (Wei et al., 2022)proposed a solution to the travelling issue using time windows: the lowest journey time trajectory for the UAV. UAV-assisted wireless-powered IoT network resource allocation was addressed through a dynamic system. Attaining a Nash equilibrium is the best way to distribute resources according to Bellman's dynamic programming. As a result, the unmanned aerial vehicle (UAV) manages its wireless power transfer resources optimally.

4.5 SYSTEM MODEL

A Rotational Dynamic Wireless power transfer (RDWPT) system in which a random distribution of N and wireless devices is analyzed is shown. WPT-enabled UAVs can be denoted by =... 1, 2, M. Unmanned aerial vehicles (UAVs) gather data and transmit wireless energy to RDWPT devices via the air. A UAV j's altitude is indicated by the coordinates (xi, yi), whereas device i's position is given by (xj, yj, h). then one UAVj may service multiple devices. Devices connected to the RDWPT send power and data packets to the most appropriate unmanned aerial vehicle (UAV), hoping for a stable connection and high performance. Device I and UAV j must decide whether to send data at time t based on the current system state. We're looking at the feasibility of wireless energy transmission in this network as well. As a result, any device that lacks the power to send data may ask the UAVs for help transferring energy. We only consider one of the two options when configuring an RDWPT device for any energy-limited device, the downlink is used to gather and transmit energy, while the uplink is used to send information. However, UAV j is aware of the

current state Qj of its data queue and the current state Pj of its energy storage device. A list of data is shared each time an association is made. For example, an IoT device can show the size of the packet to broadcast, or the amount of energy required. The buffer and energy units used by UAVs are a way of describing their available resources. Each IoT device is assumed to be LOS-dominated, hence a route loss model like that used is used for the wireless channel.

Equation 4.1

$$\bar{L}_{ij} = Storage_{Los}^{ij}\mu_1\left(\frac{4\pi f_c d_{ij}}{c}\right)^{\beta} + Storage_{NLos}^{ij}\mu_2\left(\frac{4\pi f_c d_{ij}}{c}\right)^{\beta}$$

$$Storage_{ji} = \frac{e_t^i}{g_{ij}}$$

4.6 METHODOLOGY AND IMPLEMENTATION

The input power can be used to increase the load power, as shown in equation 4.2. Only the transmitter's input power can provide feedback for optimizing the efficiency of the power transmission. As a result, the extremum seeking controller's (ESC's) objective function is as follows:

Equation 4.2

$$f(theta) = RI^2 + (R_3 + R_L)\frac{w^2 I^2}{(R_3 + R_L)^2 + X_3^2} \times$$

$$(M_{13}(alpha)\cos(theta) + M_{23}(alpha)\sin(theta))^2$$

The equation 4.3 which is about f of theta differential equation explained below.

Equation 4.3

$$f(theta) = f^* + \frac{f''}{2}(theta - theta^*(t))^2$$

Where, theta is the system input and theta prime are the optimal input value which is equal to the differential equation f prime.

RDWPT system begins to identify optimal differential input value which enhance the self-reliant function of WPT receiving station. The charging station is controlled by rotating magnetic resonance field since the power transmission is omnidirectional. As a result, it will also cover the two that are left. 2nd differential order integrator s12 included with respect to the optimal input power varies with time owing to movement of the receiving station.

After all the ESC settings have been established, the independent frequency of the input system and output system are utilized for better adjustment. Using MATLAB Simulink model to show the proposed RDWPT method, reveals that the maximum is accurately tracked near real time movement of the transmitter and receiver. Using a reaction time of 8 seconds, the controller can keep track of the receiver's angle and achieve its maximum power transmission.

4.7 SYSTEM SPECIFICATIONS

If the UAV is within the charging lane's range, the dynamic charging mechanism should be able to take up steady electricity. The genuine system is three times smaller because of the restricted space. A three-fold reduction in the permissible misalignment and a decrease in the diameter of the coil result. The circular coil's corresponding radius is approximately 14 cm. 23 centimeters of space is sufficient for charging electric unmanned aerial vehicles. 8 cm is the estimated airgap. It is possible to simulate and test the coupling factor for misalignment. As a rule of thumb, 14.2, 14.5

V are the most common operating voltages.

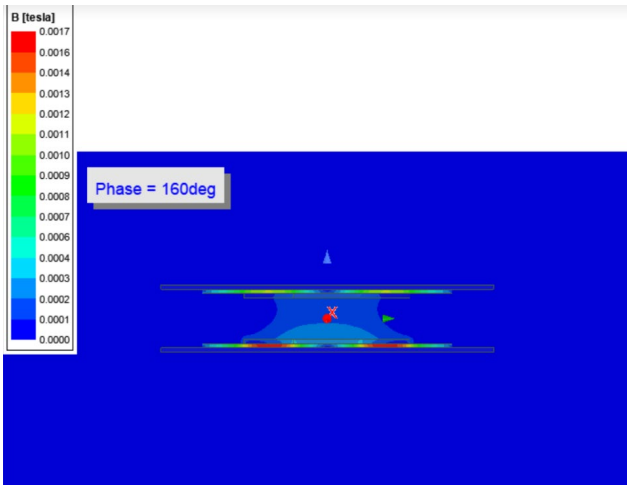

Figure 4.3 WPT MISALIGNMENT

The misalignment of the RDWPT was simulated using ANSYS software in figure 4.3. At first, transmitter and receiver coils 3d model were developed using the Maxwell electronic suite and then simulate the RDWPT airgap misalignments.

4.8 WPT MOTOR

The UAV is propelled by an AC electric motor with electronic speed controller. The RDWPT-POLICY system is controlled by DC motor attached with slip ring to rotate the transceiver in opposite directions. Traditional dynamic WPT system works by moving aerial vehicle wirelessly charge by static multiple transmitting stations in the ground. The proposed system in this chapter focuses on the novel method of rotating transmitter and receiver in the reverse direction to increase the charging distance of the RDWPT-POLICY system.

Equation 4.4

$$[v_s] = [R_s][i_s] + \frac{d}{dt}[\varphi_s].$$
$$[\varphi_s] = [L_{ss}][i_s] + [\varphi_f].$$
$$[\varphi_f] = \varphi_{sf}\begin{bmatrix}\cos(\theta)\\ \cos\left(\theta - \frac{2\pi}{3}\right)\\ \cos\left(\theta - \frac{4\pi}{3}\right)\end{bmatrix}$$

We need to identify and model this system to understand it. What's left in this section consists of a modelling exercise. A series of assumptions were made during this phase, as outlined in the following four points: the permeability of magnets is near to atmosphere and iron losses are omitted. Permanent magnet synchronous machines are shown in schematic and composition. Voltage and flow equations and sf denotes the magnet's peak (constant) value as it passes through the stator windings, and Equation 4.4 expresses this flux expression in that form. Because of the nonlinearity and coupling in Equation 4.5, we must adjust the variables and convert the system to make it simpler.

Equation 4.5

$$\frac{d}{dt}i_d = \frac{1}{L_d}\left(v_d - Ri_d + L_q\omega_e i_q\right).$$
$$\frac{d}{dt}i_q = \frac{1}{L_q}\left(v_q - Ri_q - L_d\omega_e i_d - \varphi_f p\Omega\right).$$

Electromagnetic Torque Equation:

$$C_e = p\left(\left(L_d - L_q\right)i_d i_q + \varphi_f i_q\right).$$

Mechanical Equations:

$$\frac{d}{dt}\Omega = \frac{1}{J}(C_e - f\Omega - C_r)$$

$$\frac{d\theta}{dt} = p\Omega$$

4.9 SIMULATION OF THE RDWPT-POLICY

The RDWPT-POLICY SPICE model from Efficient Power Conversion (EPC) is used to simulate the inverter architecture in this section of LTSpice. An inverter's first harmonic is exactly proportional to its dc voltage, VD D, hence this parameter serves as external radio frequency power control.

Equation 4.6

$$DT = (2C_{\text{off}})\frac{V_{DD}}{I_{max}}$$

Figure 4.4 Simulation Results of RDWPT-POLICY

Table 4.1 Drain Voltage

	18 km/h	20 km/h	40 km/h
Gcoil (%)	0.23%	0.09%	0.06%
Transmitter coil (T) in seconds	0.1	0.047	0.029
Total Gsoc (%)	0.59%	0.42%	0.29%
SOC max (%)	52.6348%	52.6331%	41.6318%

The simulation uses DT with a range of 8 to 10 nano seconds. Simulated dc input voltage is linearly modulated from 14 to 5.7 volts, while the DT value is dynamically modified. Figures 4.4 depict the simulation's outcomes.

4.10 COIL DESIGN CONSIDERATIONS

Magnets are used to transport high-frequency AC impulses over an air gap. The system's capacity to transfer electricity and the distance it can travel are determined by the design of these coils. A wide variety of planar coils have been studied because of WPT technology advancements throughout the years. Non-Polarized Pads often come in the following shapes: round, rectangular, and hexagonal.

The magnetic flux distribution is directly influenced by the diameter change. It has been shown that the effective flux distribution area of rectangular coils is greater than that of circular coils. However, the system weight is increased due to the need for additional materials in these designs than in conventional systems. To minimize misalignment when working as a secondary component, the flexible design has been implemented. Copper coils have been replaced by High-Temperature Superconductors (HTS) that have proven a 92.34 percent efficiency.

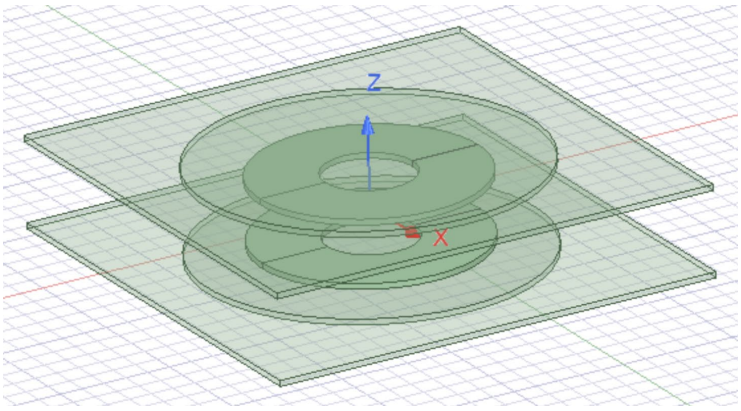

Figure 4.5 RDWPT ANSYS SIMULATIONS

Magnetization losses were found to rise as the frequency and density of the magnetic field increased. There were less losses of magnetization in the spiral and solenoid coils, respectively. Aside from the fact that skin effect causes excessive cooling power consumption, HTS coils are inefficient for high-power applications because of this. However, the small size of the UAV's frame restricts the use of numerous coils. As a result, the transmitter and receiver circuits use a basic circular coil construction. Electronic circuits can be damaged by the electromagnetic radiation (EMF) emitted by the coils. Internal circuit damage occurs when rogue currents are generated in the PE circuit because of being exposed to EM radiation. When working with high-frequency electromagnetic waves, precautions must be taken (Prithvi Krishna et al., 2021). The coil design from ANSYS is shown below in figure 4.5 with above configurations.

4.11 MATHEMATICAL ANALYSIS

An orthogonal transmission-end coil (Tx, Ty) and a centrally aligned receiving-end coil (Rx) make up the system that moves in the (x, y) plane at a variable speed. To boost the WPT's efficiency, the coils are linked to serial capacitors and resistors. AC sources are used to supply power to the transmission side and a resistive load is attached to the receiving side of the coil.

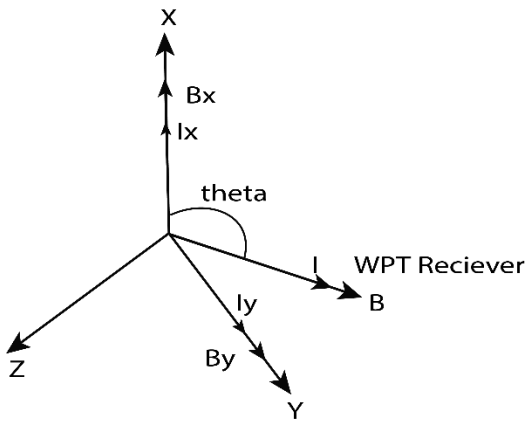

Figure 4.6 Magnetism and Electricity of WPT

The magnetic fields BxBy in figure 4.6 are produced by the currents ixiy passing through the transmitting coils.

Equation 4.7

$$B = \frac{\mu_0 I}{4\pi r^2} \oint dl \cdot (\hat{\imath} \times \hat{r}) = \frac{\mu_0 I}{2r} \cdot (\hat{\imath} \times \hat{r})$$

There are two ways to look at Equation 4.7: one is to look at it in terms of the Cartesian plane, which has the same directionality for each of these components. As a result, even if the transmitter isn't moved, the magnetic field may be steered. It is possible to change the amplitude of the magnetic field to any desired location in the Cartesian plane by altering this feature. WPT's transmitting-end coils create a theta vector (magnetic field).

Equation 4.8

$$B = B_x + B_y = \frac{\mu_0}{2r} \cdot \left(i_x \hat{\imath} + i_y \hat{\jmath}\right)$$

Magnetostatic and electrostatic fields are seen in the (x, y) plane in Figure 4.8. To target any load in the plane, we can simply move the resultant theta vector.

Equation 4.9

$$\begin{cases} i_x = I \times \cos\ \theta \\ i_y = I \times \sin\ \theta \end{cases}$$

4.12 Results

The simulation trajectory with maximum power may be achieved by a receiver that turns at an angle of 90 degrees. As a result, the 2D orthogonal coils system achieves maximum power transmission in both rapid mobility and static load instances. However, even with 612 rad/s of receiver rotation, controller can drive system to maximum power transmission.

Table 4.2 Control Parameters

Control parameters	Mathematical Form
Proportional Integral Gain	PI
Low Pass Filter	$\text{asin}\,(\omega s)$
High Pass Filter	$\dfrac{k}{k + w_s^*}$
Error factor	$-(k+1)$

Table 4.2 shows the control parameters of the RDWPT system. Once installed, the controller will just monitor and optimize the input power signal and will not require any other information from the receiver. The power provided to the load may be increased by altering the coil design parameters, and the benchmarking chapter's parameters were utilized to model the system in this study. There is more detail on the reciprocal coupling relationship and receiver's angle of rotation in this work, though. This chapter focuses input power calculation matches the experimental results thanks to the Ansys software simulation. This research uses an efficient control approach based on adaptive control theory. As previously published work has shown, ideas for charging batteries and supplying electricity to moving loads may be extended and improved upon. Under high transmitter-receiver misalignment circumstances, omnidirectional techniques are shown in the study that has just been developed in this chapter.

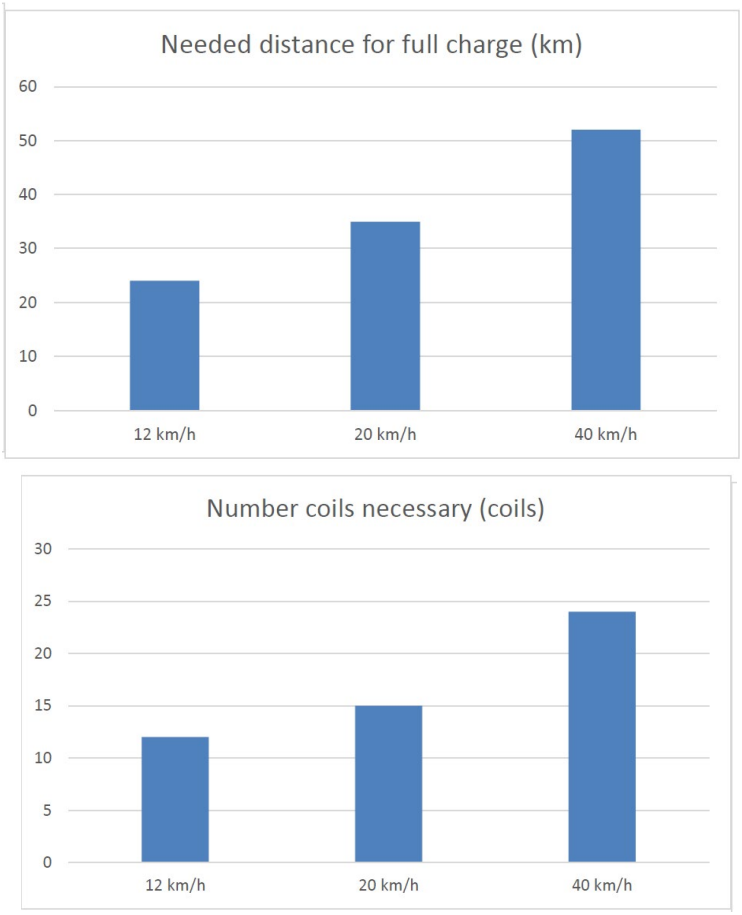

Figure 4.7 Number of coils and speed of RDWPT

Table 4.3 Number of coils and speed of RDWPT

Speed	Needed distance for full charge (km)	Number coils necessary (coils)
12 km/h	24	12
20 km/h	35	15
40 km/h	52	24

4.13 Stationary System Analysis

Variation of input voltage VIN topology was employed by the nominal airgap of 120 mm was maintained without misalignment for the aerial vehicle-side coil. An 88 kHz inverter working frequency was maintained throughout the entire experiment. The efficiency was 92.2 percent with a power load of 200W at 48.6 VDC. A theoretical output voltage V'L of 24 volts. Voltage L was measured at 401 volts, though.

4.14 Dynamic System Analysis

The rotational dynamic WPT system photographed in the subsequent bench tests. Each ground-side coil was separated by 120 mm. The aerial vehicle-side coil was moving at 32 mm/s. Constant values of 240 VDC and 90 kHz were used to manage the input voltage VDC and frequency. This system has no additional feedback loops built.

For an aerial vehicle-side coil in motion, the changes in input and output power with time. Maximum values in Figure were obtained by aligning the coils on the UAV with the coils on the ground. PS features and a resistive load were the outcome of this event. Furthermore, the amount of energy conveyed quadrupled when the coil on the vehicle side's side was slowed by half. Throughout the test, electricity was continuously transferred from the experimental road to the UAV.

4.15 Applications

A rotational dynamic WPT system is shielded using the shielding approach provided in the method under consideration utilizes numerous successive short-track main pads positioned on the lab. Coils in the primary ignition switch are turned on one at a time for security and efficiency, and only when an underbody-mounted secondary coil is recognized. Because the secondary coil may be placed anywhere along the electrified road, this system can be studied in the same way as a

normal static WPT system. The main coil's exterior dimensions are 150 cm long and 50 cm wide. Because the long side of the secondary coil is oriented to compensate for any conceivable misalignment, this coil is rectangular in form. There are two secondary coils: one that has a diameter of 50 cm and the other that has a diameter of 60 cm. A reduction in reluctance in the magnetic field allows for improved electrical performance via improving magnetic field behavior. A UAV has been used in our simulations. Its length is 423 cm, its height is 144 cm, and its breadth is 180cm in the metallic bodyshell seen in Figure 26. For the body, thin 2-mm aluminum alloy panels with 30-MS/m electrical conductivity are used.

Table 4.4 Coupling Factor of Secondary Coil

Secondary Coil Center Position along x Axis	k1	k2	k3
x1 = 0 cm	0.0649	0.0397	0.0215
x2 = 15 cm	0.066	0.0395	0.0213
x3 = 20 cm	0.0686	0.0395	0.0101

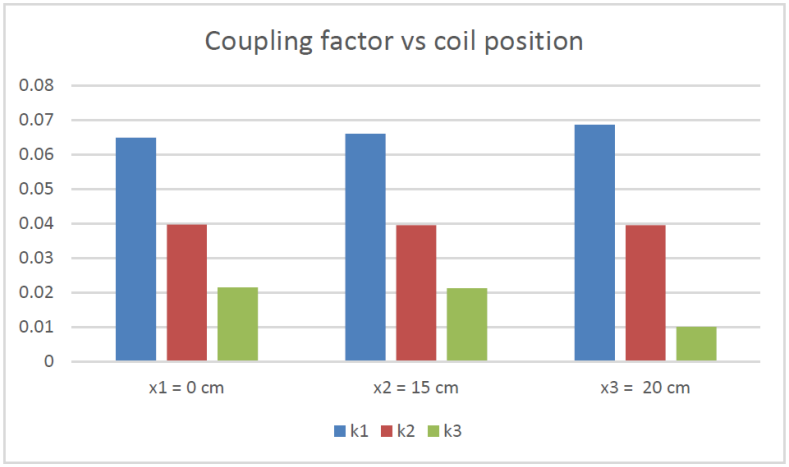

Figure 4.8 Coupling Factor of Secondary Coil

4.16 Efficiency of WPT

The efficiency of the RDWPT-POLICY under investigation in this section. In this case study, the suggested mutual inductance analytical behavioral model is validated using a series–series compensation architecture. This work does not include the optimal design of both power conversion stages and resonant compensation systems.

Additionally, R2 contains the resistances of both rectifier diodes and the L2-C2 series of resistors. LTX, LRX, RTX, RRX, and R1 and R2 are all used respectively. This allows the receiver's diode-bridge rectifier to be linked to the load (battery). Using phase-shift control, the transmitter rms current I1rms may be set to a certain value, ref. The investigated DWPT had the following operational parameters and component values. Additional information on dynamic power control and demand regulation may be found in the reference section.

The equation below presents the phasors of voltage and current at the transmitting and receiving coils, respectively.

Equation 4.10

$$P_1 = \frac{1}{2}\left[R_1 + \frac{(\omega_0 M)^2}{R_2 + R_{ac}}\right] I_1^2, P_2 = \frac{1}{2}\frac{R_{ac}(\omega_0 M)^2}{(R_2 + R_{ac})^2} I_1^2$$

$$\eta = \frac{(\omega_0 M)^2 R_{ac}}{[(\omega_0 M)^2 + R_1(R_2 + R_{ac})](R_2 + R_{ac})}$$

the inverter phase-shift control sets the TX coil current magnitude I1 to p2 I1rms, ref. I1 = p2 I1rms The WPTS efficiency is affected by the mutual inductance M, as shown in Equation 4.10. Furthermore, the efficiency rises with increasing mutual inductance indicates.

4.17 Experimental Verifications

Single rotating motor-powered transmitters and a receiver make up this prototype. Segmented switches can be ignored since the movement speed is believed to be low enough ref. Three parallel inverters are powered by a single DC power supply.

According to the position of the receiver, segmented wireless charging can be accomplished. The experimental prototype's complete set of parameters may be seen in the table below. Immediately following the switchover point, U45 is activated, whereas U12 is shut off. U3 is always active during this experimental validation since both G1 and G2 require it. There is currently some distortion, and this will be rectified in future work. While in motion, the secondary side may have induced a tiny shift in resonant state. Overall, a 220 V output voltage with oscillation waves of less than 18 V is attained (8 percent of the nominal voltage).

4.18 Performance Comparison

The intended dynamic WPT system's performance to that of prior systems (see ref) and lists the differences. This design has an unusually high tolerated offset ratio of 1.4. According to the prior research, there are two ways for calculating efficiency. Efficiency is measured from a direct current (DC) source to a direct current (DC) load. A typical dc–dc efficiency is 90 percent or higher ref due to the inclusion of Tx and Rx power converter efficiency. Consequently, the system's efficiency is satisfactory. A steady, efficient, and restricted coupling flux is used in this article's misalignment-tolerant coils. In addition, the landing and charging are more stable due to the coils and accompanying landing basins. The four-channel prototype has a maximum output power of 200 Watts.

4.19 Electrical Performance

The initial tests were carried out to verify the electrical performance numbers reported in the preceding section. Consideration was consequently given to a more streamlined electrical system design.

Table 4.4 Experimental results

	(Watts)	Efficiency	Power Efficien	Total Energy (Wh)
Resistance	9.1	81.3%	76%	420
Battery	9.4	81.7%	67.12%	201
WPT UAV test	4.3	72%	82%	5.70
RDWPT UAV test	6.3	79%	89%	2.1
Stationary WPT system	18	91.0%	92.0%	401

When comparing actual measurements to findings from a finite element model, the numerical results are displayed in Table 4.4. Then, with the output power set at PL = 166 W, a comparison of efficiency was made between three distinct Rx coil alignments. A flawless alignment was achieved in the first example, however the secondary coil was laterally misaligned by 100 mm and 200 mm about the main coil, as well as by 35 and 70 millimeters in y-axis direction.

The output power was maintained at PL = 166 W in all the studied scenarios by altering the input voltage V1. A variety of x- and y-axis misalignment circumstances are investigated, and the resulting electrical performances are analyzed and compared. Table 2 shows that computations and observations are in good agreement.

All the true electronic components of the system are considered and applied to the drone in the second test. It has been replaced with a rectifier and a battery on the Rx side of the drone. The rectifier, which is made up of four Schottky diodes with extremely low forward voltage, mounted on the landing gear with compensating capacitors.

Charging this type of battery requires a constant-current/constant-voltage method. The suggested

solution has been tested in several operational scenarios. After the drone is automatically landed, the battery is charged for roughly an hour. Additionally, the drone's ECU and communication components are unaffected by the magnetic field emissions.

4.20 Discussions

According to our findings, the following issues must be addressed to enhance the dynamic WPT system under consideration in this work. A way of switching might be devised to lessen the impact of this. As a comparison, look at the RDWPT-POLICY and WPT systems. A rotational dynamic WPT system was the subject of this work. But we also evaluated a dynamic WPT system based on a series-series model. The two systems should be compared. (d) Strengthen the ground-side coils' ability to receive electricity. There were power dips between the coils in the system studied in this research.

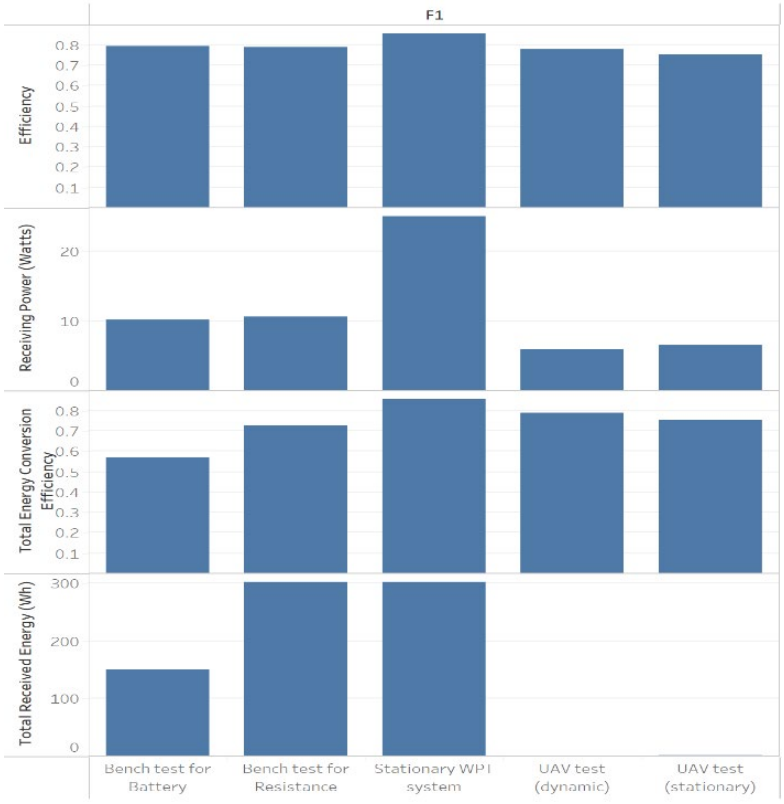

Figure 4.9 Experimental Results

As seen in figure-4.9, this chapter's experiments are summarized with the experimental results. Drone power energy conversion efficiencies are challenging to measure because of the inconsistencies in the timing of vehicle passings over ground-side coils. According to our calculations, the total energy received is a reliable indicator of vehicle speed and input power.

4.21 Conclusions and chapter summary

Fast evolving technologies has led to the innovation of powerful wireless powered unmanned aerial vehicles (UAV), also known as WPT drones, for the purpose of working in dangerous environments which human won’t be able to travel. To begin, the study's theoretical analysis indicated that the system under consideration might make use of a circuit equal to that found in test in a variety of scenarios to verify the theoretical analysis. In this chapter, we designed and experimented the RL-POLICY, the working Principe of the proposed methods including short- and long-range methods. As a final step, two new factors were also introduced to help us gauge how well rotational dynamic WPT systems function in a variety of settings. Finally, the future of WPT transfer using electrostatic resonant coupling method using earth as a return wire. In the next chapter, we will be experimentation of this method to power the UAVs efficiently, the safely and reliability of sending power to longer distances.

5 DESIGN AND Implementation of autonomous rotational dynamic wireless charging for UAVs

- Chapter 5 continues with implementing the design of Reinforcement Learning Policy (RL-POLICY) system into the autonomous UAV.

5.1 Introductions

Studies on WPT with UAVs have covered a wide range of topics including far-field and near-field transmissions, operating frequencies and frequencies with misaligned coils and mismatched capacitance values, as well as target loads in various environments and operating situations. Many critical concerns, including weight limits, comparability of existing charging methods, shielding approaches, and many more, are not addressed in this chapter. Rotational Dynamic WPT must determine whether to request data transmission, request wireless energy transfer using a drone. Charging stability is improved by the structure's many, null-cross-coupled transmission pathways. Using the input voltages of the active coils to ensure a constant charging power and the best transmission efficiency of UAV battery. Due to its low battery capacity, a UAV's flight time is generally constrained by these opportunities. As a result, the UAV's payload is restricted. There are several advantages to using an autonomous drone that can recharge its batteries wirelessly and autonomously without the need for human involvement, such as increasing the overall mission duration. In comparison to a proposed search methodology, simulation results demonstrate the superiority of the offered strategies.

Control of both location and attitude (inner loop) is handled by the UAV's flight controller. The UAV's on-board CPU typically handles the inner-loop control, while the base station's processor handles the outer-loop control. To implement their own control algorithms, multiple UAV research groups all around the world frequently create a control algorithm. By using a precise position-feedback mechanism, such as that proposed by (Xia et al., 2017), a UAV may do even the most

daring maneuvers, such as multi-flips.

The device which was used to experimented in this chapter consists of raspberry pi camera at high frame rates (30 fps) to detect even the tiniest motions of the drone. The wireless powered drone with cameras seen in (Hoseini et al., 2021) are conceivable in a properly calibrated setting. Using this pi motion capture technology with Nvidia Jetson AI powered controller and flight control electronics, this research achieves the exact outer-loop or position control it sets out to achieve.

Using a wireless charging station, this study presents an inexpensive way for drones to extend their flight life for long-term missions without the need for human interaction. Also, if a UAV's battery is low, it will be automatically sent to a charging station presented in chapter 4 which made of novel techniques called rotational dynamic wireless power transfer. As a result, a UAV will be able to begin landing on the station for recharging as soon as it notices that its battery is becoming low. Recharging has been completed, and the drone is ready to begin its mission.

Figure 5.1 Custom Made Quadcopter

UAVs, like traditional helicopters, may hover, but they also offer significant benefits, such as piloting ease and mechanical simplicity, which make them a viable alternative to helicopters.

UAV's' flight time is severely constrained by the high current demands of their motors, making them unsuitable for extended use. Even with a completely charged battery, the UAV can only fly for a few minutes in a controlled setting. It will take longer to fly if it has additional weight, such as a camera or a measuring gadget. Thus, it is evident that the battery of the UAV must be recharged. This chapter's proposed method was developed using custom made quadcopter shown in figure 5.1.

As it is, a direct human interaction is required for this charging operation; hence, an automatic technique is needed to land and recharge a UAV without the continual requirement for human participation. An effort to build a battery exchange station for tiny coaxial helicopters (Gómez & Green, 2017) has also been underway by the researchers. There are a few other ground robots with comparable self-recharging capabilities, but UAVs have yet to be effectively deployed in a mainstream application. Contact-based charging stations are both more expensive to produce and more difficult to design due to their complicated mechanical implementation.

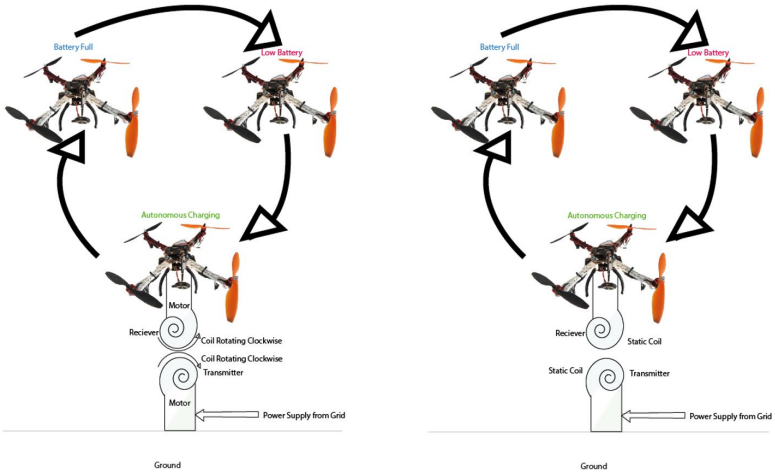

Figure 5.2 Comparison between traditional approach right Static and proposed method left Dynamic Wireless Power transfer for UAV concept

An efficient and high-power transmission of up to 2 meters may be achieved using the strongly coupled magnetic resonant induction (WPT) which the radiation would be dangerous to the person

who stay near to the field. Due to the low interference and disruption caused by magnetic resonant induction based WPT, UAVs can take use of this technology (Jia & Yan, 2020) for its advantage. UAVs have also been used to power sensor networks wirelessly using the WPT principle (Le et al., 2020b). All these papers demonstrate the usefulness of WPT in a variety of (mostly low power) contexts. These research' findings about the effectiveness of WPT technology in extending UAV flight periods have led to the current proposal to use relatively high-power WPT technology to achieve this goal. It is the originality of the proposed research that WPT integration in UAVs would enable the capability of autonomous recharge and extended flight periods without human involvement.

Even though this is a complex and time-consuming process, this study proposes a low-cost and easy to install solution for any commercially available UAV, as well as a ground station enabling WPT and UAV. Figure 5.2 shows that the comparison between traditional approach right Static and proposed method left Dynamic Wireless Power transfer for UAV concept which was proposed in this chapter.

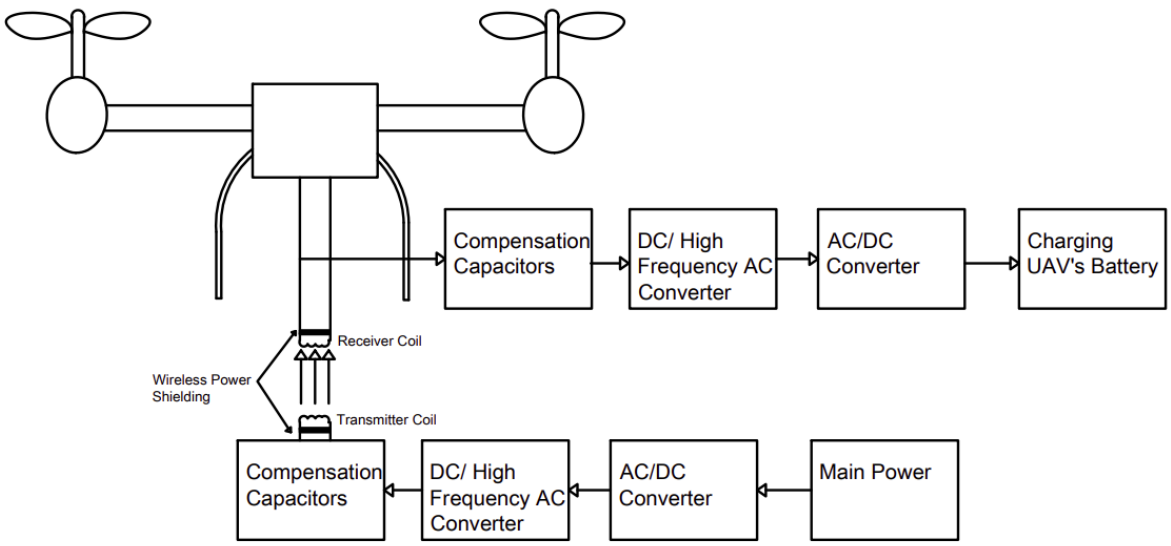

Figure 5.3 UAV's WPT Block diagram

5.2 System Model

There are three different shielding models, and their corresponding evaluations are explored in this section for the DWPT of the UAV. When utilizing a constant operating frequency for the series–series (SS) compensation topology, a FEM software solver is utilized to examine the impacts of shielding strategies on the WPT system power transfer efficiency (based on the coupling coefficient) and system inductances of the UAV. The ferrite shielding is shielded using the lumped circuit model from Reference (Mohamed et al., 2017), while the resonant reactive current shield is shielded using the circuit model described in this section. The internal resistance of the power supply and the resistance of the load are set to 150 W and 200 W, respectively, as the default values.

Ferromagnetic material might complicate the analysis because of the nonlinear behavior, which is caused by both hysteresis and eddy current losses in Tx and/or Rx coils. The magnetic dipole moment Pm of a material change because of an applied magnetic field H. Because of this, the

macroscopic magnetic dipole density or simply, a magnetization M shown below.

Equation 5.1

$$M = \chi_m H$$

The magnetic susceptibility is a constant that measures the amount of magnetization a material has in reaction to an external field. Relative permeability is defined as the ratio of material permeability to free space permeability, and the relationship between B, H and M may be summarized as follows:

Equation 5.2

$$B = \mu_\circ(H + M) = \mu_\circ(H + \chi_m H) = \mu_\circ H(1 + \chi_m) = \mu_\circ \mu_r H = \mu H$$

As a result, the magnetic flux density comprises both the external field mH and the material reaction m–M. It is therefore possible to use the WPT model outlined in the presence of ferromagnetic material. The FEM software solver is utilized to implement the effects of ferromagnetic materials on WPT system design in the analysis. Two iron cores are added to the same circular coils to make them more powerful.

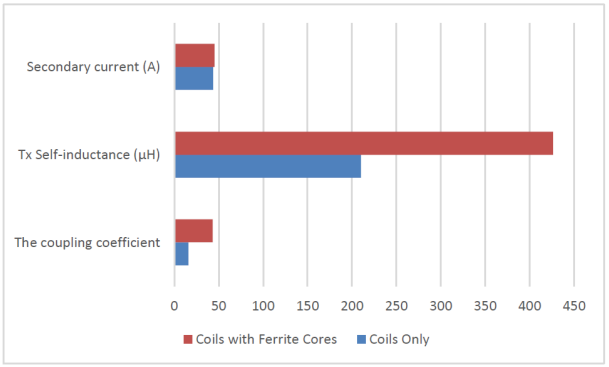

Figure 5.4 Coil comparisons for current, self-inductance and coupling coefficient

When ferrite cores are added to the Tx and Rx coils of the SS design with a 22 W load resistance, the efficiency of power transmission is shown in Figure 5.4 for different frequencies solely for the

two coils. The resonant frequency is altered because the compensating capacitors are the same as in the version without cores. According to this diagram, the WPT system is vulnerable to ferromagnetic materials. Therefore, the system must automatically alter the capacitors or the operating frequency to compensate for this.

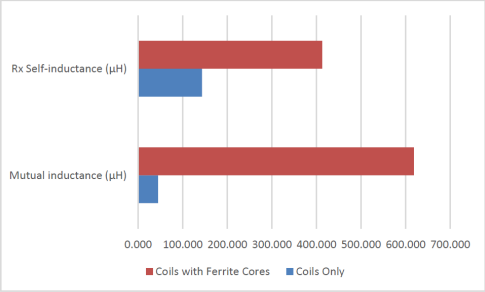

Figure 5.5 Coil comparisons for self-inductance and mutual inductance

The system's efficiency increases from 59 to 81 percent with the addition of ferrite cores. Increased system performance and resonance may be achieved by changing the compensating capacitors following the addition of ferrite cores as indicated in Figure 5.5. The magnetic coupling will improve because of the reduction in leaky magnetic flux. As the XY measurement plane 40cm positioned 8 cm above the secondary coil can provide more information than the shielding efficacy alone when comparing the magnetic field strength (A/m) of the coil's alone vs the shielded coils. Because the magnetic plates channel the magnetic flux along and inside the plates, it is obvious that the magnetic shield has strong shield efficiency. The magnetic shield is a very effective shield.

Table 5.1 Coil Comparison

Parameters	Coils Only	Coils with Ferrite Cores
Mutual inductance (µH)	44.611	618.300
Rx Self-inductance (µH)	142.96	412.6
Primary current (A)	12.43	5.38
The coupling coefficient	15.8	43.400
Tx Self-inductance (µH)	210.1	426.1
Secondary current (A)	43.47	45.47

Two coils with ferrite cores with their self and mutual inductances, as well as additional simulation data. Ferrite cores can increase the self- and mutual inductance, which will lead to a rise in coupling coefficient. For the same amount of power transmission, adding a magnetic core can reduce the current stress on the primary coils.

The excited coil B1(T) produces the following magnetic flux density. Eddy current (mirror loop) B2(T) generates a magnetic flux density. The overall density of magnetic flux is Coil and shielding plate eddy current mutual inductance is represented by M. The eddy current circuit's self-inductance and total resistance are denoted by the notation La, Ra. There, r is the wire diameter. If the eddy current's breadth and d is its skin depth, and these values are provided as follows:

Equation 5.3

$$B_1 = \frac{\mu_\circ a^2}{2(a^2+z^2)^{\frac{3}{2}}} I_1.$$

$$B_2 = -\frac{\mu_\circ a^2}{2(a^2+(z-d)^2)^{\frac{3}{2}}} \frac{j\omega M}{R_a + j\omega L_a} I_1.$$

$$B = B_1 + B_2$$

$$M = mu_\circ a\left(\log \frac{8a}{breadth} - 2\right)$$

$$L_a = a\left(mu_\circ\left(\log \frac{8a}{diameter} - 2\right) + \frac{mu_\circ}{4}\right)$$

$$R_a = \frac{2\pi a}{\alpha\delta}$$

$$\delta = \sqrt{\frac{\rho}{\pi f \mu}}$$

5.3 Simulations

Simulink's simulation output waveform is depicted in Figure 36 based on the coil parameters computed in 1st model. Rather than using resonant coils and their mutual inductance, we utilize a transformer to replace them. We employ AC power to create the high-frequency AC power needed

by the system. The series inductance and capacitor architecture are used in both the double transmitting and single receiving circuits. The output voltage waveform is shown in other figures 37 as Uout. Uin is the active coil's input voltage. Iin is the active coil's input current waveform. The output current waveform is denoted by Iout. The system's output active power is represented by output power, while the system's input active power is represented by input power1 and input power2. The system's transmission efficiency, which is 89%, may be determined using the simulated voltage and current. The output power inaccuracy is less than 8% when the simulation results are compared to the theoretical values.

A variable power output may be accomplished by varying the input voltage. The theoretically derived theoretical output power is quite close to the simulated output power. There will be less inductance between the receiving and transmitting coils due to radial misalignment, which in turn reduces power. For example, when both active coils are powered by 480 V peak input voltage, the output power is reduced by radial misalignment.

Table 5.2 Outcome of the verifications

	Value-1	Value-2	Value-3	Value-4	Value-5
Theoretical (W)	296	430	635	772	849
Simulation (W)	290	420	610	750	820
Peak Amplitude (V= 14)	410	510	610	680	710

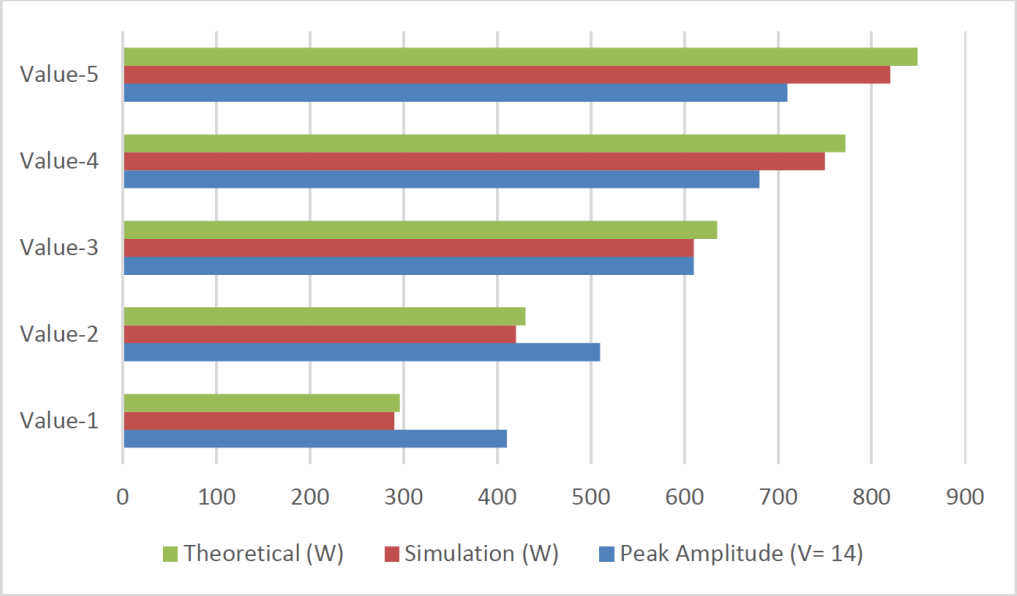

Figure 5.6 Outcome of the verifications

Finally, the simulation between the output power and the input voltage of the second active coil proves the validity of the control strategy when the radial misalignment is constant with the input voltage of one active coil. Table 5.2 and Figure 5.6 depicts the outcome of the verification. Currently, the system has a radial misalignment of 6 cm and a voltage input of 480 V to an active coil. Increases in active coil voltage led to an increase in system output power.

5.4 UAV Experimentations

The UAV's flight controller design effort, time, and expense may be considerably reduced by utilizing a commercial inner-loop control system. RDWPT-POLICY experiment prototypes have been built to test the design process proposed in this chapter. In the prototype, there are four RDWPT-POLICY channels with four Tx coils, four Rx coils, four inverters, and one rectifier. The established motor powered dynamic WPT coils are attached to the UAV's landing gear. The transmitter pad size is 17 cm x 17 cm, which includes the charging zone in the middle (8 cm x 8 cm) and the edge sliding region.

Table 5.3 The measured values for the established coils and compensations

Parameter	Value-A	Value-B	Value-C	Value-D
Cth (nF)	51.83	56.99	57.96	51.09
Lso (µH)	24.85	25.75	15.87	25.8
Lpn (µH)	228.94	227.31	226.4	228.2
Cpn (nF)	5.3	5.3	5.6	5.8
Lth (µH)	8.2	8.53	9.67	9.91
Cso (nF)	28.84	21.65	21.77	21.27

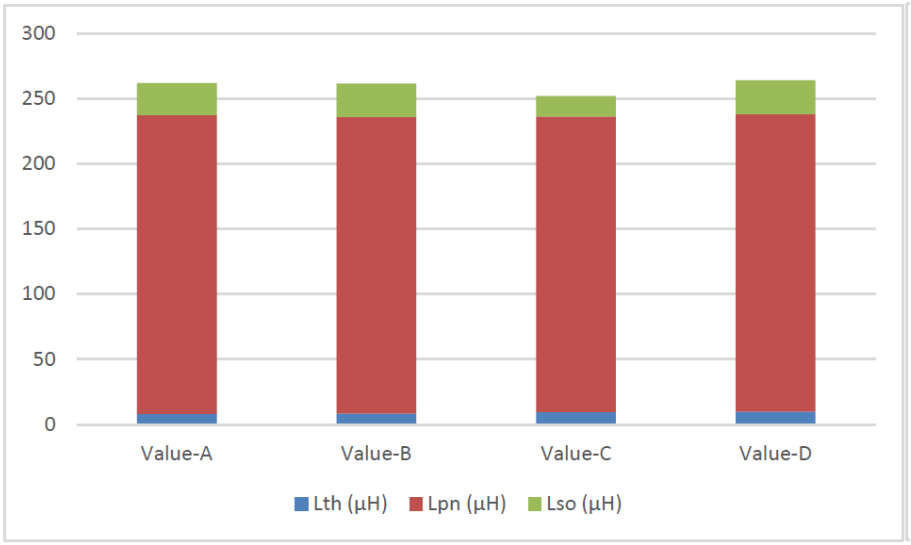

Figure 5.7 The measured values for the established coils and compensations

The source's dc voltage is 12 V. 220 kHz is the system's operational frequency, which is within the power matters alliance standard's acceptable frequency range. The airgap is 8 millimeters wide. Table 5.3 and Figure 5.7 shows the measured values for the established coils and compensations.

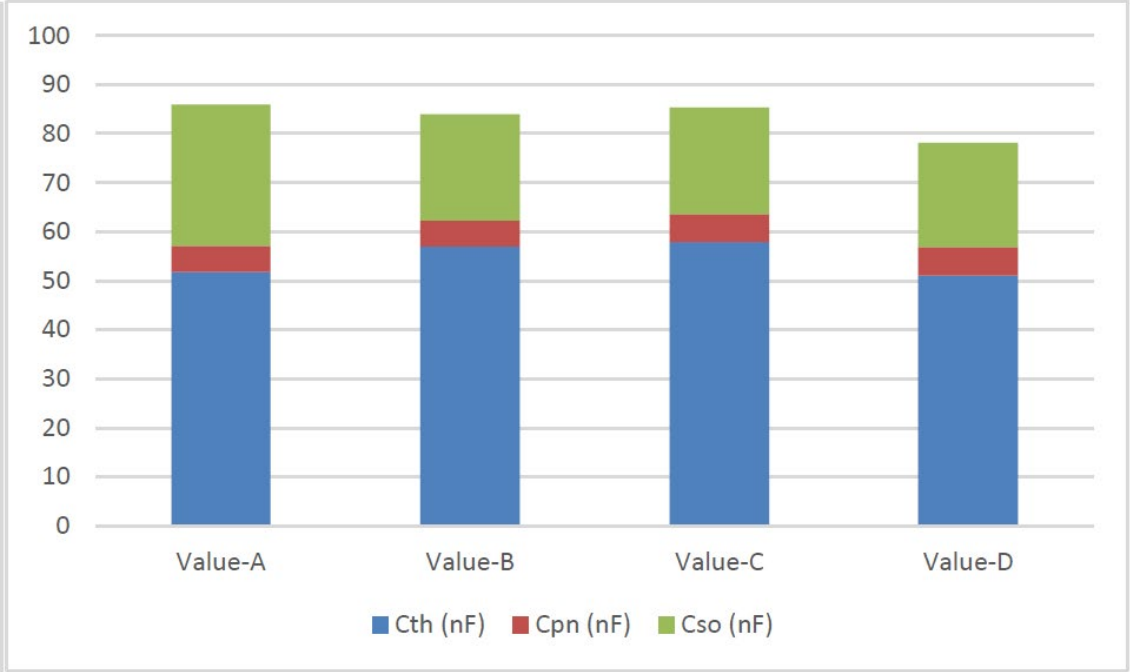

Figure 5.8 The measured values for compensations

Details of the main converters, such as full-bridge inverters, LPFs, phase comparators, sampling circuits, sensors, etc. are depicted in Fig 5.8. A phase comparator circuit is used to obtain the phase difference between voltage and current, which minimizes the cost of the processor and simplifies control. The controller uses a high-speed analog-to-digital converter to transform the phase and current signals. After that, using the estimated voltage and sampled current amplitudes, the desired gain may be readily attained. Primary and auxiliary controllers are configured with output current estimate controls. Onboard Rx switches SN are activated upon startup and during malfunctions. Cables and printed circuit boards intended to protect against electromagnetic interference (EMI) are used for signal transmission. The primary converters can also be shielded from electromagnetic interference (EMI) by adding exterior shielding metal shells.

The electronics prototyping UAV's platform Nvidia Jetson Nano serves as the foundation for this project. To avoid interfering with the onboard device's inner-loop control mechanism, this

interface provides the ability to manage the location and navigation. The ground station sends orders to the APM through the alternative micro-controller, which interprets them for the APM controlled by the Windows 10 laptop. 200 Watts WPT module with Jetson Nano embedded computer is the alternative micro-controller offered in this research. It's a Raspberry Pi and Jetson nano-based variation.

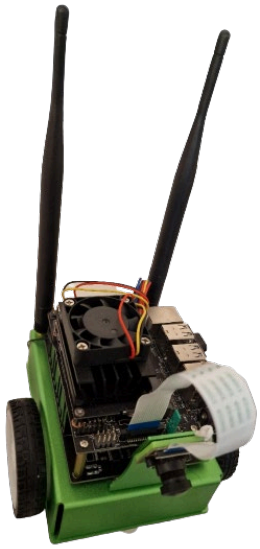

Figure 5.9 Jetson nano with camera

The Artificial Intelligence (AI) integrated arm processor is used in Jetson Nano module. Jetson Nano 's usage of the AI arm processor as its only micro-controller makes it more affordable and easier to use than previous Raspberry Pi controllers. The Jetson Nano socket and three sensor extension pins on the 200 Watts WPT module are equipped with this APM flight controller. One of the most often used AI prototyping devices is the Jetson Nano in figure 5.9.

With the socket, RDWPT-POLICY device may be directly connected to Wi-Fi and Bluetooth modules, as well as RF modules, such as the Jetson Nano. The 200 Watts WPT module board has a Jetson Nano connector. The APM is responsible for UAV inner-loop control. Different signals can be recognized by varying the pulse width modulation (PWM) pulses of the drone motor shown

in figure-42. In this example, the RC remote control sends a normal RC signal to the APM input. Using the wireless Jetson Nano link, the alternative controller installed on the UAV now generates this RC control signal, which the APM uses for self-flying flight operations.

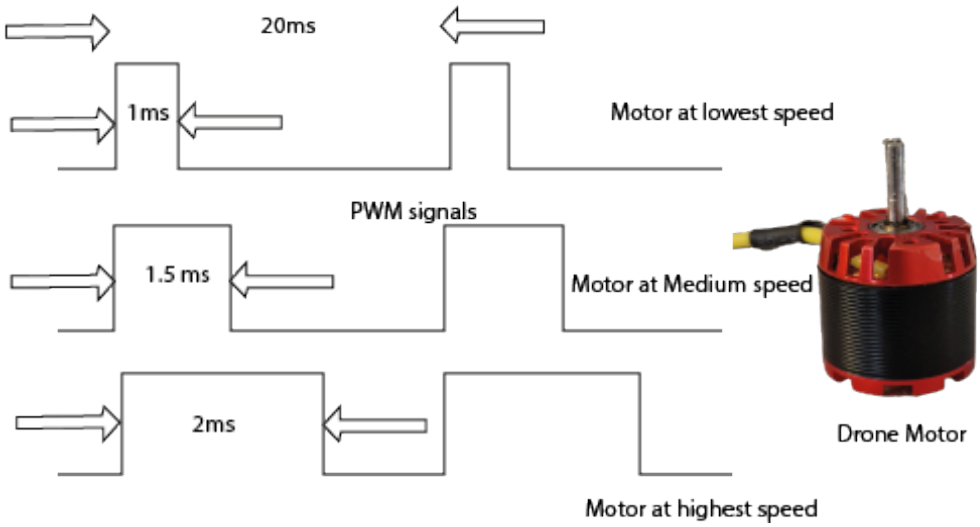

Figure 5.10 Drone PWM signals

The UAV is activated after receiving input from an alternate controller. Since the APM's extremely dependable inner-loop control cannot be disrupted in this scenario (Fig. 5.10), the construction of the UAV's flight controller may be streamlined, which saves money and time. A drone with four motors with a payload capacity of one kilogram was developed in the current study of this chapter. PI CAMERA's motion capture technology, as previously indicated, provides exact input on the location of a defined item (in this case, the hex copter) in a predetermined environment, all of which is captured by PI CAMERA cameras. The ground station can see the object's X, Y, Z, roll, pitch, and yaw position and angular data (PC). Once MATLAB/Simulink has been installed on the ground station, it manipulates the positional and angular data to generate a sequence of outer-loop inputs.

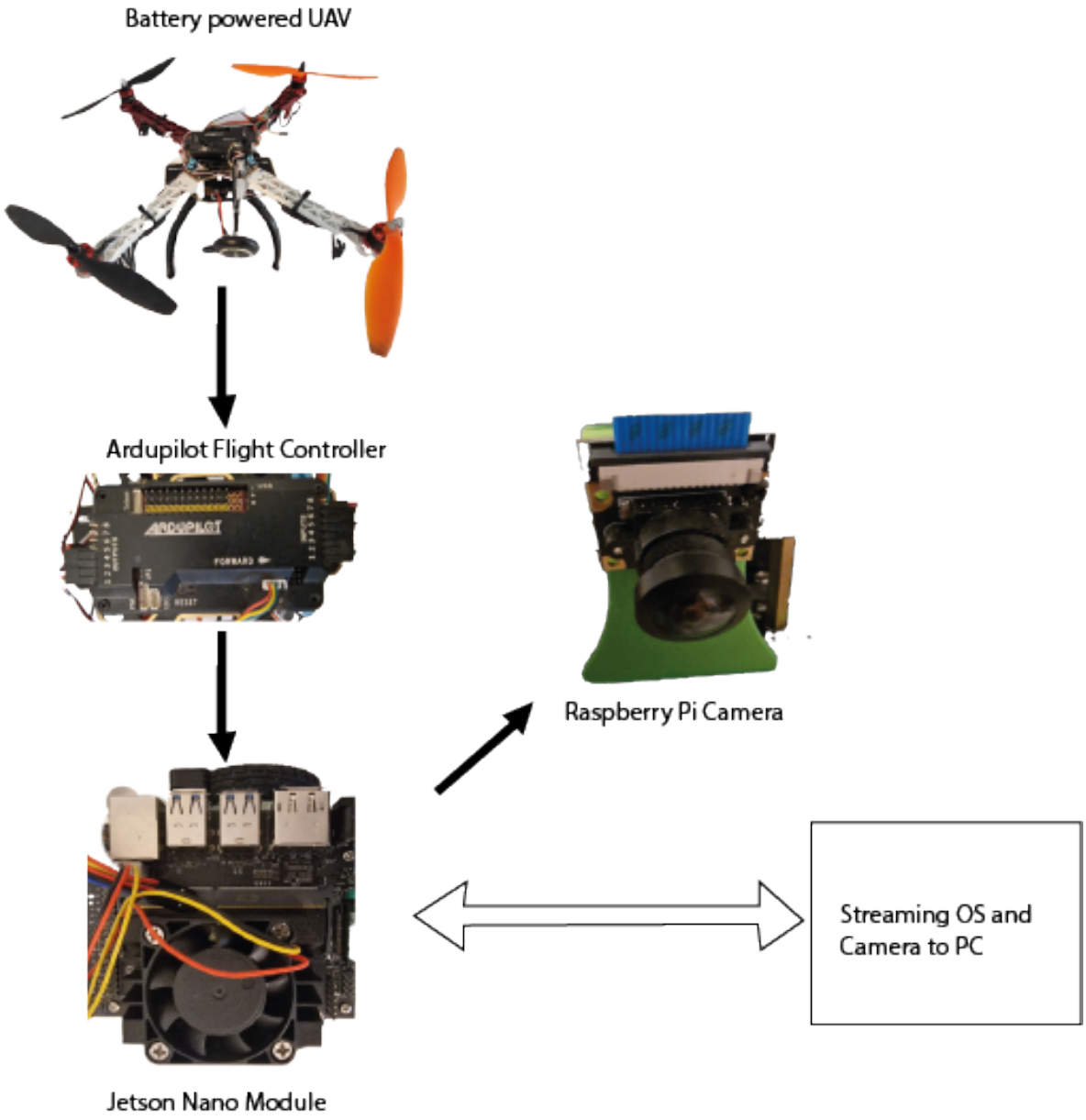

Figure 5.11 Experiment Setup of UAV

DC power manipulation is the primary focus of WPT. DC power must be converted into magnetic induction at a certain frequency. A resonator, inductor coupling, and rectification are involved in this process. Because of the magnetic field, secondary wires generate current when they are put in the field that a magnetic field may be used to drive a load.

Using non-resonant induction coupling over long distances is exceedingly inefficient since the main coil's resistive losses squander most of the power that would otherwise be delivered.

Resonant connection of the coils improves the overall efficiency of the device. Resonant coupling and power transmission are accomplished with the help of an AC source.Power may be transferred between the coils across an area many times larger than the diameter of the coils at a tolerable efficiency. Input power should be converted as efficiently as possible while minimising conversion losses in this inverter. Setting up the experiment and running the simulation.

5.5 Development of a UAV testbench

Four propellers were used in the experimental configuration of the suggested method above. Pi Camera motion capture is being used in this study with the drone equipped with reflective markers on the transmitter pad.

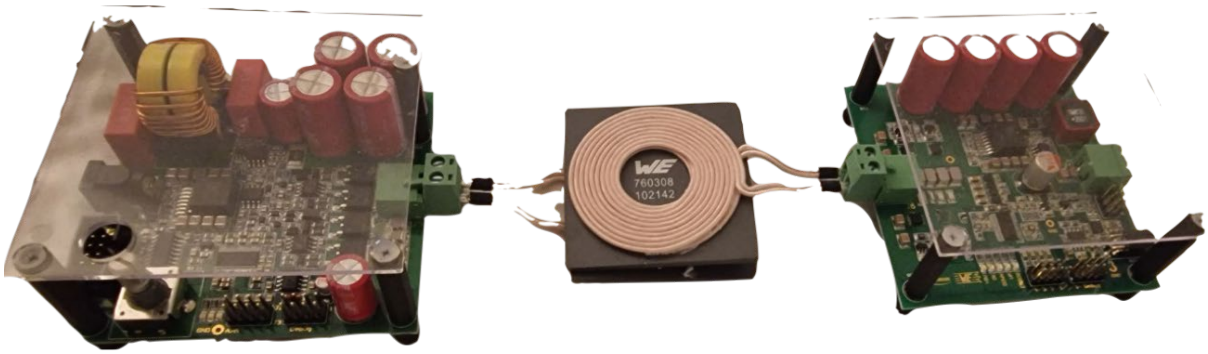

Figure 5.12 Transmitter and Receiver with 200 watts wireless power transfer Circuit Board

Using infrared cameras, the PI CAMERA motion capture system can identify moving objects in real time with a high frame and sampling rate. Drone's reflective markings are used to create an object that can be tracked with PI CAMERA. The three-dimensional (3D) environment created by cameras for the purpose of tracking a moving RDWPT-POLICY device. Using a Simulink block diagram, location data from the PI CAMERA environment may be received. The drone control algorithm uses these data to process and maintain the location and navigation of the UAV.

The inductors are connected by tuning them to a certain resonance frequency. To provide a usable DC power supply, the coupled magnetic resonant phenomena induce an AC voltage at the receiver end, which is rectified and filtered before being used. The ZVS inverter is seen in Figs. 5.12. To ensure that the circuit design described above could be implemented, simulation was performed prior to implementation. The results of the simulation demonstrate that a certain resonant frequency may be achieved in the conversion of DC power to AC power using the ZVS inverter. When the simulation was verified, the relevant circuit was built.

The size of the UAV dictates the form, size, and number of turns on the coil that will be utilized for inductive coupling. With the usual tiny UAV in mind, the coil's total size was selected between 12 and 20 cm. High-frequency Structural Simulator (HFSS) was used to simulate the construction of the transmitter and receiving coils. This program was also used to simulate the efficiency of the power transfer. Between the coils, the distance was designed to be ZVS inverter simulation scheme.

The geometry and spacing between the transmitter and receiver coils. One of the most efficient WPT configurations as a rectangular coil with a hole in the center. The resonant frequency of about 220kHz is achieved with this shape. To increase WPT efficiency, a higher resonance frequency might be employed. Further (manual and discrete) optimization was performed about the number of turns 3-8 and the size of the coil 12-20 cm. Eight coil turns with a 22-centimeter coil size had the highest efficiency (6.15 dB) among the combinations evaluated.

5.6 Autonomous charging and long-term mission control

Upon Autonomous UAV started the process of landing, the drone generates a signal to begin charging and a current sensor monitors the charging status. To determine when the charging has

been completed, the current sensor reads zero. The drone is armed and ready to fly after the charging process is completed.

The drone's real-time reaction to a Vertical-axis instruction. The drone retains its set Vertical position quite precisely, with a median value of Receiver coils are shown in 0.6 mm. The measured values are up to 0.17 m off from the mean. The drone's response to a Horizontal axis instruction while it is being provided in real time. Up to 0.193 m of deviation from the mean was found in the measured values. The drone can be seen in the figure staying within 0.4 m by 0.5 m of the required spot (0, 0). As a result of the suggested remedy, the computational cost is minimal, and the performance is enough for use in self-charging wireless devices.

5.7 Analysis of wireless energy transfer

In this section, the WPT and analysis findings are presented in terms of efficiency. There was a 12.2 V (volts) input voltage and a 14 V output voltage regulation. It took 38 minutes to recharge the drone's battery from an 8% starting charge. To compute both the input and output energy utilized throughout the process. The charging procedure uses a total of 0.98 kJ of input energy and produces an output energy consumption of 0.610 kJ. Wireless energy transmission efficiency thus comes to 62%.

Accordingly, the greater distance one must cover, the less efficient one will be when the inter-coil distance exceeds a particular threshold, the WPT efficiency is zero. In addition to the draw load, input power limits the distance at which this threshold may be crossed, causing this distance to vary. The efficiency of WPT as a function of distance as it moves horizontally. Again, if the applied load is lower or the available input power is greater, the threshold distance might be increased at the expense of efficiency. Furthermore, it has been discovered that the WPT's efficiency increases with increasing distance.

The RDWPT-POLICY efficiency reported in this study is realistic and attainable for the intended uses. According to previous studies, the suggested solution has a maximum efficiency of 71% and lowest efficiency of 31%, which is significantly better than the 41% and 58% stated in the previous studies. Note: In addition, the suggested RDWPT-POLICY solution's maximum efficiency may be raised even further by raising the resonant frequency and using an impedance matching approach (Nguyen et al., 2020a). RDWPT-POLICY findings provided here are thought to be sufficient evidence that the proposed approach is successful. The evident novelty of this research is in its application to actual unmanned aerial vehicles (UAVs). The drone might fly for considerably longer than an hour thanks to this self-charging.

5.8 Results

An electric UAV with VTOL capability utilizes a RDWPT-POLICY technology developed in this chapter. For the sake of reducing weight and size, all the on-board components have been developed using lightweight and compact materials in mind. In the design process, a two-turn secondary coil was designed and mounted on a drone landing gear. The RDWPT-POLICY system is more efficient when the primary and secondary coils have a tiny air gap between them. The ground station of a RDWPT-POLICY charging system may also be improved using a process to create an array of separate main coils. This method helps to minimize the problems that may arise from a drone landing that isn't flawless, such as coil misalignment.

The suggested RDWPT-POLICY application's validity has been demonstrated mathematically and experimentally in terms of electrical performances. It is possible to obtain strong electrical performance and excellent tolerance to coil misalignment by using the recommended technique. This is critical for the drone's battery to be automatically recharged.

Table 5.4 Electrical Performance

Pbat(W)	Vhdr (V)	ηtotal(%)	Ich(A)	r(W)	Battery Status (%)
63.4	23	81	5.2	75.7	21
68.6	25.4	83	5.1	83.9	68
76.5	27.4	87	5.1	96.2	99

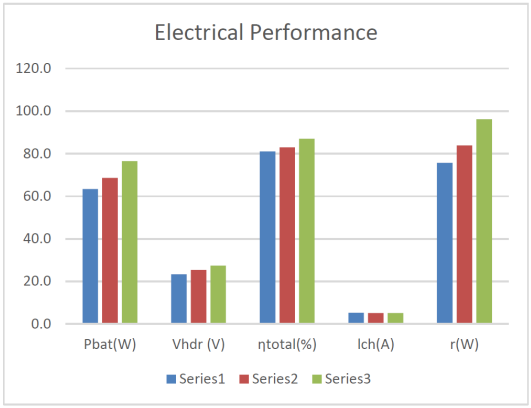

Figure 5.13 Electrical Performance Comparisons

The electrical performance shown in table 5.4 and figure 5.13 depicts the relationship between series 1,2 and 3 of the variation of the RDWPT-POLICY transceivers.

5.9 Conclusion and chapter summary

Small customized electric powered UAVs was tested on a bench proposed in this study, which can be used for a variety of UAV and ground vehicles research applications. This type of interface frequently necessitates a significant investment of time and money. The drone's addition of rotational dynamic wireless charging paves the way for long-duration missions free of human interference. The battery capacity of today's UAVs severely restricts their flight duration. Using wireless charging, the drone can recharge itself when its battery is low, allowing it to continue its task without interruption. This enables missions requiring extensive flight periods to be completed without the need for human interaction. Many drones with the capacity to wirelessly charge may

be examined, and missions can be organized such that the multiple copters fly in synchronization, resulting in a shortened flight duration. Rotational Dynamic Wireless charging, on the other hand, is more efficient if the design of its linked components can be improved. Resonant frequency and coil characteristics are the focus of this design. Reduced conversion losses, because of improved inverter design, will boost overall efficiency. Increasing the resonance frequency of the inductive connection can also enhance the wireless power transmission distance. Increase the resonance frequency of the system to improve its performance. Increasing productivity is one way to allow for a reduction in charging time by raising the charge rate. Next chapter, deep learning-based reinforcement learning Kalman Filter with RL-POLICY method will be explored to improve the flight autonomy.

6 Deep Kalman Filter and Dynamic Wireless Power Transfer for UAVs

- Chapter 6 introduces the method of Deep Kalman Filter and Dynamic Wireless Power transfer approach for UAVs charging based reinforcement learning techniques.

6.1 Abstract

Unmanned Aerial Vehicle (UAV) needs to continuously estimate its position for carrying out a safe and successful autonomous indoor flight operation. The estimation of UAV's Attitude obtained through using Global Positioning Unit (GPS) may often be unreliable due to the possibility of surrounding high-rise buildings blocking the satellite signals transmitted from earth orbits. This chapter establishes that a more reliable estimation of the UAV's attitude can be achieved through using the UAV's on-board sensors, such as the Inertial Measurement Unit (IMU) sensor and the obstacle avoiding sensors. The approach developed by the author that localizes the UAV position through fusing the UAV's on-board (IMU) sensor and the obstacle avoiding sensors to eliminate sensor noise to obtain better estimate of the UAV's attitude from the raw data unstable outputs. The methodology involves use of deep Kalman filter with sensor fusion algorithm and sensor noise cancellation algorithm. Deep Kalman filter is an improved version of Kalman filter and Extended Kalman filter which uses deep learning techniques for faster prediction. The results achieved from testing on various indoor flight trajectories proved the approach presented in this paper is better in localization and the estimation of the attitude of UAV than the approaches that use GPS.

Keywords: Attitude estimation, Kalman Filter, UAV Localization, Indoor Localization, Sensor Fusion

6.2 INTRODUCTION

Unmanned Aerial Vehicle has found widespread use in practically every part of life today; with many applications increasingly requiring its autonomous flight operation. Henceforth, it is important to be enabling UAV to fly and hover stably in air and to continuously estimate its attitude. UAVs which normally has more than two rotor propellers, has the benefits of taking off and landing vertically with high portability with basic structure and simple support. In such cases, to enhance the vehicle's security and irreconcilability, to make it fly independently or be guided physically, is exceptionally valuable. Attitude estimation is a critical piece of the control framework in UAVs and the accuracy of the attitude estimation impacts control execution altogether (W. Li & Wang, 2013). Application of Deep Kalman filter for estimation of UAV attitude using IMU sensors has been proven as an effective approach.

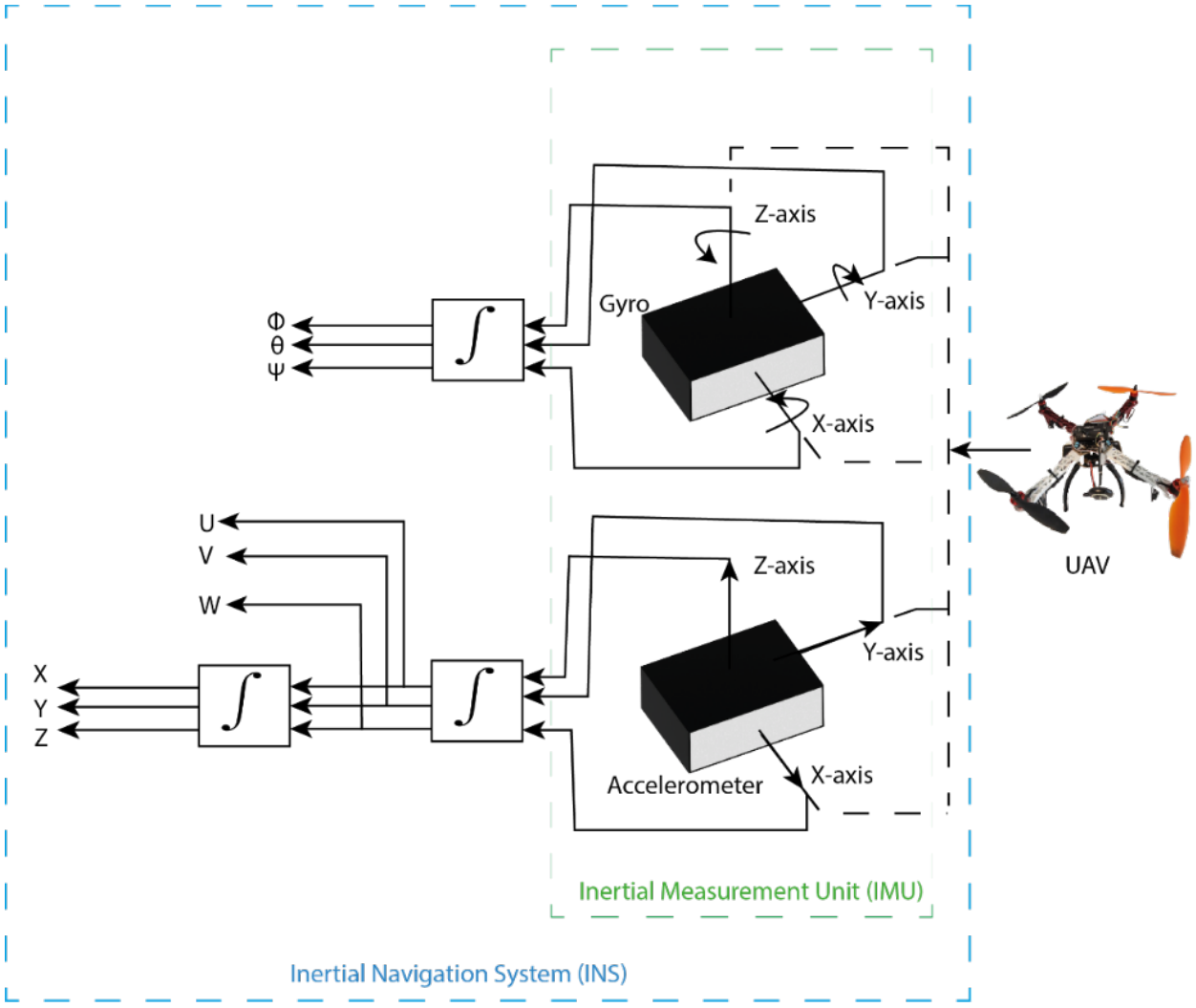

Figure 6.1 Architecture of Inertial Navigation System of an UAV

Unmanned Aerial Vehicle's indoor flight attitude estimation is a technique wherein the position and direction of the versatile robot is resolved regarding the indoor condition and is a significant piece of any autonomous self-ruling portable robot. Self-governing robot frameworks are generally being utilized during catastrophe reaction ventures as assistive UAV robots and so on. To help the compelling working of robots in such situations there is a requirement for precise and productive estimation of the attitude of indoor flight UAV and the mapping of its trajectories. One of the central difficulties in indoor flight situations is when the GPS signals are out of range. In this chapter our essential objective is to eliminate the need for UAV to rely on GPS signals for

estimation of its attitude.

Equation 6.1 General Navigation Equation

$$\begin{bmatrix} \dot{\emptyset} \\ \dot{\theta} \\ \dot{\varphi} \end{bmatrix} = \begin{bmatrix} p \\ q \\ r \end{bmatrix} \begin{bmatrix} 1 & sin\emptyset tan\theta & cos\emptyset tan\theta \\ 0 & cos\emptyset & -sin\emptyset \\ 0 & sin\emptyset sec\theta & cos\emptyset sec\theta \end{bmatrix}$$

Attitude estimation is essential for any types of unmanned aerial vehicles (Jing et al., 2017). On the other hand, it is complicated to estimate aerial vehicle's position due to issues related with the minimal effort locally available sensors. These minimal effort sensors are yet favored in UAVs because of their reduced size, little weight, and low power utilization.

$$\begin{bmatrix} X \\ Y \\ Z \end{bmatrix} = \int C_{bn}^{T}(\emptyset, \theta, \varphi) \begin{bmatrix} U \\ V \\ W \end{bmatrix} dt$$

Equation 6.2 Nonlinear model using Euler angles

The main approaches for attitude estimation are for efficient flying experience by combining the estimations of various small sensors, are right now used to make up for the sensors' course precision.

$$\begin{bmatrix} \dot{U} \\ \dot{V} \\ \dot{W} \end{bmatrix} = \begin{bmatrix} a_x + Vr - Wq + g_e sin\theta \\ a_y + Ur + Wq - g_e cos\theta sin\emptyset \\ a_z + Uq - Vq - g_e cos\theta sin\emptyset \end{bmatrix}$$

Equation 6.3

Distinctive methodologies have been used for estimation of UAV's attitude. However, when the UAV's flight time increases, the precise estimation of the UAV attitude may be difficult due to the influence of heavy wind or other natural conditions in the air. This may result in an erroneous attitude estimation. Additionally, the vibration of the UAV rotors also influences the estimation of the accelerometers. These challenges prompt the need for a more reliable and robust methodology for estimation of the UAV's attitude.

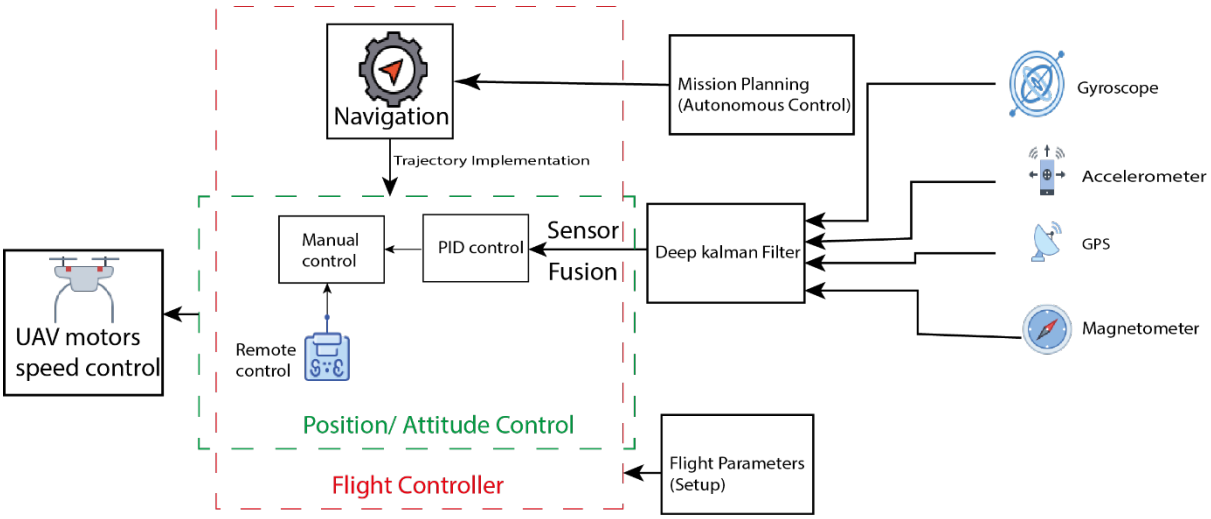

Figure 6.2 Deep Kalman filter-based UAV flight control

The main issue in relying on using any algorithm for control of small UAV, however, is the restricted precision of the raw sensors data (A. Gupta & Fernando, 2022). Furthermore, these vehicles require a greatly improved precision in the navigational estimations, only because of their little sizes. The most regular case of this issue is GPS (Global Positioning system) that is generally connected to UAVs. The precision of accessible little GPS beneficiaries is insufficient for such vehicles, whose range is limited underground areas. Consequently, the coordination of GPS with IMU through the Kalman channel is very anticipated. Along these lines, numerous scientists have attempted to build up a proper Kalman filter to address this issue (Hide et al., 2003). However, the nearness of deficiencies of sensors or actuators, which destabilizes the vehicle elements and what for all intents and purposes makes it hard to control. Along these lines, a deep Kalman filter ought to be produced separately to the issue.

IMU commercial devices reported in (S. Han et al., 2020) utilize controlled situations, for example, turntable, to gauge and eliminate precise errors. The sensor adjustment methods related with controlled condition are expensive and it can't eliminate for all environments. The methodical and irregular calibration of IMU can be assessed if the connection between these mistakes and the

perceptions are known. At the point when IMU calibrated, they are expelled from IMU perceptions and IMU situating turns out to be progressively precise. Shockingly, the previous models of IMU errors are not exact and they depend on some measurable suppositions that may not hold. For example, the traditional Kalman filters, have a few impediments that may present some issues in eliminating IMU errors. For example, the regular Kalman filter is direct and can't deal with non-linear model. As of now, researchers recommend displaying IMU's errors independently. In this chapter, we acquaint the deep learning based Kalman filter with at the same time experimented with IMU sensors errors. As opposed to recently proposed methodologies, our methodology uses learn from its mistake method. As opposed to recently proposed approaches, we can precisely show non-straight, time-variation, exceedingly related IMU mistake sources.

6.3 Contributions

The following is a summary of the chapter's key contributions:

1. The proposed reward function is based on a sensor error in location estimation. Using this method, the gradient computation is simplified.

2. Experiment the proposed method using a wide range of real-world data. Under a wide range of conditions, the experimental findings show that the suggested UAV WPT system achieve great performance in terms of location, velocity, and course angle.

The proposed method also provides several existing adaptive navigation algorithms in the discussion of this topic. Our experimental assessment and comparison with other traditional Kalman filter approaches.

Table 6.1 Deep Kalman Filter

Field	Symbol	Description
Kalman filter	δx	Error state in the prediction phase
	P	The covariance matrix of the predicted error
	δz	Error state obtained from the measurement
	H	The observation matrix
	Q	Process noise covariance matrix
	R	Measurement noise covariance matrix
RL	s	State of RL, which is defined as the value of the current process noise
	α	Action of RL, which is defined as the change of the current process noise
	r	Reward of RL
	E	Environment of RL
DDPG	θ^{μ},$\theta^{\mu\prime}$	The parameters of Actor network
	θ^{v},$\theta^{v\prime}$	The parameters of Critic network
Sensors	ω_t^{IMU}, α_t^{IMU}	Gyroscope and acceleration output at time t
	r_t^{IMU}	The predicted position at time t
	r_t^{RTK}	The measurement position at time t

6.4 SYSTEM OVERVIEW

Before discussions of the methodology of this chapter, UAV robot parts are initially presented with its framework, and its sensors. The UAV's type is a quadcopter and independent light weight robot. And its using Raspberry Pi, Navio 2 flight control unit and ultrasonic sensor. To estimate the position of the UAV, IMU sensors are installed in the center of the UAV for best estimation. It must be noticed this is a motor driven drone and motors speed is controlled by Electronic Speed Control unit (ESC). The IMU sensors furthermore give us an estimate of the UAV's direction. Ultrasonic and IR sensors are inserted on either feature in front of the UAV. Each sensor returns the separation between the obstruction and robot. This record serves to offer us with an additional control in indoor flight operation.

Among navigation options, odometry and inertial navigation are cheap and don't need any infrastructure. IMU sensors' error characteristics are complex. They vary to a different varieties maker's technology, and sensor. The less noise IMU (Y. Liu et al., 2022), however it is pricey and not appropriate such as mapping. The procedures connected with surroundings are pricey and errors cannot be completely removed by it. In the association between also the observations and

these mistakes are understood IMU's random and systematic errors could be estimated. These mistakes are approximated using this procedure and IMU error versions is named IMU calibration when GNSS positioning can be obtained. They're eliminated from IMU observations when IMU mistakes are estimated and IMU positioning becomes even more precise.

Additionally, Bayes filters, like particle filters and the Kalman, have some constraints which could introduce error. As an example, the Kalman filter can't handle error resources that are non-linear and is linear. Compared to previously proposed strategies, the proposed strategy doesn't have any IMU error version that is pre-defined, and it are heard from observations. The system doesn’t have to presume some deterministic or stochastic behavior of IMU mistakes. Compared to previously proposed strategies, it could be simulated, time variant IMU error resources that are non-linear. Then, it will be united with the detectors using Sensor fusion algorithms to use the position of UAV.

6.5 Sensor Fusion Filters

6.5.1 Kalman Filter

Using Kalman filter for object detections, sensor fusion, and attitude estimation in unmanned aerial vehicle. The filter can also make prediction with past performance of the inputs. There are two types of tracking method which are continuous estimation and discrete estimation. Discrete estimation is multi-model and continuous estimation is uni-model and the comparison is shown in figure 6.3. Kalman filter estimate the state using continuous estimation method.

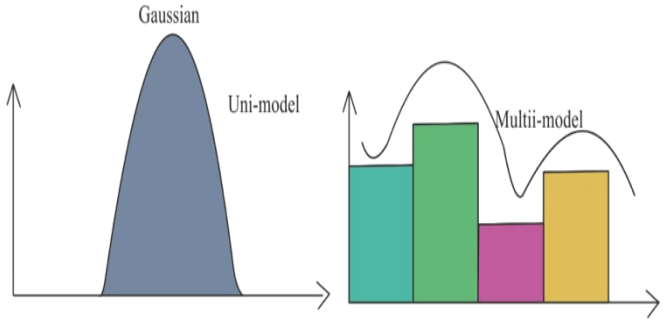

Figure 6.3 Uni-model and multi-model comparison

There are two parameters of Gaussian characteristics such as Mean (μ) and Variance (σ^2) which represents height and width. The one dimensional for Gaussian Kalman filter in figure 6.4 is defined by below equation.

Equation 6.4

$$f(x) = \frac{e^{-(x-\mu)^2}/2\sigma^2}{\sqrt{2\pi\sigma^2}}$$

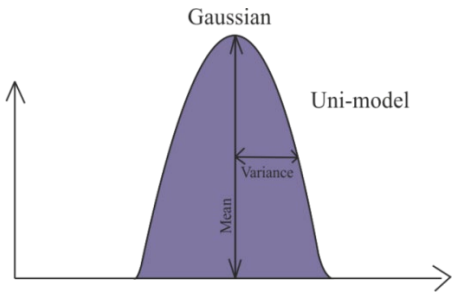

Figure 6.4 One dimensional Gaussian Kalman Filter

In figure 6.5, variable Gaussian transformed into predicted Gaussian which is closer to measurement position and peak is a little above measurement position Gaussian to get real time data.

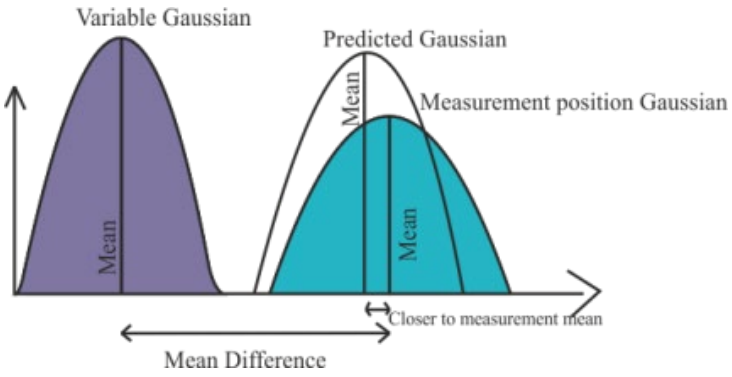

Figure 6.5 Predicted Gaussian

To find the predicted value, we can use below equation to find new mean and new variance

Equation 6.5

$$\mu_3 = \frac{\sigma_2^2\mu_1 + \sigma_1^2\mu_2}{\sigma_2^2 + \sigma_1^2}, \sigma_3^2 = \frac{1}{\frac{1}{\sigma_2^2} + \frac{1}{\sigma_1^2}}$$

Where,

μ_1 = original variable mean

μ_2 = Measurement position mean

μ_3 = Predicted mean

σ_1^2 = original variable width

σ_2^2 = Measurement position width

σ_3^2 = Predicted width

6.5.2 Deep Kalman Filter

Our goal is to predict and update sensors for indoor UAV flight estimation using Deep

Reinforcement Learning based Kalman Filter. The use of Deep Kalman Filter (DPF) shows significant increase in the process of sensor fusion method by eliminating most of sensor noises. For nonlinear indoor UAV flight operation, the system needs to estimate its position by fusing IMU sensors and ultrasonic sensors were GPS signal weak or unavailable. In tradition Kalman filter system, UAV's inertial measurement unit noises influence on other different environment conditions such as extreme hot or cold, but these conditions cannot be detected automatically. For the type of estimations presented in this chapter, the latent state vectors of measured raw sensor data from IMU and Ultrasonic depends on each other state vectors to estimate UAV's positions. So, these vectors work in opposite way with a stochastic process (future states influence upon present states) which was used with other tradition Kalman filters methods. The first modelling process of this chapter presents that the state estimation of indoor UAV's estimation by sensor fusion algorithms and the second process be training and testing of this tuned sensor data in deep learning frameworks for better estimation without using GPS sensor data. The difference between machine learning and deep learning is that the machine learning used for linear operation where input data is known when modeling the networks, but deep learning completely based on nonlinear operations. Our approach simplifies the Kalman filter approach with better estimation over time with deep learning frameworks.

6.6 Materials and Methods

The proposed system included Dynamic Self-Learning Kalman Filter (DSLKF) for UAV navigation using reinforcement learning techniques shown in figure 6.6 below. The system estimates the sensor Noise Covariance Matrix (NCM) based on self-adaptation method.

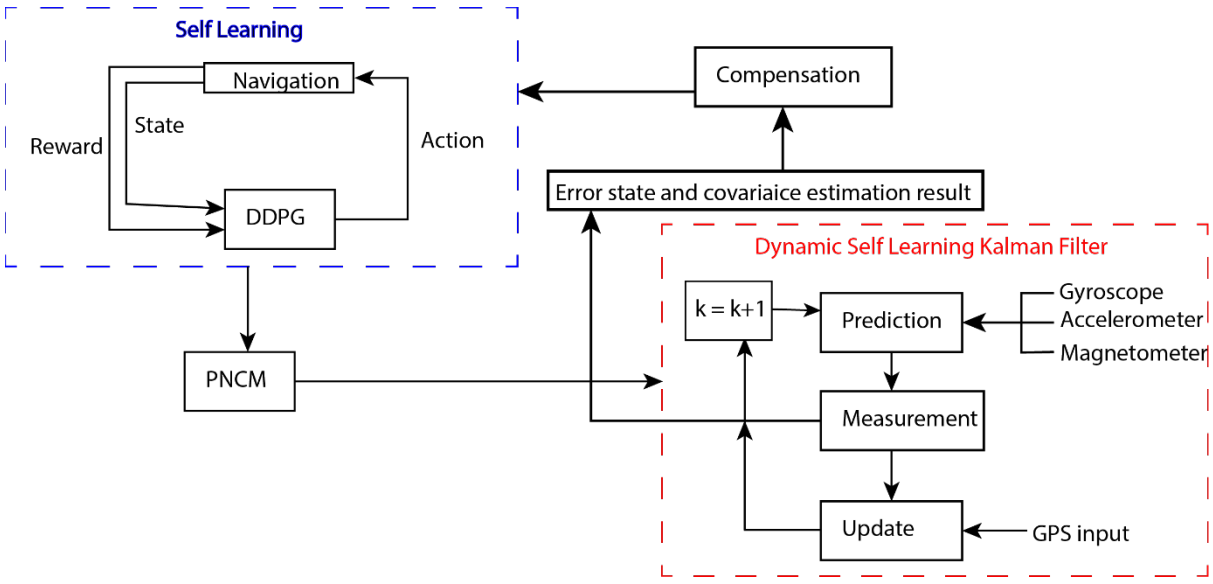

Figure 6.6 Dynamic Self-Learning Kalman Filter (DSLKF) for UAV navigation using reinforcement learning techniques

The DSLKF method is based on the notion of adaptively changing the NCM to achieve high-accuracy placement of the integrated wayfinding system. The inputs included gyroscope, magnetometer and an acceleration which is usually called Inertial Measurement Unit (IMU) are obtained at each sensor data update time by the procedure. In the DSLKF module, based on the starting state and the initial state covariance matrix (SCM), the prediction error state is calculated. To acquire the final error state estimate result, the DSLKF will perform a measurement update if GPS data are currently present. In this case, the current location approximation result is obtained after compensating from the inaccuracy of the sensor data. The initiations of the proposed algorithm, the NCM details are sent using tuned sensor data of the previous output of DSLKF.

The proposed algorithm that regularly observing if the GPS positioning state is available which is necessary since the wayfinding results have high accuracy but require multiple details about UAV flying territory. This system can determine the wayfinding inaccuracy of the present Kalman-filter

system if NCM error is observed. Different variance in NCM leads to incorrect Kalman-filter values if the estimated error is higher than the threshold. It next gathers gyroscope, accelerometer, magnetometer, and GPS sensor data near the present instant, does self-learning of the NCM process, and ultimately returns the learnt data into the preceding sensor-fusion method for UAV. The system also updates online using dynamic self-learning Kalman filter, the goal is to reduce the location error of gathered data by learning the NCM process. The necessary components of reinforcement-learning consist of agent (UAV model), environment (flying environment), state (UAV's position), action (flying from one state to another) and reward (each action gave better reward if fly properly otherwise bad rewards).

The initial state is represented by the value R0. There are several qualities that make it possible to characterize the system as an MDP where operator actions affect the value of rewards. Finding good strategies for ramping-up observable states, from which we can also derive the learnt ideal state, is made possible by machine learning by capturing relationships between actions and reactions.

6.6.1 Environment Definition

As a projection and integral operation, inertial navigation may be described as such. Over time, its navigational errors mount up. Due of accuracy divergence, Inertial Navigation System (INS) must be used in conjunction with other navigation and positioning systems. It is possible to increase navigation accuracy and redundancy by utilizing the complimentary information offered by several sensors. The selection of a suitable optimum estimate technique necessitates the successful integration of data from many sensors.

6.6.2 Forwarding INS mechanization

The alignments of the location (r0), velocity (v0), and attitude (0) must be completed to initialize

the INS system. An orientation alignment is done using either stationary or in-motion approaches, and the first two may be derived straight from the GNSS measurement. The forward INS mechanization algorithm has been thoroughly examined (Chiang et al., 2013). Using time tk1, gyro meter, it is possible to determine the attitude, velocity, and location of the inertial measurement unit (IMU) at time tk using these inputs.

6.6.3 Error Model based on Kalman Filter

The link between the prediction and measurement, i.e., rRTK k, is described by an error model in our navigation system. At this point in the prediction process, the error state vector is specified as:

Equation 6.6

$$\delta x = \begin{bmatrix} \delta r^T & \delta v^T & \phi^T & b_g^T & b_a^T & s_g^T & s_a^T \end{bmatrix}^T$$

This may be stated as follows: where the error in location, velocity, and attitude is represented by:

Equation 6.7

$$\begin{aligned} \delta r &= [\delta r_N \quad \delta r_E \quad \delta r_D] \\ \delta v &= [\delta v_N \quad \delta v_E \quad \delta v_D] \\ \phi &= [\phi_{\text{roll}} \quad \phi_{\text{pitch}} \quad \phi_{\text{course}}] \end{aligned}$$

6.6.4 Feedback Correction

Navigating at low latitudes is straightforward because of the error compensation:

Equation 6.8

$$r_k^{IMU} = \hat{r}_k^{IMU} + \delta r_k$$

6.7 State System

For example, Wk is a 21x1-dimentional process noise vector and Q is its covariance vector. Using the manufacturer's calibration data, State system shows the meaning and beginning value of each noise component.

6.7.1 Positive for NCM

This criterion cannot be satisfied with the existing mechanism of state transition. We rewrite the computation procedure of Q to ensure that the new state always meets this requirement.

The current Wk is used to define the state will be stated as follows when a new action is taken:

Equation 6.9

$$Q' = E[e^{W_k + a_k}(e^{W_k + a_k})^T]$$

Agent System

Instead of relying on a Q(s, a) table, we want an algorithm that can select the best course of action from a continuous space.

6.7.2 Action generation with DDPG

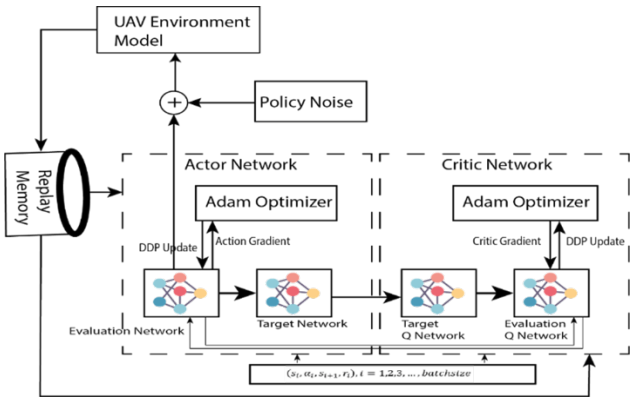

Figure 6.7 Agent generation with actor and critic

Equation 6.10

$$(s_i, \alpha_i, s_{i+1}, r_i), i = 1,2,3, \dots, batchsize$$

The DDPG performs a certain time step for each episode. When the ACTOR module selects ai at each time step. Next, the weight of the network is revised in preparation for the following round of computations.

Low-dimensional observations have been used to demonstrate the method's ability to develop effective policies for a variety of activities. The upcoming section will examine the deep learning for actor and critics.

6.8 Deep Learning for actor and critics

Two completely interconnected networks are the actor assessment and target networks. The input layer has a size of 19 and the hidden layer has a dimension of 41, after which a ReLU activation function is used. Finally, we can get the desired response by activating the output layer neurons with a tanh activation function. A dimension of 31 is the input dimension. Hidden layers h1 and h2 are learned by state and action inputs, respectively, over time. An activation function called ReLU is then employed to extract the value of the buried layer.

6.9 Results

6.9.1 Evaluation Metrics and Compared Methods

In this chapter, the application did an error computation in comparison with the integrated navigation results. The evaluation may be achieved at any moment, meeting the accuracy requirements of this method.

Position error is calculated in two separate modules in the RL-AKF technique. The calculation here is the difference in latitude and longitude between two points. After calculating each Q

matrix's anticipated positioning error, the reward is the negative number of the positioning error. Position error calculation methods are unified in the references. For example, 8 seconds, 18 seconds, and 58 seconds are all examples of time-based statistics. For distance-based statistics, such as 80 metres, 180 metres, and 280 metres could be used.

The formula for calculating position error uses latitude and longitude as inputs, with the subscripts true and pred serving as placeholders for the actual value and expected value, respectively.

Equation 6.11

$$e = 2 \times a \times \operatorname{asin} \sqrt{\sin^2\left(\frac{la_{\text{pred}} - la_{\text{true}}}{2}\right) + \cos\left(la_{\text{pred}}\right) \times \cos\left(la_{\text{true}}\right) \times \sin^2\left(\frac{la_{\text{pred}} - la_{\text{true}}}{2}\right)}$$

Finally, the proposed system come up with the following testing strategy.

1. Use the Kalman filter with the current NCM.

2. The GNSS measurement update is skipped for 10 seconds between 80 and 90 seconds to mimic a lost GNSS signal.

3. Step 3 must be repeated until the IMU or GNSS signal is limited.

6.9.2 Data collection and Training

We used sensor raw input data from the UAV as well as data from the open-source flying drone data to create training data.

6.9.3 Experiment Setup

Our suggested approach is described in depth in this part, which includes information on the context in which it will be used and how it will be put into practice. We use the TensorFlow module in Python3.5 to implement the whole procedure noise covariance matrix adaptive estimation.

Equation 6.12 contains the default Q matrix value for the current condition. There are two upper and lower bounds for current actions, which are created by the state through an action assessment network. In addition, the algorithm will tack on zero-mean, two-variance Gaussian noise to the projected outcome. Configuration of these parameters is done in the following manner:

Equation 6.12

$$U_p = [0, 10^{-7}, 10^{-9}, 10^{-13}, 10^{-9}, 10^{-10}]$$
$$L_p = [0, -10^{-8}, -10^{-10}, -10^{-14}, -10^{-10}, -10^{-11}]$$
$$\sigma^2 = [5 \times 10^{-8}, 5 \times 10^{-8}, ,5 \times 10^{-10}, 5 \times 10^{-14}, 5 \times 10^{-10}, 5 \times 10^{-11}]$$

The testing platform is built on a Windows 11 64-bit Intel Core i7-11800H processor with computer. 4.6 GHz is the primary frequency of the CPU. GPU is GeForce RTX 3070 8 GB GDDR VRAM. The memory is DDR4 and has a capacity of 16 GB.

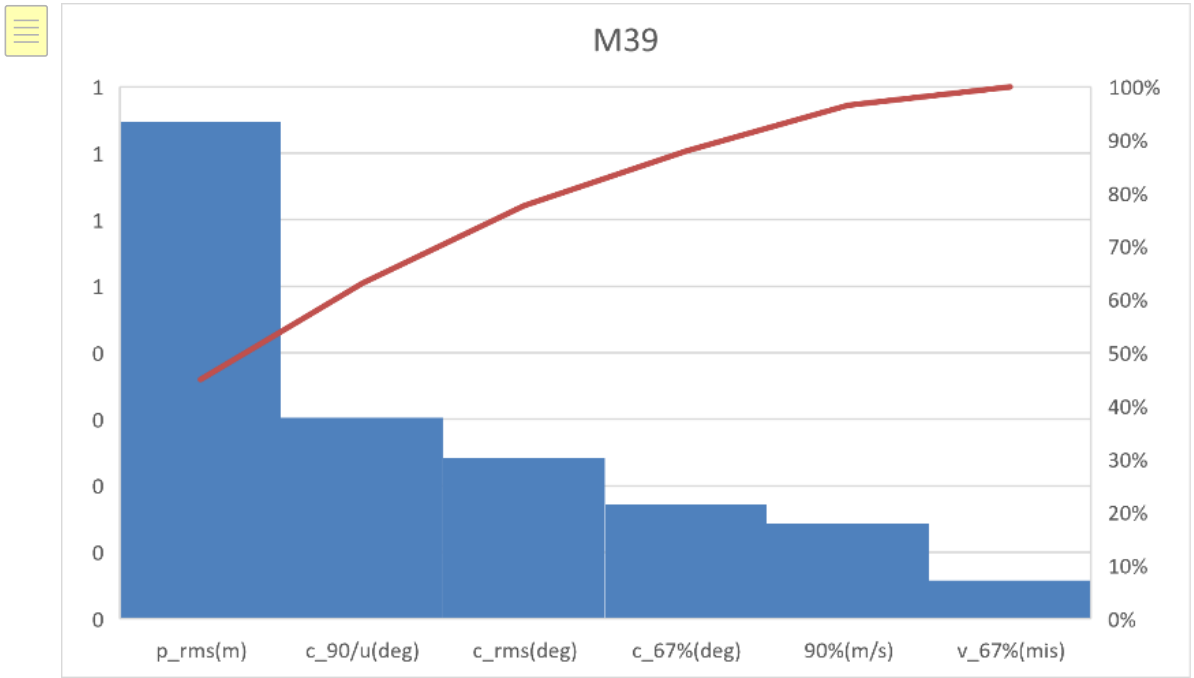

Figure 6.8 M39 Performance

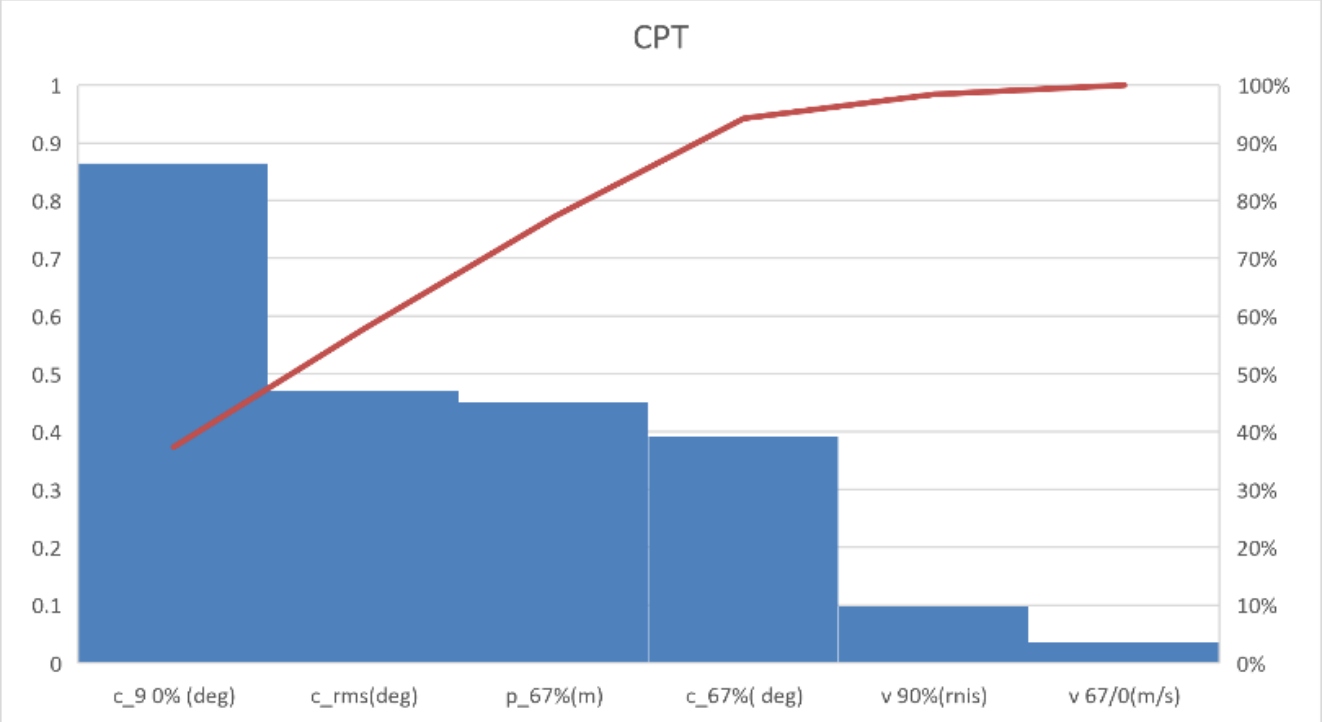

Figure 6.9 CPT performance

This RL-AKF algorithm's final Q matrix value, with training time indicated in the last column. It takes roughly twice as long to train M39 compared to CPT equipment because of its high sampling frequency.

Training time rose by 28.52 percent when the duration was raised to 280 seconds, however the placement error decreased by just 0.85 percent throughout this time span. SPAN-CPT yields a similar outcome in this case as well.

Training sequence duration has a direct influence on memory needs for embedded platforms. IMU's data collecting frequency, for example, is 60 Hz when using SPAN-CPT equipment. There are three types of data in each collection: time, acceleration, and gyroscope.

A 180-sequence-long Q matrix was used to train our current inertial sensor device's calibration model, which was then compared to the positioning accuracy and training time/storage

requirements.

To evaluate the results, this chapter focused on different approaches which is estimation of Kalman filter and deep learning based on Kalman filtered sensor data. The UAV equipped with cloud internet to send data into the computer system where deep learning operations can only be done because of the usage of processing data for deep learning operation is extremely high. The results concluded that the proposed system is the best optimized the system with improved accuracy of indoor UAV estimation without the need of GPS signals.

6.9.4 Accuracy

Latest UAV sensor data were collected using M39 to see if the training results will hold up over the course of time. This path is very level and has less turns than the data route on July 10, which is quite a contrast. The GNSS antenna is unplugged three times during the data gathering procedure, which is more consistent with the real-world positioning situation.

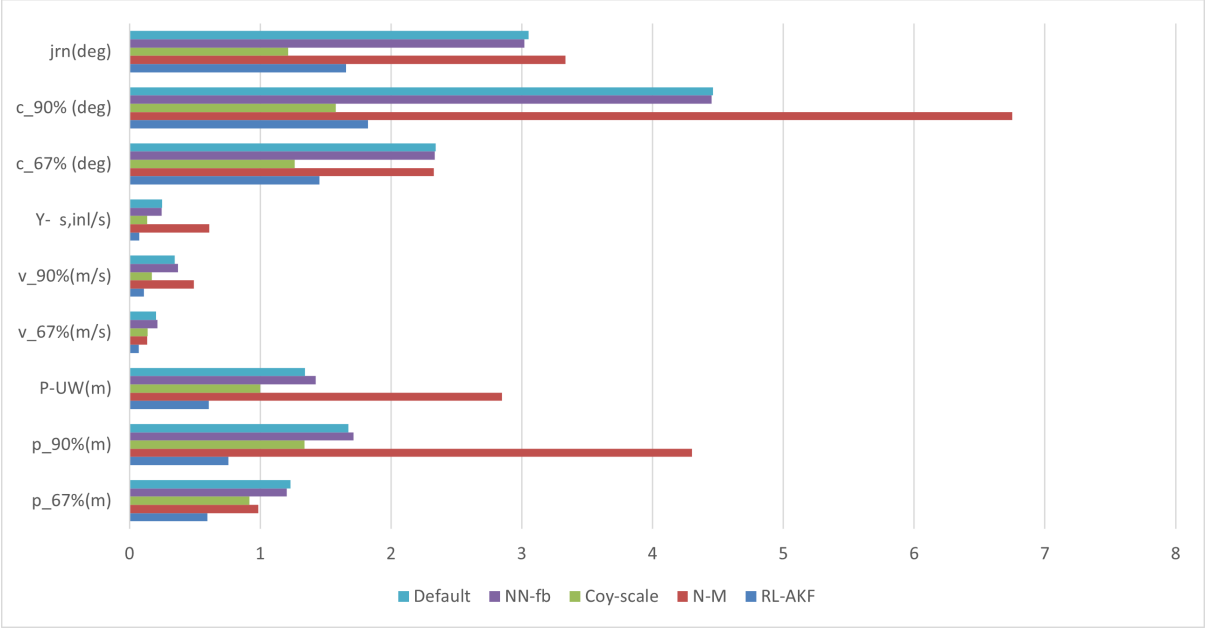

Figure 6.10 RL-AKF has the best overall performance

There is still a sub-meter degree of positioning inaccuracy, according to testing data. Both the forward and rightward position faults appear to be flat. To see the positioning findings beneath one stretch of the route, go no further than the figures 6.10. The lack of a GNSS measurement update is used to mimic GNSS signal loss during the blue triangle periods.

Our suggested RL-AKF has the best overall performance, as shown by the results of the experiments. To put it simply, the default process noise covariance matrix is as good or better than any of the NN-feedback algorithms tested. Even though algorithm's estimated course error is slightly lower than the RL-AKF algorithm's, the latter still surpasses the former when it comes to estimating location and velocity.

6.10 Discussions

It's clear from the proposed research that the used algorithm's primary benefits include the three points listed below. A more precise location, velocity, and course estimation may be achieved by using the RL-AKF approach compared to other current methods. An adaptive covariance matrix for Kalman Filter (RL-AKF) may be generated using various data, making it appropriate in a variety of applications.

When no additional measuring aids are present, pure inertial navigation has a 10-second inaccuracy of 0.475 m. To put it another way: if you use the average air speed of 22 kilometers per hour, as a benchmark, it can be determined that the overall location inaccuracy. The UAV displacement after 2800 m of flying cannot exceed 8 m, as measured by the odometer. The high-accuracy and continuous location requirements in challenging environments like lengthy tunnels and dense forests can already be met through integrated navigation.

Temperature affects the process noise covariance matrix. However, for a brief amount of time, the

temperature won't vary that much. The sensor's intrinsic performance will be reflected in the covariance matrix, thus there will be little change there either. On the ground in the real placement scene there is also an odometer, empirical measurements, and opportunistic measures like zero restrictions.

Kalman filters can benefit from velocity detection. This algorithm's process NCM accurately anticipate the navigation state during inertial navigation phase. In the Kalman filter, the RL-AKF method may be used to increase or reduce the number of distinct measurements.

However, the RL-AKF algorithm has certain drawbacks. Even though its robustness decreases the RL part's training frequency. In addition, the technique necessitates the storing of 180 s of IMU and GNSS data on the integrated navigation device, which increases the device's storage requirements. Our future effort will focus on optimizing and improving these two features.

6.11 Conclusions and chapter summary

It is possible to greatly increase the integrated navigation's positioning performance when the IMU signal is unavailable in this chapter. Experiment findings show that employing the NCM process using reinforcement learning computed from presented technique may provide reliable location prediction, regardless of time, IMU outage time periods, or navigation fusion approaches. Orientation quotes from obstacle avoidance methods are fused using the orientation quotes of the gyroscope. Our experiments have demonstrated that using gyroscopes as and if needed and using the data the place accuracy enhanced. It's seen that because surroundings have challenges, and UAV must navigate them around. Next chapter will be focus on the design of vision-based object detection using deep learning for reliable autonomous charging technique.

7 Design of vision-based object detection using Deep Learning for reliable autonomous charging of UAV

- Chapter 7 presents vision-based object detection using deep learning for reliable autonomous charging of UAVs

7.1 Abstract

This chapter is concerned with the application of Deep Learning techniques for analyzing image data for operations such as search and rescue, 3-D mapping of Unmanned Aerial Vehicles (UAVs). For intelligent charging of UAVs in air, vision-based object tracking system is needed to find the transmitter using deep learning techniques and hover above it charge efficiently. Using deep vision method to localize the charging station whenever there is low percentage in the usage of battery while UAV in operation and automatically execute the process of powering it. With the advancement in inexpensive hardware such as Jetson nano, Raspberry pi which connected with a camera, it is plausible to use pretrained deep learning techniques on board with UAV sensors and actuators. The proposed system uses Keras and its TensorFlow backend to model a deep Convolutional Neural Network (CNN) Learning technique and train the model with input image dataset of transmitter to predict the WPT device from the image data received from the ground level. This chapter also explains the stages involved in the implementation of LeNet method of Deep Learning techniques for developing a classifier for long distance recognition of wireless transceiver. It is shown in the present investigation that drone path planning controller are used with the connection with autonomous object detection methods. An experimental test was conducted on a custom-made quadcopter and identify the ground charging station to confirm the effectiveness of the designed system. Multiple tests were implemented under a variety of conditions. Using the suggested approach, the drone was able to locate the charging station and

charge safely.

Keywords—Deep neural network; deep learning; convolutional neural network; MNIST; Lenet; image processing; unmanned aerial vehicle; Tensorflow; Keras

7.2 Introduction

The use of unmanned aerial vehicles (UAVs) for non-military purposes is on the rise (S. G. Gupta et al., 2013) like catastrophe recovery and security measures. A tremendous growth in the usage of unmanned aerial vehicles in search and rescue efforts has occurred during the last three years, particularly in the maritime and mountainous regions (Howard, n.d.), (Klemas, 2015), (H. Li et al., 2014), (Nonami et al., n.d.), and (Pereira et al., 2009). To maximize the odds of the victims' survival, the primary goal of a search and rescue (SAR) operation is to locate and rescue the intended victim as quickly as feasible (Szegedy et al., n.d.). For effective and quick identification, and, for long distance recognition of images, UAVs need to be equipped with intelligent devices and systems that can help them quickly recognize the images from long distances (Colomina & Molina, 2014).

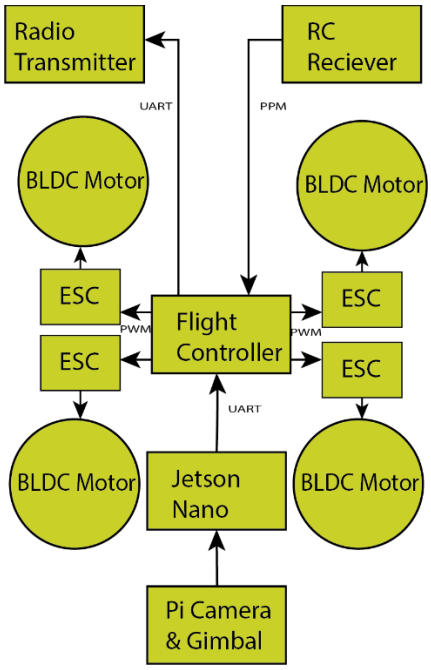

Figure 7.1 Block diagram of the proposed system

Many fields of engineering have investigated how to recognize objects and features in digital images, a process known as image recognition or object recognition, with many types of algorithms being developed to facilitate these processes, for example, images may be recognized by using image recognition algorithms When it comes to OCR (optical character recognition), matching, learning, or pattern recognition algorithms that depend on appearance or feature-based approaches are often used.

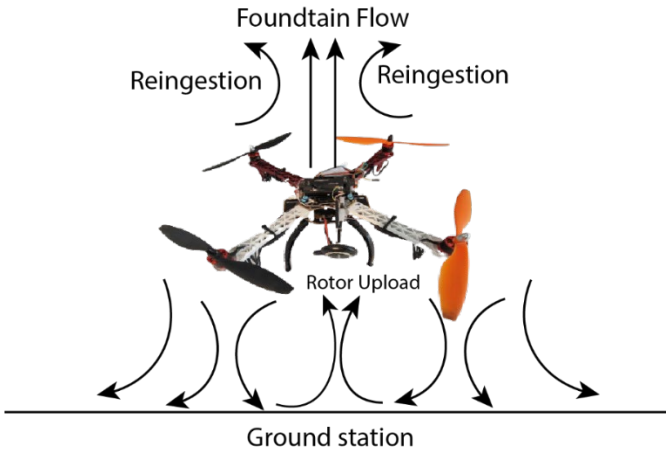

Figure 7.2 Drone thrust force under in-ground effect

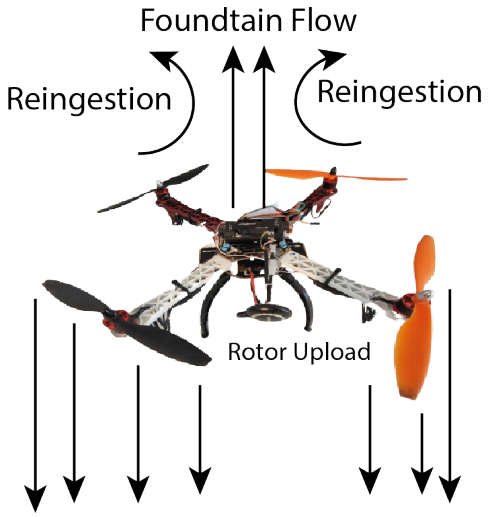

Figure 7.3 Drone thrust force under out of ground effect

Current development in image recognition or processing involves object detection with trained data set. It is called machine learning (ML), It makes it possible for AI systems to gain knowledge from data. ML can now be part of image processing (Simonyan & Zisserman, 2014). The currently available Machine Learning algorithms can facilitate the three types of learning are super-vised, unsuper-vised, and reinforcement-based. Algorithms in supervised learning are given a dataset that includes a set of features. Each sample is also given a label or target value. The information is

contained in this feature-to-label mapping of goal values. Once the algorithm has trained, it should be able to identify the proper labels or target values for unseen samples based on their attributes. It is a subclass of machine learning techniques known as deep learning, which is used to generate complex notions out of smaller ones.

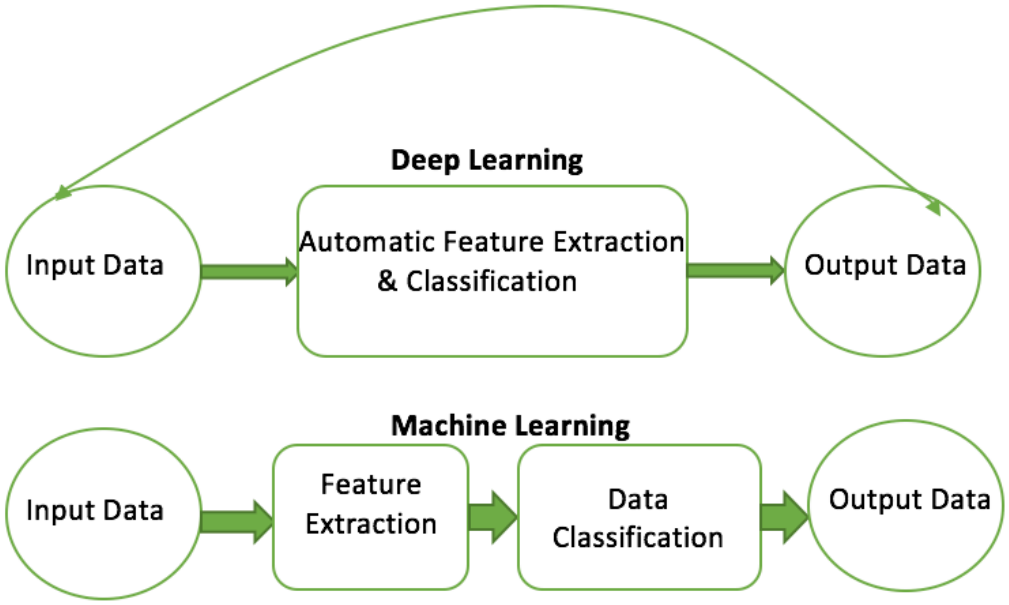

Figure 7.4 Deep learning vs Machine learning

Robotic challenges ranging from perception, planning, localization, and control may be solved using deep learning, which has lately shown impressive results (Schmidhuber, 2014). Image processing applications benefit greatly from its outstanding learning capabilities from complicated data obtained in actual scenarios. Fig. 7.4 compares the working of Deep Learning vs Machine Learning.

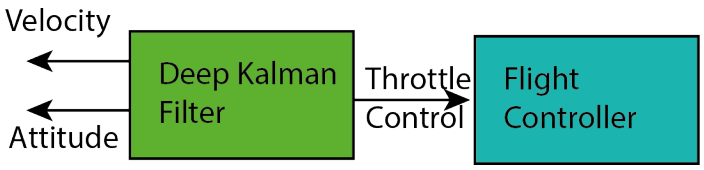

Figure 7.5 Block diagram of a deep Kalman filter based controller

As shown in Fig. 7.5, the deep Kalman filter approaches worked in a way that required the first attempt at a feature extraction method, and it was hampered by a lack of precision and required a lot of complicated arithmetic (complex design). After that, you'll need to create a comprehensive classification model to categorize your input based on the characteristics you've retrieved.

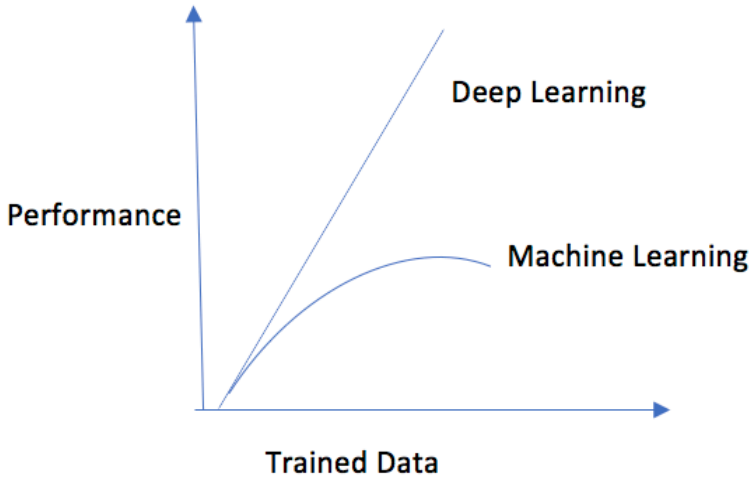

Figure 7.6 Performance comparing of two models.

Feature extraction and classification may be done in one step using deep networks, reducing the number of models to be built. Fig. 7.6 compares the efficiency of Deep Learning vs ML. When the amount of training data increases in machine learning, the performance of ML decreases but the Deep learning get the maximum performance with huge amount of data with the same situation

7.2.1 Deep Convolutional Neural Networks (CNNs) and the Training (Learning) Process

There are several deep learning technologies available in supervised learning; the most relevant algorithms nowadays in supervised learning are:

Convolutional neural networks (CNNs), recurrent neural networks (RNNs), and long short-term memory (LSTM) models are prominent variations of feedforward neural networks.

In supervised learning, feedforward neural networks, also known as multilayer perceptrons (MLPs), are the most often used models. A trained algorithm is anticipated to provide an output value or classification category consistent with the mapping between inputs and outputs supplied in the training set when given a sample vector containing features. Many hidden layers are triggered sequentially to provide the desired output in an estimated function. The phrase "deep learning" comes from the word "depth of the model," which refers to the number of hidden layers. This paper uses Keras and Tensorflow backend platform in python to design and train a designated deep Convolutional Neural Network architecture with the given sample image data set, and then applies the trained network to new image data taken by UAV camera for identification and recognition of the image.

7.2.2 Modelling Deep Learning with TensorFlow

TensorFlow software library help tackle implementation of machine learning and deep learning methods. These libraries are very broad enough to implement many types of methods and algorithms which are included seeding, loading data, designing neural network architecture, compiling and training of the machine learning or deep learning model. The technique has been used in areas such as robotics, voice recognition devices, map extracting, object detection (Tompson et al., 2014), etc. (Cireşan et al., 2012).

In addition, the Tensorflow backend called Keras (Deng, 2014) is also used for detecting hand

written digits or MNIST data. The Convolutional neural network (CNN) (Ren & Xu, 2015) is used to determine MNIST image into words by transforming multi-Dimensional images into characters. Open source Tensorflow made by Google team to model CNN with MNIST digits. The reason of using MNIST digits for modelling deep learning is because a person called Yann LeCunn already released hand written datasets in 1998 which then main source for data scientists and researchers for classifying objects in Deep Learning. Modelling and Simulating Deep Convolutional Neural Network using Tensorflow and Keras. A deep convolutional neural network is built in this paper using Keras with TensorFlow backend library tool for modelling and simulating of handwritten digits by training with MNIST dataset sample image data of handwritten images.

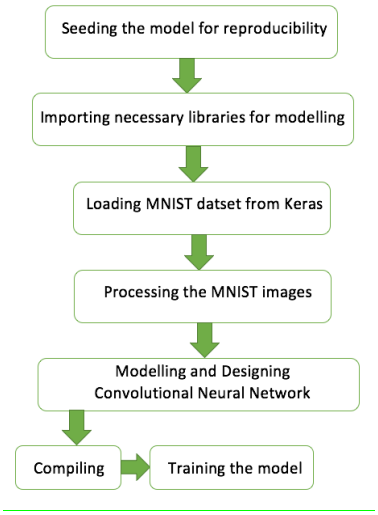

Figure 7.7 Model system approach flow diagram

The flow diagram for the proposed model system is shown in Fig. 7.7. The modelling process for testing and training include 7 stages described as fellows.

Stage-1

In the first stage, Neural network may not be predicted precisely because of instability of the

algorithms being trained with same dataset with unusual results. To overcome this complexity, random seeding to start the system with random weights applied on the neurons respectively. This causes the system to automatically learn each time if the identical neural network train with identical result.

Stage-2

Importing Keras library to use all the necessary libraries from that framework to model and simulate the MNIST datasets. Given dataset can be loaded into the system to classify handwritten images already uploaded in the Keras. After that, a sequential model needed to perform and design neurons by stacking layers of that neurons using Dense layer which implement the operation of the neural network. The system can cause overfitting by using complicated neurons in the model. To avoid that, overfitting neural layer was used using with the Dropout layer which set a fraction rate of input to 0 at each update during training and flatten the input using Flatten layers. To create successful deep convolution neural network for 2-Dimensional images, Maxpooling2D layer was used to operate spatial data of each pixel of the image which presents same pixel detection to get accurate output.

Stage-3 & 4

In this stage, loading the hand-written images from the dataset stored. For testing and training the data, it included in the dataset are images with its respective labels. When training the input data, the total of digits is 60000 and only 10000 are being tested for training and testing the data. The value of each pixel is 255 pixels in processing the MNIST images.

Stage-5

Using Sequential model to initialize and stack all the neural layers.

2-Demensional convolutional layer uses lenet-5 have 32 neurons which is the first convolutional

layers. The size of the pool size is 3 by 3 kernel size pixels. As with the Dense layer, a recommended neuron called Relu should be activated. MNIST digits input is (28 by 28) pixels with 1 depth black and white image.

Second 2-D Convolutional layer, on the other hand uses 64 layers and remaining values are same as first layer.

Third layer is 2-D MaxPooling, for every 4 pixels reduce them to one with 2 by 2 pool size.

Dropout layers produce results from training apply well to the validation data, going to dropout 0.25 of the neuron.

We have to flatten everything, so we have more than one dimension at this point, dense fully connected layer is going to able recombine all these possible representations stored by convolutional neuron, represent 3 by 3 corner, feed that into dense layer with any kind of configuration. Multi dimension to one dimension by flattening.

```
In [8]: model.summary()
```

Layer (type)	Output Shape	Param #
conv2d_1 (Conv2D)	(None, 26, 26, 32)	320
conv2d_2 (Conv2D)	(None, 24, 24, 64)	18496
max_pooling2d_1 (MaxPooling2	(None, 12, 12, 64)	0
dropout_1 (Dropout)	(None, 12, 12, 64)	0
flatten_1 (Flatten)	(None, 9216)	0
dense_1 (Dense)	(None, 128)	1179776
dropout_2 (Dropout)	(None, 128)	0
dense_2 (Dense)	(None, 10)	1290

Total params: 1,199,882
Trainable params: 1,199,882
Non-trainable params: 0

Figure 7.8 Convolutional neural network model summary

Dense layer with 130 neurons and activation of RELU configured. This layer will be cut in half for us. Softmax activation on Dense layer of 12 neurons. It's common for users of machine learning models to be curious in the state of the model and how it evolves over time. A variety of summary operations may be added to the graph in the final output using TensorFlow and Keras. Figure 7.8

summarizes the model of a convolutional neural network.

Stage-6 & 7

In this stage included compiling and training on 10000 from 60000 sample MNIST images with validation.

7.3 Results

This model is testing with only 1 epoch and the validation accuracy is 98.36 % (see Fig. 7.9).

```
In [10]: model.fit(X_train, y_train, batch_size=128, epochs=1, verbose=1, validation_data=(X_test, y_test))

         Train on 60000 samples, validate on 10000 samples
         Epoch 1/1
         60000/60000 [==============================] - 319s - loss: 0.2410 - acc: 0.9267 - val_loss: 0.0518 - val_acc: 0.9836

Out[10]: <keras.callbacks.History at 0x7f5202ce6898>
```

Figure 7.9 Trained data results

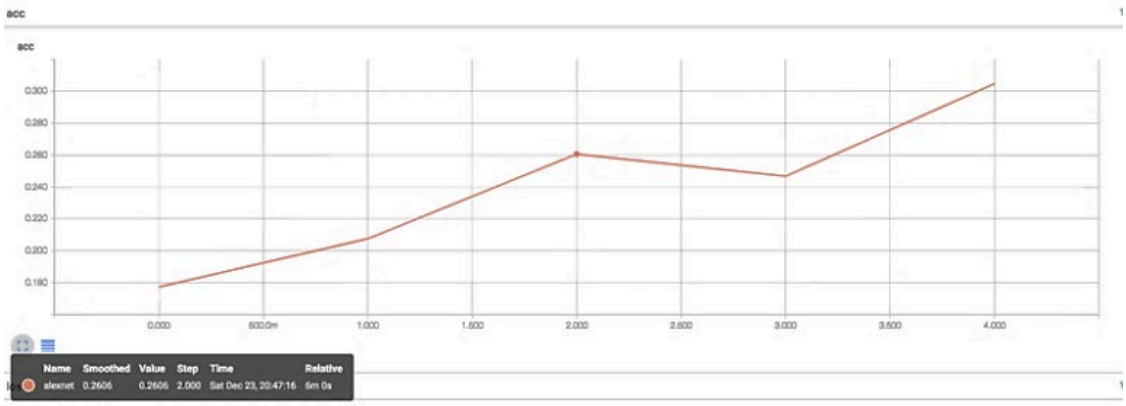

Figure 7.10 Accuracy Results

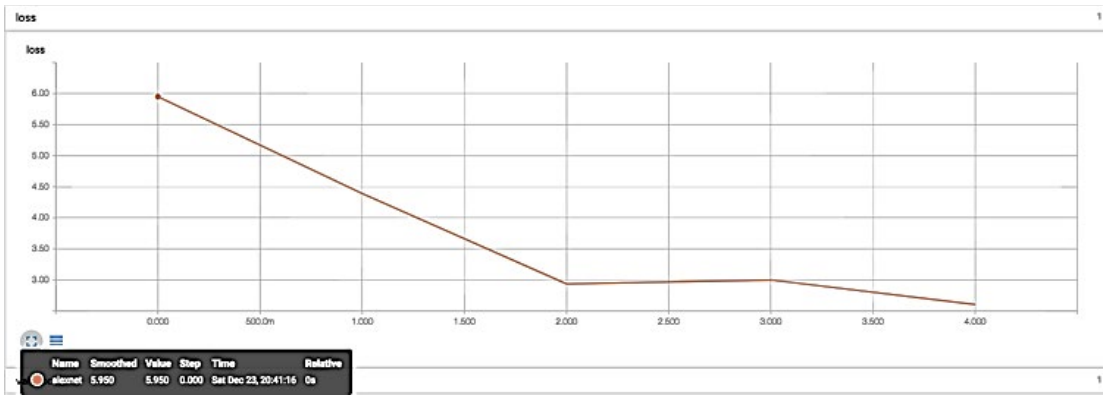

Figure 7.11 Loss values to the training data decreases

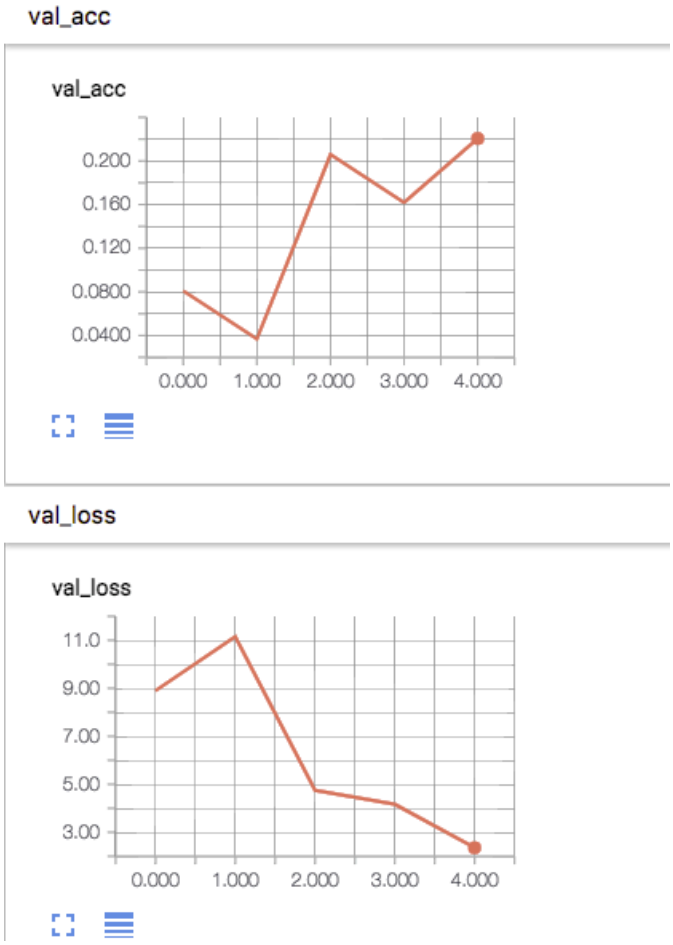

Figure 7.12 Validated accuracy and loss after feedback from output

The results from Fig. 7.12 verify that when predicting accuracy increases, the amount of loss data

on the trained data decreases over the result. The validation accuracy and loss get from feedback received from fully connected deep neural network enhance the system performance.

The system's classification accuracy was tested using Relu Activation functions, which yielded a classification accuracy of 98.36 percent on the test data.

7.4 Conclusion and chapter summary

When it comes to retrieving information or high-quality photos from risky settings, unmanned aerial vehicles (UAVs), often known as drones, have emerged because of rapidly expanding technology. To help with picture recognition for Unmanned Aerial Vehicles (UAVs) in search and rescue (SAR) operations, we showed in this work a unique solution using deep learning technology (as part of Machine Learning –ML). The deep Convolutional Neural Network (NN) architecture was designed and trained using TensorFlow (an Open-Source software library) and Keras (a Python backend platform). Using a pre-trained NN and new picture data from an unmanned aerial vehicle camera, the researchers were able to demonstrate that the newly trained system is capable of accurately recognizing images. In the next chapter, multi agent deep reinforcement learning method was introduced to tackle the problem of controlling multiple UAV charging process.

8 Multi-Agent Deep Reinforcement Learning for UAVs Charging

- Chapter 8 brings together with using Reinforcement Learning (RL) techniques to train and test multi agent self-learning system to automate collaborate flying and charging process.

8.1 Abstract

This chapter research findings emphasis has focused on multi-agent unmanned aerial vehicles (UAVs) using RL techniques, which are finding usage in a variety of WPT fields. Despite this, the amount of time that they can spend in the sky is still limited by their energy supply. This is especially true when UAVs are used to supplement the wireless network as transceiver stations (TS). Simulated findings reveal that, compared to baseline techniques, the suggested RL-POLICY-MA approach has significantly improved the trajectory optimization and energy consumption of TS.

8.2 Introduction

A wide range of applications and services based on Unmanned Aerial Vehicles (UAVs) have emerged, from parcel delivery and public safety to disaster management and monitoring (Rejeb et al., 2021). The UAV WPT charging network's lifespan which uses the methods of energy-efficient techniques is only slightly extended by these enhancements, which needs major improvement (Townsend et al., 2020). Furthermore, this limitation necessitates that the onboard batteries be changed or recharged on a regular basis, which has a significant impact overall multi agent UAV collaborative network performance.

Although RF-based far-field WPT is a potential way to powering UAVs, it is not the only option. A wide range of mobile networks, including 4G onwards, are likely to make use of WPT technology with the conjunction with UAVs in the future (see (H. Zhang et al., 2021). However,

lengthy distances between transmitter Tx and receivers Rx severely reduce the performance of WPT systems because of the problem of restricted power transfer, resulting in substantial RF signal propagation loss.

There are two possible solutions to this problem for UAVs equipped with Tx and RX which are the drone should land whenever battery low and charge in the ground station or it automatically hover above transmitter and charge while on operation. A significant number of Multi agent WPT UAVs may be mass-deployed (Shakhatreh et al., 2019) on the ground charging station. There are several ways in which WPT might potentially be used, however this rotational dynamic WPT option discussed and experimented in chapter 3 would be flexible and require the use of low altitude flying by unmanned aircraft (UAV) to load RL-POLICY with power.

There are key problems that must be addressed for controlling multiple UAVs using RL method to carry out their duties, and this research is aimed at solving them. Firstly, remote-area multiple UAVs need to be constantly recharged or replaced with new batteries to minimize the need for human involvement, which necessitates a vast deployment of DWPT charging stations (DWPT-CSs). Installing and maintaining DWPT-CSs will be expensive, and there may be other issues, especially if the deployment area is limited. As a result, operations take longer to complete, and the network suffers, especially when UAVs are used to service ground customers. As a result, the DWPT efficiency is reduced, and the quantity of energy captured by UAVs is reduced accordingly. A viable solution should solve all the above identified difficulties and improve the WPT's performance. Air-to-air refueling of military aero planes by aerial tankers is the inspiration for our solution (Yan et al., 2020). A series of intelligent DWPT-CSs working independently with the express purpose of effectively recharging UAVs is proposed in this approach (see Fig. 8.1). To transmit energy from a WPT RL-POLICY-equipped transmitter to an RL-POLICY-equipped

UAV's receiver, DWPT-CSs must have a larger energy capacity than conventional UAVs. Ground RL-POLICY charging station powered by either main AC supply directly or with the use of renewable energies such as solar powered or wind, which are UAVs in and of themselves.

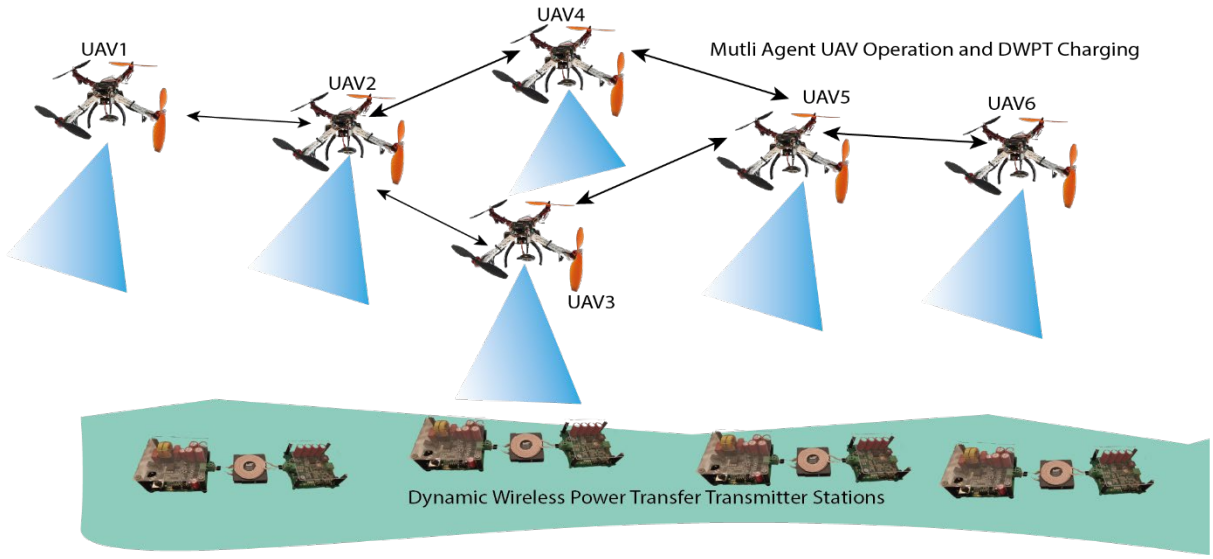

Figure 8.1 Purpose of effectively recharging multi-agent UAVs

When it comes to charging the UAVs, rotational dynamic wireless energy beamforming allows the DWPT-CSs to keep RF connections in good state of service while also shortening their lengths. The implementation of DWPT-CSs, on the other hand, presents significant obstacles. Because low-energy unmanned aerial vehicles (UAVs) might come at any time, DWPT-CSs must constantly hover and supply the UAVs with the energy they need. Since all multi-agent UAVs fly in the same area, they are at risk of colliding with one other and with other flying. When all drones must constantly move around and communicate with others, that will be going to use a lot of electricity. RL-POLICY Energy sources are forced to modify its own flight paths to minimize the distance between them and UAVs to carry out the energy transfer successfully.

Our approach is based on RL-POLICY-DL-RL approaches, which have proved their ability to

analyses vast state spaces and dynamic contexts, such as multi-agent systems.

- Achieving a reasonable amount of efficiency in the charging of UAVs while also optimizing the trajectory of DWPT-CSs and keeping them from colliding with one another.
- Taking into consideration the energy requirements of RL-POLICY while optimizing the loading procedure from the ground charging station.
- Analytical and numerical support for the evaluation of the suggested strategy and the evaluation of its efficiency is provided in this study.

A new wireless powered UAV network architecture is introduced in this chapter, along with a problem description. Also discusses the multi-agent RL-POLICY-DL-RL based methodology and gives a collection of DL-RL preliminaries.

8.3 Related Work

8.3.1 Global WPT charging station deployment research on UAVs

DWPT charging station position, and energy resource allocation is all tuned together to enhance the system's downlink sum rate. (Ding et al., 2018) optimized the deployment of UAVs, as well as the scheduling of energy recharging procedures for UAVs, to maximize the coverage of UAVs. Dynamic wireless charging via unmanned aerial vehicles (UAVs) is the focus of (T. Yang et al., 2021), where a ground-based mobile control system provides critical assistance. Before being deployed to air operations, each unmanned aerial vehicle (UAV) must be fully charged and location of the transmitter should be stored inside the drone control system (Haque et al., 2017). Study (Ghazzai et al., 2019) investigated how many DWPT charging stations are needed and how to best deploy them collaboratively so that multiple UAVs may recharge their batteries and take

to the skies once more. (Q. Tang et al., 2020) investigates the impact of dynamic wireless charging station on overall UAVs network performance. Optimal coverage may be achieved by minimizing charging time and installing lower density dynamic WPT stations, according to the latter study. To date, existing DWPT-based techniques on the ground have shown to be effective in extending the operating time of deployed UAVs. To complete the given air operations, unmanned aerial vehicles (UAVs) must stop and return to a Control Stations whenever there will be low on power. This prohibits them from completing their responsibilities over a longer charging period. When it comes to emergency situations or time-sensitive applications, this might be an inflexibility issue.

8.3.2 UAVs enabled flight path planner aware WPT

Many studies have been done to improve the WPT energy transfer mechanism of UAV flight path planner. The two scenarios were designed to maximize the power efficiency of UAVs that could be processed at any one time with an effort was made by (Xu et al., 2018b) to create a flight path planner that would enhance energy use efficiency and hence extend sensors and WPT network lifespans. UAV-aided wireless power transfer networks have been suggested in (Masroor et al., 2021). The flight path planner of the UAV was optimized using a heuristic technique that considered several channel characteristics.

However, in UAVs enabled flight path planner aware WPT techniques, several restrictions are overlooked. When it comes to transferring energy, for example, multiple UAVs working together may be all that's needed. There are several methods that use more than one unmanned aerial vehicle (UAV); however, they don't consider concerns like as collisions, energy transfer, or completion time. As a result, the proposed methodologies are necessary because of the lack of consideration for the energy consumption of UAVs.

8.3.3 Reinforcement Learning enabled WPT's UAVs

Reinforcement Learning approaches have recently re-emerged, and this is of special significance. A stationary WPT method was used by the authors of (Azar et al., 2021) to charge UAV electric batteries. As a result, a UAV uses a Deep learning-based RL approach with resource management strategy to optimize data collecting, power transfer, and the accompanying modulation scheme for robotic IoT nodes. The Deep learning-based RL approach is used to optimize by (van Huynh et al., 2022) proposes the use of a UAV to gather data from a target device while simultaneously charging additional covered devices. In a particular mission duration, this strategy maximisers aggregate data rate, maximisers total collected energy, and minimizes the UAV's energy consumption by using an appropriate Deep learning-based RL version. Drawbacks include a reliance on a single UAV to serve as the WPT devices in all but the simplest of cases.

8.4 Performance Comparison

As a cooperative UAV's RL-POLICY charging task, the beginning position of the pursuers is critical. Using a K-means clustering technique, the system was able to identify three centroids among the first 953 points of successful episodes. Using this initial position as a starting point, pursuing multiple UAVs agent may be sent to specified places for improved pursuit charging performance. With the beginning of the DL training point set, the multi-agent RL model is implemented, and rewards system connection is disrupted by a huge difference resulting in a collision between UAV agent 3 and UAV agent 5. This error demonstrates that when the evader makes an abrupt turn and escapes successfully, his UAV agent lose track of another agent.

UAV agent 1 and 2 work together closely to locate the other agents even when the agents make an unexpected turn in RAD2. UAV agent 4 waits for the other agents to be intercepted while it hovers below the communication coverage. RAD2's intended communication-awareness reward makes it

possible for the other UAV agents to leverage the cellular network to establish high-quality communication, reducing the need for individual agents to do partial observational tasks. Simulates UAV RL-POLICY charging with randomly generated starting positions. Unauthorized Unmanned Aerial Vehicles (UAVs) invade no-fly zones more frequently when master UAV agent 1 catch them. On the other hand, the UAV agents form small groups to focus on a single charging one by one. So, their collaboration is less successful because they cannot use their numerical advantages to enclose and capture the charging agents are clear.

For the Multi-agent collaboration part, the UAV agents work in unison to surround each other and prevent it from collision while they move closer to capture it. This is mostly due to the RAD2 curriculum, which teaches the agents to first encircle the other agents to meet the Besieged Status requirement, and subsequently to reduce the encirclement until the agent is apprehended and started the process of WPT charging simulations.

There are 900 episodes gathered with the fixed beginning location for general comparison tests and the results are shown in fig 8.2. Based on the results, the proposed RAD2 and its variations outperform all other techniques in terms of both capture probability and average time cost. The results show that the proposed RAD2 creates more efficient cooperative wireless charging methods in urban airspace than the state-of-the-art techniques. A low battery UAV agent may be captured by three cellular-connected master UAV agent in 14.2s, where the current system is 2.1 times quicker than the agent, using the cooperative pursuit tactics discovered.

The study demonstrates that master and slave agent’s accidents are far less common than those between pursuer and flying environment model. In the case of UAV agents, learning the collision avoidance approach is substantially more difficult than for stationary objects.

RAD2 without WDAT has a bigger reward variance than RAD2, which can be seen when

comparing RAD2 and its variations. From the comparison, it appears that WDAT is a more reliable tool for simple 2-dimensional environment but for complex 3-D environment RAD2 outperform it. As a result, WDAT can decrease environmental uncertainty by emulating the behaviors and observations of unconnected UAV agents. As a result of the experiments, WDAT's performance is also evaluated. In the experiment, 95-episode vectors with the conjunction of deep learning-based training data are used to represent a sequence of observations and actions.

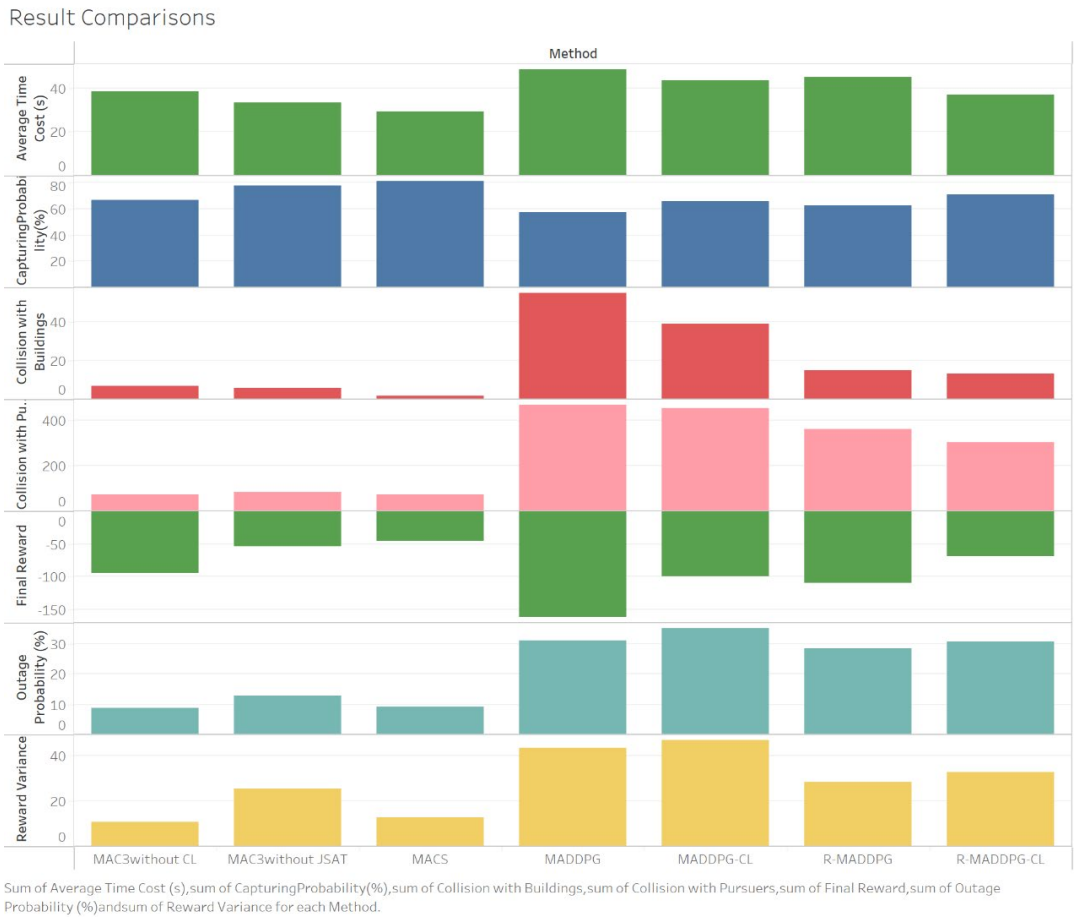

Figure 8.2 Result comparison

WDAT efficiently reflects the spatiotemporal dependency of the following's observations and actions, as demonstrated by the findings in other dimensions, the prediction error is minuscule or nonexistent. As a result, the cumulative prediction error does not grow exponentially as the

prediction step rises. When communication is disrupted for an extended period, WDAT has the capacity to forecast the actions and observations of other pursuers within a given range of prediction steps. Two factors account for the proposed RAD2's enhanced performance: Partial observation and nonstationary are reduced because of cellular-enabled parameter exchange, which streamlines the investigation process. Curriculum learning, which aims to overcome the issue of scant rewards and teaches the UAV agents how to work together more effectively in pursuit.

8.5 Simulations

Decentralized FARCA and DWPT-DL-RLFAS both recorded three performance metrics for each episode in accordance with previous research. As for success, it refers to the number of times an episode ends without a deadlock or a collision. After that, the average time it takes each agent on a particular mission. Observations were made both experimentally and virtually in two different settings. On the outside corners of a 3-dimensional environment with a radius of 3.2m, 1.27m-radius UAV agents begin the episode.

The agents must avoid colliding with one other to achieve their antipodal objectives as rapidly as feasible. At a 3.2m with 2 different environment with UAV agents with a radius of 1.27m begin the episode in an unknown position. The environment inside is filled with random targets that do not overlap. All the simulated testing demonstrates that DWPT-DL-RLFAS is superior to DFARCA in terms of performance.

Using 900 simulated episodes and varied numbers of agents, the performance metrics in experiments are summarized in the following. Two controllers, FARCA and DWPT-DL-RLFAS, represent situations where a random number of UAV agents were assigned a non-colliding velocity toward their objective in the simulation. DWPT-DL-RLFAS had a success rate of 86% in homogenous settings with 19 agents, but the DFARCA success rate was just 69%. Routes are up

to five seconds quicker on average because to this technology. As a result, in busy areas, DWPT-DL-RLFAS provides UAV with faster and safer charging options. As a result, DWPT-DL-RLFAS can be seen to travel longer distances in sparse surroundings. As a result, the average time to reach the objective is on par with DFARCA in both circumstances, despite the greater distance travelled When there are fewer agents around, the DWPT-DL-RLFAS policy causes the agents to travel at a faster rate.

Individual short-term reward is sacrificed in favor of the objective of maximizing speed and episodic reward in DWPT-DL-RLFAS. The above policy obtains a success rate of 91% and varies from 96% to 98.87% in 2-dimensions in settings with similar density to the 15-agent randomized simulations both, but DWPT-DL-RLFAS is the winner. In addition, DWPT-DL-RLFAS has a 97.7% success rate when evaluated in situations with constant-velocity agents. Adding non-policy actors has no effect on DWPT-DL-RLFAS's success. While FARCA has a 62% success rate in the same situation, other leading techniques have not been created for this kind of situation. Using DWPT-DL-RLFAS' training methodology instead of other ways shows the advantages of this approach.

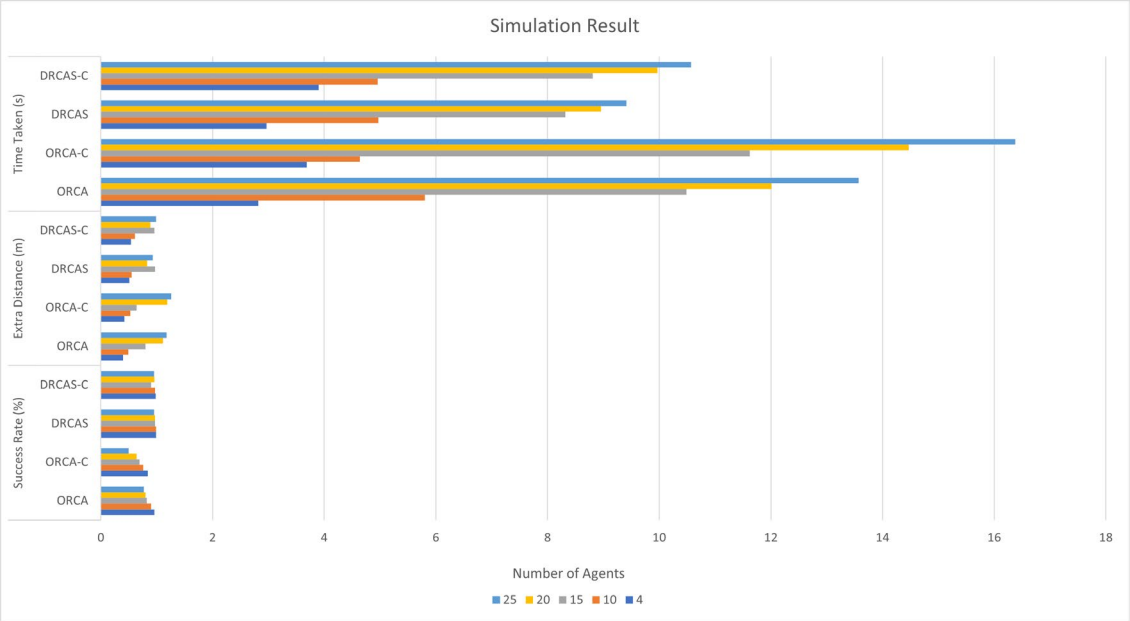

Figure 8.3 Simulation result

As it is difficult to convey 3-dimensional flight path planner through a textual medium, 2-dimenional simulations were also done. For example, DFARCA produces more direct parallel lines whereas DWPT-DL-RLFAS provides asymmetric paths in which the blue UAV agents move more directly but the green UAV agents which do not. When the population density is higher, DFARCA is more likely to direct UAV agents to a center roundabout, where they all slow down since the computed velocity obstacle offers fewer possibilities for their flight path planner. Figure 8.3 shows how DWPT-DL-RLFAS, on the other hand, uses cooperative behavior to keep agents moving at a faster pace.

According to documented performance metrics, DWPT-DL-RLFAS travels shorter distances in less time than its competitors. Despite the huge number of UAV agents, stalemate is not observed with DWPT-DL-RLFAS, and the success rate remains high. If an UAV agent can travel straight to its objective under DWPT-DL-RLFAS, it will do so. Gradients-inspired attractive forces are responsible for this. Since this route was extremely unlikely to be sampled during training, other

deep reinforcement learning algorithms couldn't achieve the outcome.

As a result, the hybrid policy adopted is no longer necessary thanks to DWPT-DL-RLFAS. DWPT-DL-RLFAS, on the other hand, ensures that all agents remain inside the confines of the cuboid habitat, thereby minimizing the footprint. Instead, DFARCA takes agents on courses that take them far from other UAV agents' itineraries, especially in real-world experiments, thereby increasing travel time. As a result of the negative penalty applied in the reward function, DWPT-DL-RLFAS avoids this.

8.6 Evaluation Results

Proposed method is compared to Random Scheduling and Random Sharing in this section. Figure 8.4 shows the scheduling and energy sharing aspects of this simulation-based evaluation are examined and summarizes this simulation-based performance evaluation.

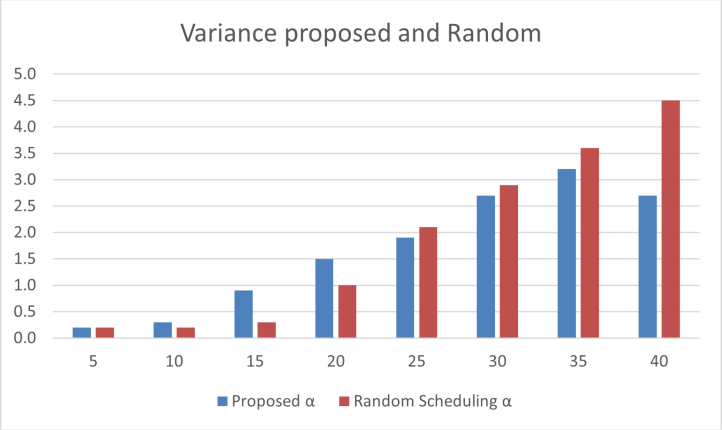

Figure 8.4 variance proposed and random

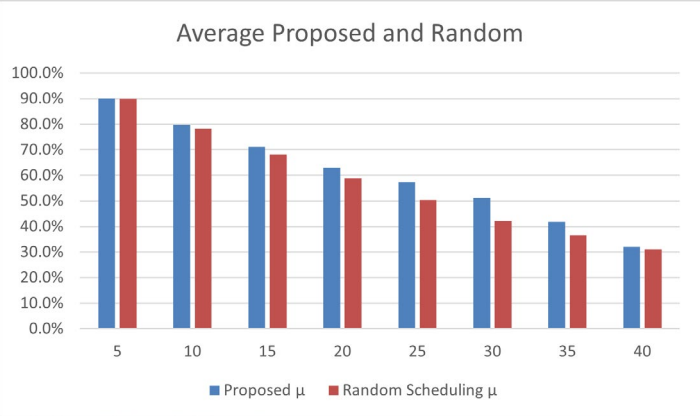

Figure 8.5 average propose and random

In this section, the suggestion was made for a time for balancing the energy resources of charging towers of UAVs. Thus, the performance review is carried out in this way. Unmanned aerial vehicles (UAVs) start with batteries whose mAh values are randomly chosen accordingly. The Proposed method outperforms the Random Scheduling algorithm in terms of energy-awareness. UAVs' remaining battery/energy quantities are summed for both proposed and random scheduling, with averages and variances shown for both cases. In figure 8.5, we see that the average residual energies for the whole time are larger in the proposed approach. As a result, the Proposed method has a greater number of charge UAVs ratio than the Random Scheduling algorithm does. As an advantage, the proposed method has a lower standard deviation meaning the proposed algorithm is capable of charging services that consider load balancing and fairness in wireless energy charging.

Charging tower energy consumption for the proposed and random scheduling algorithms. Proposed and Random Scheduling algorithms with their differences in terms of energy consumption compared to each other. Comparing the proposed and random scheduling algorithms with traditional system, it can be shown that the proposed approach has a much better long-term

energy usage. The Proposed algorithm and the Random Scheduling algorithm, the charged WPT energy from the local energy is noticeably less than that because of the uniqueness of the Proposed algorithm. This suggests that the recommended timing is efficient in terms of charging tower load-balancing.

8.7 Performance Results

Figure 8.6 shows the tradeoff between task failure rate (Rf) and search time (Ta) vs constraint scaling parameter (m) in relation to these two variables. The following conclusions may be drawn from this figure.

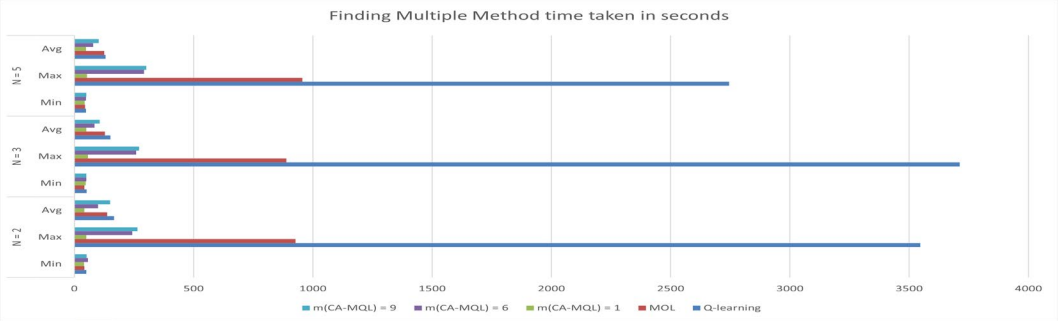

Figure 8.6 multiple method time taken

The amount of time it takes to conduct a search gets shorter as the number of UAVs increases. Increasing the constraint scaling parameter m further demonstrates this impact. We can see that a higher m places a tighter cap on the anticipated cost. In this situation, the UAV will choose activities based on the immediate benefit to avoid the expense (negative reward) of superfluous actions. To put it another way, the UAV is more likely to ignore the ground server's instructions and not take the desired action. CA-search CGL's time performance is comparable to CGL's with a big m (example., m = 8). With CA-CGL, when m drops, even with a small number of UAVs, there is a considerable reduction in searching time.

Task failure rates rise as the number of unmanned aerial vehicles (UAVs) rises. As a result of the coordination mechanism, erroneous reference points and reward information may be transferred between UAVs. As m lowers, the rate of task failure increases. Excessive restrictions on the UAV operation might have resulted in an under-exploration. It is possible for the UAV to surpass its maximum search duration if the reference point estimation is not good enough. It is more likely to fail a task with a big m than with a small m, because of its faith in its own observation rather than the inference based on prior experience. The task failure rate vs. search time tradeoff is an intriguing one, as can be seen from the previous two data. Thus, our design of the constraint scaling parameter allows UAV tracking to be more adaptable to diverse performance needs.

8.8 Proof of theorem

Steps to prove to pay off at s+1 is no smaller are summarized in this section. As can be shown, the limited reward-system is equivalent to the instantaneous reward-system. There is a correlation between (s) and (a) in equation 8.1. As a result, we are left with the following:

Equation 8.1

$$J\left[\sum_{s=0}^{T-1}\gamma^{s}R_{n,c}(s_t,a_t)\right]\leq J\left[\sum_{s=0}^{T}\gamma^{t}R_{n,c}(s_t,a_t)\right]$$

$$\begin{aligned}J\left[\sum_{s=0}^{T}\gamma^{s}R_{n,c}(s_t,a_t)\right] &= J\left[\sum_{s=0}^{T-1}\gamma^{t}R_{n,c}(s_t,a_t)\right]\\ &\quad +\gamma^{T}R_{n,c}(s_T,a_T),\\ &\geq J\left[\sum_{s=0}^{T-1}\gamma^{t}R_{n,c}(s_t,a_t)\right].\end{aligned}$$

8.9 Conclusion and chapter summary

Multi-agent unmanned aerial vehicles (UAVs) utilizing RL approaches have been the focus of this chapter's research discoveries, which have been employed in a range of WPT applications. As a result, their stay in the sky is limited by their energy source. Even more so when UAVs are deployed as transceiver stations in the wireless network (TS). Based on the results of the simulations, the RL-POLICY-MA strategy proposed here has greatly improved TS's trajectory optimization and energy usage over baseline solutions.

9 Conclusion and Future Works

- Chapter 9 brings the overall discussion of all results and concludes this research with a contribution to the science community, limitation, and future research possibilities.

The conclusions and subjects discussed in this thesis are summarized in this chapter. Section 9 gives an overview of the problem and the solution offered in the thesis. We'll go through the major contribution of this research, which is the use of novel techniques of rotational dynamics of WPT with deep reinforcement learning, deep neural networks to train a control strategy for an unmanned aerial vehicle's autonomous charging, along with all the advantages it has over human agents and existing WPT solutions. The thesis' primary objectives are also summarized in this Section. Lastly, additional research directions are also proposed.

9.1 Overview

Unmanned surface vehicles' autonomous WPT charging remains a challenge despite the efforts of the scientific community for UAVs. The aerial vehicles are particularly vulnerable to limited battery with limited flying time while it’s on operation, where they represent a major disadvantage. That is why the work done and reported in this thesis was motivated by the requirement for an unmanned aerial vehicle (UAV) WPT receivers that can cope with dynamic rotational WPT transmitters and charging whenever there is a low charge autonomously using DL-RL and DL Kalman filter. The control system can use deep Kalman filter sensor fusion data from an unmanned aerial vehicle (UAV) flying over the rotational dynamic WPT transmitter to navigate and charge autonomously. As a reminder, this is a multi-faceted problem that was never meant to be solved in single research; hence, the data acquired are of great value to the larger purpose.

UAV networks are extensively and actively employed in the design and implementation of the

next-generation WPT charging according to the autonomous and flexible properties of UAV networks. Possibility of search and rescue operation with high mobility and dynamic wireless power transfer network base station deployment may be performed using autonomous UAV systems using deep learning and deep reinforcement learning techniques, enabling large-scale adaptable big-data processing based on data collected by many UAVs.

9.1.1 Design Rotational dynamic Wireless Power Transfer system

Powerful wirelessly powered unmanned aerial vehicles (UAVs), also known as wireless power transfer (WPT) or WPT drones, have been developed to function in hazardous areas where humans cannot. An initial theoretical analysis showed that, under several test situations, the system under consideration might employ a circuit identical to that discovered in the theoretical analysis. Based on the RL-POLICY, the working Principe of all the suggested techniques including short and long-range approaches, we developed and tested it in this chapter. At the end of the process, we added two more variables to assist us determine how effectively rotating dynamic WPT systems work in various environments. Finally, the future of WPT transfer employs the earth as a return wire for the electrostatic resonant coupling approach.

9.1.2 Design and implementation of autonomous rotational dynamic wireless charging for UAVs

The bench suggested in this paper was used to test small customized electric driven UAVs, which may be utilized for a range of research purposes. An enormous amount of effort and money is usually required to create this kind of user interface. It is now possible to conduct long-duration flights completely unhindered by humans thanks to the drone's new rotating dynamic wireless charging capability. Today's unmanned aerial vehicles (UAVs) have a limited flying time because

of their battery capacity. When the drone's battery runs low, it can be recharged wirelessly so it may continue its mission uninterrupted. With the use of this technology, it is now possible to perform long-distance missions without human intervention. Missions may be set up such that many drones fly in sync and therefore save flying time if they are equipped with wireless charging capabilities. A more efficient charging method would be Rotational Dynamic Wireless Charging, provided that the associated components could be improved in design. This design's primary considerations are the resonant frequency and the properties of the coil. Improved inverter design will lead to a reduction in total efficiency. Wireless power transfer may be improved by increasing the inductive connection's resonance frequency. Improve the system's performance by increasing its resonance frequency. Raising the charge rate may help reduce charging time by increasing productivity.

9.1.3 Deep Kalman filter and Dynamic Wireless Power Transfer for UAVs charging

In this method, it is feasible to considerably enhance the integrated navigation's positioning performance when the IMU signal is missing. Using reinforcement learning calculated from experiment results, experimenters found that the NCM process can reliably forecast position, independent of time, IMU outage periods, or navigation fusion methodologies. This is because of the NCM process' use of reinforcement learning. The gyroscope's orientation quotes are utilized to combine the quotes from several obstacle avoidance algorithms. Our research has shown that the precision of a system may be improved by employing gyroscopes when required and analyzing the data that they provide. For this reason, it has been observed that UAVs must deal with a variety of obstacles in their surroundings.

9.1.4 Design of Vision-based Object detection using Deep Learning for reliable autonomous charging of UAV

Unmanned aerial vehicles (UAVs), sometimes known as drones, have developed due to fast developing technology when it comes to recovering information or high-quality images from dangerous locations. This method demonstrated a new method using deep learning technology (as part of Machine Learning –ML) to assist with photo identification for Unmanned Aerial Vehicles (UAVs) in search and rescue (SAR) missions. Programming libraries TensorFlow and Keras were used to develop and train the deep Convolutional Neural Network (NN) architecture' (a Python backend platform). The author of this thesis was able to show that the freshly trained system is capable of successfully detecting pictures by using a pre-trained NN and new picture data from an unmanned aerial vehicle camera.

9.1.5 Multi-agent Deep Reinforcement Learning for UAVs charging

This research proposal focuses on multi-agent unmanned aerial vehicles (UAVs) that use RL techniques and have been use in a variety of WPT applications. This means that their time in the sky is limited by the power they have available to them. Even more so when UAVs are used in the wireless network as transceiver stations (TS). In comparison to the baseline solutions, the RL-POLICY-MA technique provided here has significantly enhanced TS's trajectory optimization and energy utilization.

9.2 Contribution to the scientific community

There has never been an attempt to employ an established approach to identify the dynamic wireless power transfer can be used by rotating them in opposite direction to increase the distance

of the charging of UAVs or other electronic devices. Using Unique Deep Learning and Reinforcement Learning based Kalman Filter model, the UAV's RL-POLICY charging process can be automated efficiently which was studied in this research. The RL model is used as a self-learning system that can be applied easily to determine the autonomous charging RL-POLICY UAVs without relying on traditional dynamics of the system. Research also incorporates numerical data from vision-based object detection study to estimate the charging location of RL-POLICY system using deep learning method. Multi-agent deep reinforcement learning for intelligent charging of UAVs designs were also developed, and the findings demonstrate that RL method gives a greater level of trajectory optimization and energy consumption than other designs. It is possible for electric UAV, boat, and automotive makers to utilize the findings of this study to evaluate prospective design adjustments to enhance operation time of the vehicles.

9.3 Limitation of this PHD thesis

The following are some of this PhD 's limitations:

- DL simulation results were compared and found to be in excellent efficiency, although the RL simulation of the UAV designs had a restriction in slow processing speed that computer which needs expensive artificial intelligence based neural engines to train faster.

- The limitation of using UAV sensors due to the budget of the PhD such as IMU, GPS which got more noise compared to the expensive ones with less sensor noise for better testing with accuracy used by military aircrafts or other large organization.

9.4 RDWPT UAV of the Future

Nikola Tesla patented first design of wireless power transfer around 1900s using earth surfaces as a ground and high-pressure atmosphere as a conductor to transfer electricity from one distance to another. Even this closed-circuit design may work, if we want to apply it practically would be impractical and risk of clashing communication with passenger flights because we must raise hydrogen balloon to the height above sea level of more than 30 thousand feet. Tesla proposed not only that earth atmosphere become conductive like wire when it reaches certain pressure levels but also using reactive power transfer method to send electricity using only ground. When Reactive power transfer method oscillate between transmitter capacitor and receiver capacitor using resonant tuned frequency, there would be standing wave pressure build up between transmitter and receiver which helps transfer usable active power to the UAV.

In the future design, reactive power transfer method works at half of 360 degree between two capacitors. When main active power activated, the power converted into reactive power by using quarter wave coils between transmitter and receiver. Quarter wave coil's purpose is that the circuit should be in resonance to transfer power efficiently. When the power activated, two capacitors exchange reverse charges simultaneously using reactive wireless power transfer method. Then, standing wave between transmitter and receiver ground formed and usable power transmitted into the UAV or load. Other type method can be used for transmitting power through one wire transmission on UAVs for the purpose of showing the working principle of RWPT system. The circuit can be tuned in the same way as using electromagnetic resonance. For the efficient power transfer method, the UAV frequency also should be in resonance with the RWPT circuit.

Despite the great deal of research work done in the field of WPT and unmanned aerial vehicles and the advancement in its technology many experts agree that one of the major drawbacks of

today's WPT UAV is that they tend to use extreme power usage, charging batteries usually takes out operation time, low range wireless power transfer and complexity of the resonance transmitter and receiver coil designs. An important consideration in connection with the WPT UAV system is that the power can be transmitter using same earth ground in which large amounts of electrons stored inside and capacitive coupling approach to the UAV which it would act as a return wire instead of sending through air. In the practice of building traditional WPT system in UAV, structures which tend to cost high and are often used to provide complicated design required for different applications. To achieve the required long-distance operation for WPT UAV, an electrostatic capacitive coupling method can be made in terms of using earth ground as conductor with desired resonant frequency are used for the UAV which would be result in the power travel faster and further.

This capacitive coupling system can be used to transfer energy to not only UAVs but also any types of battery powered system can be integrated to use this method. The 'space' between the capacitor plates or spheres and air which also as dielectric for charging and discharging electrostatic power That is, the region changed into a state against which a mechanical push could be applied. This suggested, utilizing this procedure, it ought to be conceivable to create a transmitter plant in desired area and receiver can be far away from the transmitter, if the earth resonant frequency and TX, RX resonant frequency can be tuned to work in same which could be resolved the issues of long-distance power transfer. Further investigations and experiment needed to prove these methods wireless power transfer method of UAV.

REFERENCES

Ahmed, F., Mohanta, · J C, Keshari, A., Pankaj, ·, & Yadav, S. (2022). Recent Advances in Unmanned Aerial Vehicles: A Review. *Arabian Journal for Science and Engineering 2022*, 1–22. https://doi.org/10.1007/S13369-022-06738-0

Aibin, M., Aldiab, M., Bhavsar, R., Lodhra, J., Reyes, M., Rezaeian, F., Saczuk, E., Taer, M., & Taer, M. (2021). Survey of RPAS Autonomous Control Systems Using Artificial Intelligence. *IEEE Access*, *9*, 167580–167591. https://doi.org/10.1109/ACCESS.2021.3136226

Aliakbarpour, H., Almeida, L., Menezes, P., & Dias, J. (2011). Multi-sensor 3D volumetric reconstruction using CUDA. *3D Research 2011 2:4*, *2*(4), 1–14. https://doi.org/10.1007/3DRES.04(2011)6

Alsamhi, S. H., Afghah, F., Sahal, R., Hawbani, A., Al-qaness, M. A. A., Lee, B., & Guizani, M. (2021). Green internet of things using UAVs in B5G networks: A review of applications and strategies. *Ad Hoc Networks*, *117*, 102505. https://doi.org/10.1016/J.ADHOC.2021.102505

Andreae, J. H., & Cashin, P. M. (1969). A learning machine with monologue. *International Journal of Man-Machine Studies*, *1*(1), 1–20. https://doi.org/10.1016/S0020-7373(69)80008-8

Apparatus for transmitting electrical energy. (1907).

Art of transmitting electrical energy through the natural mediums. (1900).

Azar, A. T., Koubaa, A., Ali Mohamed, N., Ibrahim, H. A., Ibrahim, Z. F., Kazim, M., Ammar, A., Benjdira, B., Khamis, A. M., Hameed, I. A., & Casalino, G. (2021). Drone Deep Reinforcement Learning: A Review. *Electronics 2021, Vol. 10, Page 999*, *10*(9), 999.

https://doi.org/10.3390/ELECTRONICS10090999

Bassolillo, S. R., D'amato, E., Notaro, I., Ariante, G., Core, G. del, & Mattei, M. (2022). Enhanced Attitude and Altitude Estimation for Indoor Autonomous UAVs. *Drones 2022, Vol. 6, Page 18*, *6*(1), 18. https://doi.org/10.3390/DRONES6010018

Bécherrawy, Tamer. (2012). *Mechanical and electromagnetic vibrations and waves*. John Wiley & Sons, Inc.

Boukoberine, M. N., Zhou, Z., & Benbouzid, M. (2019a). A critical review on unmanned aerial vehicles power supply and energy management: Solutions, strategies, and prospects. *Applied Energy*, *255*, 113823. https://doi.org/10.1016/J.APENERGY.2019.113823

Boukoberine, M. N., Zhou, Z., & Benbouzid, M. (2019b). A critical review on unmanned aerial vehicles power supply and energy management: Solutions, strategies, and prospects. *Applied Energy*, *255*, 113823. https://doi.org/10.1016/J.APENERGY.2019.113823

Busoniu, L., Babuska, R., de Schutter, B., & Ernst, D. (2020). Dynamic programming and reinforcement learning in large and contin- uous spaces. *Reinforcement Learning and Dynamic Programming Using Function Approximators*, 57–130. https://doi.org/10.1201/9781439821091-8/DYNAMIC-PROGRAMMING-REINFORCEMENT-LEARNING-LARGE-CONTIN-UOUS-SPACES-LUCIAN-BUSONIU-ROBERT-BABUSKA-BART-DE-SCHUTTER-DAMIEN-ERNST

Buşoniu, L., de Bruin, T., Tolić, D., Kober, J., & Palunko, I. (2018). Reinforcement learning for control: Performance, stability, and deep approximators. *Annual Reviews in Control*, *46*, 8–28. https://doi.org/10.1016/J.ARCONTROL.2018.09.005

Campi, T., Cruciani, S., & Feliziani, M. (2018a). Wireless Power Transfer Technology Applied to an Autonomous Electric UAV with a Small Secondary Coil. *Energies 2018, Vol. 11,*

Page 352, *11*(2), 352. https://doi.org/10.3390/EN11020352

Campi, T., Cruciani, S., & Feliziani, M. (2018b). Wireless Power Transfer Technology Applied to an Autonomous Electric UAV with a Small Secondary Coil. *Energies 2018, Vol. 11, Page 352*, *11*(2), 352. https://doi.org/10.3390/EN11020352

Canese, L., Cardarilli, G. C., di Nunzio, L., Fazzolari, R., Giardino, D., Re, M., & Spanò, S. (2021). Multi-Agent Reinforcement Learning: A Review of Challenges and Applications. *Applied Sciences 2021, Vol. 11, Page 4948*, *11*(11), 4948. https://doi.org/10.3390/APP11114948

Carrasco-Casado, A., Vergaz, R., & Pena, J. M. S. (2011). Design and early development of a UAV terminal and a ground station for laser communications. *Https://Doi.Org/10.1117/12.898216*, *8184*, 89–97. https://doi.org/10.1117/12.898216

Chargers and methods for wireless power transfer. (2013).

Chiang, K. W., Duong, T. T., & Liao, J. K. (2013). The Performance Analysis of a Real-Time Integrated INS/GPS Vehicle Navigation System with Abnormal GPS Measurement Elimination. *Sensors 2013, Vol. 13, Pages 10599-10622*, *13*(8), 10599–10622. https://doi.org/10.3390/S130810599

Chittoor, P. K., Chokkalingam, B., & Mihet-Popa, L. (2021). A Review on UAV Wireless Charging: Fundamentals, Applications, Charging Techniques and Standards. *IEEE Access*, *9*, 69235–69266. https://doi.org/10.1109/ACCESS.2021.3077041

Chow, Y. T., Darbon, J., Osher, S., & Yin, W. (2017). Algorithm for Overcoming the Curse of Dimensionality For Time-Dependent Non-convex Hamilton–Jacobi Equations Arising From Optimal Control and Differential Games Problems. *Journal of Scientific Computing 2017 73:2*, *73*(2), 617–643. https://doi.org/10.1007/S10915-017-0436-5

Cimurs, R., Lee, J. H., & Suh, I. H. (2020). Goal-Oriented Obstacle Avoidance with Deep Reinforcement Learning in Continuous Action Space. *Electronics 2020, Vol. 9, Page 411*, *9*(3), 411. https://doi.org/10.3390/ELECTRONICS9030411

Cireşan, D., Meier, U., & Schmidhuber, J. (2012). *Multi-column Deep Neural Networks for Image Classification*. http://arxiv.org/abs/1202.2745

Cockburn, I. M., Henderson, R., Stern, S., Professor, H., Management, E., Business, H., & Morgan, S. (2018). *The Impact of Artificial Intelligence on Innovation*. https://doi.org/10.3386/W24449

Cokyasar, T. (2021). Delivery drone route planning over a battery swapping network. *Procedia Computer Science*, *184*, 10–16. https://doi.org/10.1016/J.PROCS.2021.03.013

Colomina, I., & Molina, P. (2014). Unmanned aerial systems for photogrammetry and remote sensing: A review. In *ISPRS Journal of Photogrammetry and Remote Sensing* (Vol. 92, pp. 79–97). Elsevier B.V. https://doi.org/10.1016/j.isprsjprs.2014.02.013

Cui, Z. H., Hua, W. S., Liu, X. G., Guo, T., & Yan, Y. (2017). Key technologies of laser power transmission for in-flight UAVs recharging. *IOP Conference Series: Earth and Environmental Science*, *61*(1), 012134. https://doi.org/10.1088/1755-1315/61/1/012134

David Wunsch, A. (2018). Nikola Tesla's True Wireless: A Paradigm Missed. In *Proceedings of the IEEE* (Vol. 106, Issue 6, pp. 1115–1123). Institute of Electrical and Electronics Engineers Inc. https://doi.org/10.1109/JPROC.2018.2827438

de Silva, S. C., Phlernjai, M., Rianmora, S., & Ratsamee, P. (2022). Inverted Docking Station: A Conceptual Design for a Battery-Swapping Platform for Quadrotor UAVs. *Drones 2022, Vol. 6, Page 56*, *6*(3), 56. https://doi.org/10.3390/DRONES6030056

Deng, L. (2014). A tutorial survey of architectures, algorithms, and applications for deep

learning. In *APSIPA Transactions on Signal and Information Processing* (Vol. 3). Cambridge University Press. https://doi.org/10.1017/ATSIP.2013.99

Dickinson, R. M., & Grey, J. (1999). *Lasers for Wireless Power Transmission*.

Ding, J., Jiang, L., He, C., & Shen, Y. (2018). Time Splitting Concurrent Transmission Framework and Resource Allocation in Wireless Powered Communication Networks. *IEEE Transactions on Green Communications and Networking*, *2*(3), 666–678. https://doi.org/10.1109/TGCN.2018.2804339

Doole, M., Ellerbroek, J., & Hoekstra, J. (2020). Estimation of traffic density from drone-based delivery in very low level urban airspace. *Journal of Air Transport Management*, *88*, 101862. https://doi.org/10.1016/J.JAIRTRAMAN.2020.101862

Ducard, G. J. J., & Allenspach, M. (2021). Review of designs and flight control techniques of hybrid and convertible VTOL UAVs. *Aerospace Science and Technology*, *118*, 107035. https://doi.org/10.1016/J.AST.2021.107035

Duggal, R., Donald, A., & Schoemehl, T. (2009). Technological evolution of the microwave power module (MPM). *2009 IEEE International Vacuum Electronics Conference, IVEC 2009*, 353–354. https://doi.org/10.1109/IVELEC.2009.5193431

Dulac-Arnold, G., Mankowitz, D., & Hester, T. (2019). *Challenges of Real-World Reinforcement Learning*. https://doi.org/10.48550/arxiv.1904.12901

Elmeseiry, N., Alshaer, N., & Ismail, T. (2021). A Detailed Survey and Future Directions of Unmanned Aerial Vehicles (UAVs) with Potential Applications. *Aerospace 2021, Vol. 8, Page 363*, *8*(12), 363. https://doi.org/10.3390/AEROSPACE8120363

Fiala, M. (2005). ARTag, a fiducial marker system using digital techniques. *Proceedings - 2005 IEEE Computer Society Conference on Computer Vision and Pattern Recognition, CVPR*

2005, *II*, 590–596. https://doi.org/10.1109/CVPR.2005.74

Fink, O., Wang, Q., Svensén, M., Dersin, P., Lee, W. J., & Ducoffe, M. (2020). Potential, challenges and future directions for deep learning in prognostics and health management applications. *Engineering Applications of Artificial Intelligence*, *92*, 103678. https://doi.org/10.1016/J.ENGAPPAI.2020.103678

García Carrillo, L. R., Dzul López, A. E., Lozano, R., & Pégard, C. (2013). *Quad Rotorcraft Control*. https://doi.org/10.1007/978-1-4471-4399-4

Ghazzai, H., Menouar, H., Kadri, A., & Massoud, Y. (2019). Future UAV-Based ITS: A Comprehensive Scheduling Framework. *IEEE Access*, *7*, 75678–75695. https://doi.org/10.1109/ACCESS.2019.2921269

Giordan, D., Adams, M. S., Aicardi, I., Alicandro, M., Allasia, P., Baldo, M., de Berardinis, P., Dominici, D., Godone, D., Hobbs, P., Lechner, V., Niedzielski, T., Piras, M., Rotilio, M., Salvini, R., Segor, V., Sotier, B., & Troilo, F. (2020). The use of unmanned aerial vehicles (UAVs) for engineering geology applications. *Bulletin of Engineering Geology and the Environment*, *79*(7), 3437–3481. https://doi.org/10.1007/S10064-020-01766-2/TABLES/15

Gómez, C., & Green, D. R. (2017). Small unmanned airborne systems to support oil and gas pipeline monitoring and mapping. *Arabian Journal of Geosciences*, *10*(9), 1–17. https://doi.org/10.1007/S12517-017-2989-X/FIGURES/2

Griffin, B., & Detweiler, C. (2012). Resonant wireless power transfer to ground sensors from a UAV. *Proceedings - IEEE International Conference on Robotics and Automation*, 2660–2665. https://doi.org/10.1109/ICRA.2012.6225205

Grlj, C. G., Krznar, N., & Pranjić, M. (2022). A Decade of UAV Docking Stations: A Brief Overview of Mobile and Fixed Landing Platforms. *Drones 2022, Vol. 6, Page 17*, *6*(1), 17.

https://doi.org/10.3390/DRONES6010017

Gupta, A., Afrin, T., Scully, E., & Yodo, N. (2021). Advances of UAVs toward Future Transportation: The State-of-the-Art, Challenges, and Opportunities. *Future Transportation 2021, Vol. 1, Pages 326-350*, *1*(2), 326–350. https://doi.org/10.3390/FUTURETRANSP1020019

Gupta, A., & Fernando, X. (2022). Simultaneous Localization and Mapping (SLAM) and Data Fusion in Unmanned Aerial Vehicles: Recent Advances and Challenges. *Drones 2022, Vol. 6, Page 85*, *6*(4), 85. https://doi.org/10.3390/DRONES6040085

Gupta, S. G., Ghonge, M. M., & Jawandhiya, P. M. (2013). Review of Unmanned Aircraft System (UAS). In *International Journal of Advanced Research in Computer Engineering & Technology (IJARCET)* (Vol. 2, Issue 4). www.ijarcet.org

Hall, O., & Wahab, I. (2021). The Use of Drones in the Spatial Social Sciences. *Drones 2021, Vol. 5, Page 112*, *5*(4), 112. https://doi.org/10.3390/DRONES5040112

Han, S., Meng, Z., Omisore, O., Akinyemi, T., & Yan, Y. (2020). Random Error Reduction Algorithms for MEMS Inertial Sensor Accuracy Improvement—A Review. *Micromachines 2020, Vol. 11, Page 1021*, *11*(11), 1021. https://doi.org/10.3390/MI11111021

Han, W., & Kunieda, M. (2017). Research on improvement of machining accuracy of micro-rods with electrostatic induction feeding ECM. *Precision Engineering*, *50*, 494–505. https://doi.org/10.1016/J.PRECISIONENG.2017.07.005

Haque, S. R., Kormokar, R., & Zaman, A. U. (2017). Drone ground control station with enhanced safety features. *2017 2nd International Conference for Convergence in Technology, I2CT 2017*, *2017-January*, 1207–1210. https://doi.org/10.1109/I2CT.2017.8226318

Hide, C., Moore, T., & Smith, M. (2003). Adaptive Kalman Filtering for Low-cost INS/GPS. *The Journal of Navigation*, *56*(1), 143–152. https://doi.org/10.1017/S0373463302002151

Hoseini, S. A., Hassan, J., Bokani, A., & Kanhere, S. S. (2021). In Situ MIMO-WPT Recharging of UAVs Using Intelligent Flying Energy Sources. *Drones 2021, Vol. 5, Page 89*, *5*(3), 89. https://doi.org/10.3390/DRONES5030089

Howard, A. G. (n.d.). *Some Improvements on Deep Convolutional Neural Network Based Image Classification*. http://code.google.com/p/cuda-convnet

Hua, M., Wang, Y., Zhang, Z., Li, C., Huang, Y., & Yang, L. (2018). Power-Efficient Communication in UAV-Aided Wireless Sensor Networks. *IEEE Communications Letters*, *22*(6), 1264–1267. https://doi.org/10.1109/LCOMM.2018.2822700

Huan-Huan, Y., Xiang-Yu, C., Jun, G., Tao, L., Si-Jia, L., Yi, Z., Zi-Dong, Y., Hao, Z., Huan-Huan, Y., Xiang-Yu, C., Jun, G., Tao, L., Si-Jia, L., Yi, Z., Zi-Dong, Y., & Hao, Z. (2013). Broadband low-RCS metamaterial absorber based on electromagnetic resonance separation. *Acta Physica Sinica, 2013, Vol. 62, Issue 21, Pages: 214101-214101*, *62*(21), 214101–214101. https://doi.org/10.7498/APS.62.214101

Huda, S. M. A., Arafat, M. Y., & Moh, S. (2022). Wireless Power Transfer in Wirelessly Powered Sensor Networks: A Review of Recent Progress. *Sensors (Basel, Switzerland)*, *22*(8), 2952. https://doi.org/10.3390/S22082952

Ishiguro, M., Orchiston, W., Akabane, K., Kaifu, N., Hayashi, M., Nakamura, T., Stewart, R., & Yokoo, H. (2012). HIGHLIGHTING THE HISTORY OF JAPANESE RADIO ASTRONOMY. 1: AN INTRODUCTION. In *Journal of Astronomical History and Heritage* (Vol. 15, Issue 3).

Jenn, D. (n.d.). *Calhoun: The NPS Institutional Archive Short range Wireless Power Transfer*

(WPT) for UAV/UAS battery charging-Phase I. http://hdl.handle.net/10945/44092

Jia, J., & Yan, X. (2020). Application of Magnetic Coupling Resonant Wireless Power Supply in a Torque Online Telemetering System of a Rolling Mill. *Journal of Electrical and Computer Engineering*, *2020*. https://doi.org/10.1155/2020/8582131

Jiang, J., Liu, X., & Zha, X. (2018). Summary of Application of Magnetic Coupling Resonance Technology in Power Inspection UAV. *MATEC Web of Conferences*, *228*, 02007. https://doi.org/10.1051/MATECCONF/201822802007

Jiang, Z., & Lynch, A. F. (2021). Quadrotor motion control using deep reinforcement learning. *Journal of Unmanned Vehicle Systems*, *9*(4), 234–251. https://doi.org/10.1139/JUVS-2021-0010/ASSET/IMAGES/JUVS-2021-0010IEQ76.GIF

Jing, X., Cui, J., He, H., Zhang, B., Ding, D., & Yang, Y. (2017). Attitude estimation for UAV using extended Kalman filter. *Proceedings of the 29th Chinese Control and Decision Conference, CCDC 2017*, 3307–3312. https://doi.org/10.1109/CCDC.2017.7979077

Johnson, J., Basha, E., & Detweiler, C. (2013). Charge selection algorithms for maximizing sensor network life with UAV-based limited wireless recharging. *Proceedings of the 2013 IEEE 8th International Conference on Intelligent Sensors, Sensor Networks and Information Processing: Sensing the Future, ISSNIP 2013*, *1*, 159–164. https://doi.org/10.1109/ISSNIP.2013.6529782

Junaid, A. bin, Konoiko, A., Zweiri, Y., Sahinkaya, M. N., & Seneviratne, L. (2017). Autonomous Wireless Self-Charging for Multi-Rotor Unmanned Aerial Vehicles. *Energies 2017, Vol. 10, Page 803*, *10*(6), 803. https://doi.org/10.3390/EN10060803

Junaid, A. bin, Lee, Y., & Kim, Y. (2016). Design and implementation of autonomous wireless charging station for rotary-wing UAVs. *Aerospace Science and Technology*, *54*, 253–266.

https://doi.org/10.1016/J.AST.2016.04.023

Kälin, U., Staffa, L., Grimm, D. E., & Wendt, A. (2021). Highly Accurate Pose Estimation as a Reference for Autonomous Vehicles in Near-Range Scenarios. *Remote Sensing 2022, Vol. 14, Page 90*, *14*(1), 90. https://doi.org/10.3390/RS14010090

Kamalinejad, P., Mahapatra, C., Sheng, Z., Mirabbasi, S., Victor, V. C., & Guan, Y. L. (2015). Wireless energy harvesting for the Internet of Things. *IEEE Communications Magazine*, *53*(6), 102–108. https://doi.org/10.1109/MCOM.2015.7120024

Kangunde, V., Jamisola, R. S., & Theophilus, E. K. (2021). A review on drones controlled in real-time. *International Journal of Dynamics and Control*, *9*(4), 1832–1846. https://doi.org/10.1007/S40435-020-00737-5/FIGURES/16

Kerr, A. J., Jr., W. R. S., Hayes, C. E., & McClellan, J. H. (2017). Target location estimation for single channel electromagnetic induction data. *Https://Doi.Org/10.1117/12.2262892*, *10182*, 245–256. https://doi.org/10.1117/12.2262892

Kim, D. W., Chung, Y. do, Kang, H. K., Yoon, Y. S., & Ko, T. K. (2012). Characteristics of contactless power transfer for HTS coil based on electromagnetic resonance coupling. *IEEE Transactions on Applied Superconductivity*, *22*(3). https://doi.org/10.1109/TASC.2011.2179969

Kim, J., Jung, Y., Lee, D., & Shim, D. H. (2014). Outdoor autonomous landing on a moving platform for quadrotors using an omnidirectional camera. *2014 International Conference on Unmanned Aircraft Systems, ICUAS 2014 - Conference Proceedings*, 1243–1252. https://doi.org/10.1109/ICUAS.2014.6842381

Klemas, V. v. (2015). Coastal and environmental remote sensing from unmanned aerial vehicles: An overview. *Journal of Coastal Research*, *31*(5), 1260–1267.

https://doi.org/10.2112/JCOASTRES-D-15-00005.1

Kubota, Y., Ke, Y., Hayakawa, T., Moko, Y., & Ishikawa, M. (2021). Optimal Material Search for Infrared Markers under Non-Heating and Heating Conditions. *Sensors 2021, Vol. 21, Page 6527*, *21*(19), 6527. https://doi.org/10.3390/S21196527

Kumar, S., & Moore, K. B. (2002). The Evolution of Global Positioning System (GPS) Technology. *Journal of Science Education and Technology 2002 11:1*, *11*(1), 59–80. https://doi.org/10.1023/A:1013999415003

Lagkas, T., Argyriou, V., Bibi, S., & Sarigiannidis, P. (2018). UAV IoT Framework Views and Challenges: Towards Protecting Drones as "Things." *Sensors 2018, Vol. 18, Page 4015*, *18*(11), 4015. https://doi.org/10.3390/S18114015

Le, A., Truong, L., Quyen, T., Nguyen, C., & Nguyen, M. (2020a). Wireless Power Transfer Near-field Technologies for Unmanned Aerial Vehicles (UAVs): A Review. *EAI Endorsed Transactions on Industrial Networks and Intelligent Systems*, *7*(22), 162831. https://doi.org/10.4108/EAI.31-1-2020.162831

Le, A., Truong, L., Quyen, T., Nguyen, C., & Nguyen, M. (2020b). Wireless Power Transfer Near-field Technologies for Unmanned Aerial Vehicles (UAVs): A Review. *EAI Endorsed Transactions on Industrial Networks and Intelligent Systems*, *7*(22), 162831. https://doi.org/10.4108/EAI.31-1-2020.162831

Lhazmir, S., Oualhaj, O. A., Kobbane, A., & Mokdad, L. (2020). A decision-making analysis in UAV-enabled wireless power transfer for IoT networks. *Simulation Modelling Practice and Theory*, *103*, 102102. https://doi.org/10.1016/J.SIMPAT.2020.102102

Li, H., Zhao, R., & Wang, X. (2014). *Highly Efficient Forward and Backward Propagation of Convolutional Neural Networks for Pixelwise Classification*. http://arxiv.org/abs/1412.4526

Li, K., Ni, W., Tovar, E., & Jamalipour, A. (2019). On-Board Deep Q-Network for UAV-Assisted Online Power Transfer and Data Collection. *IEEE Transactions on Vehicular Technology*, *68*(12), 12215–12226. https://doi.org/10.1109/TVT.2019.2945037

Li, K. R., See, K. Y., Koh, W. J., & Zhang, J. W. (2017). Design of 2.45 GHz microwave wireless power transfer system for battery charging applications. *Progress in Electromagnetics Research Symposium*, *2017-November*, 2417–2423. https://doi.org/10.1109/PIERS-FALL.2017.8293542

Li, W., & Wang, J. (2013). Effective Adaptive Kalman Filter for MEMS-IMU/Magnetometers Integrated Attitude and Heading Reference Systems. *The Journal of Navigation*, *66*(1), 99–113. https://doi.org/10.1017/S0373463312000331

Liu, X., Zhang, S., Tian, J., & Liu, L. (2019). An Onboard Vision-Based System for Autonomous Landing of a Low-Cost Quadrotor on a Novel Landing Pad. *Sensors (Basel, Switzerland)*, *19*(21). https://doi.org/10.3390/S19214703

Liu, Y., Li, Z., Zheng, S., Cai, P., & Zou, X. (2022). An Evaluation of MEMS-IMU Performance on the Absolute Trajectory Error of Visual-Inertial Navigation System. *Micromachines*, *13*(4), 602. https://doi.org/10.3390/MI13040602

Lu, P., Yang, X. S., & Wang, B. Z. (2017). A Two-Channel Frequency Reconfigurable Rectenna for Microwave Power Transmission and Data Communication. *IEEE Transactions on Antennas and Propagation*, *65*(12), 6976–6985. https://doi.org/10.1109/TAP.2017.2766450

Lu, X., Yang, W., Yan, S., Li, Z., & Ng, D. W. K. (2021). Covertness and Timeliness of Data Collection in UAV-Aided Wireless-Powered IoT. *IEEE Internet of Things Journal*. https://doi.org/10.1109/JIOT.2021.3137846

Ludeno, G., Catapano, I., Renga, A., Vetrella, A. R., Fasano, G., & Soldovieri, F. (2018).

Assessment of a micro-UAV system for microwave tomography radar imaging. *Remote Sensing of Environment*, *212*, 90–102. https://doi.org/10.1016/J.RSE.2018.04.040

Ma, H., Li, X., Sun, L., Xu, H., & Yang, L. (2016). Design of high-efficiency microwave wireless power transmission system. *Microwave and Optical Technology Letters*, *58*(7), 1704–1707. https://doi.org/10.1002/MOP.29885

Masroor, R., Naeem, M., & Ejaz, W. (2021). Resource management in UAV-assisted wireless networks: An optimization perspective. *Ad Hoc Networks*, *121*, 102596. https://doi.org/10.1016/J.ADHOC.2021.102596

Means for increasing the intensity of electrical oscillations. (1900).

Miller, J. S., Bassani, C., & Schultz, G. (2015). Extended-range electromagnetic induction concepts. *Https://Doi.Org/10.1117/12.2177476*, *9454*, 133–140. https://doi.org/10.1117/12.2177476

Mnih, V., Badia, A. P., Mirza, L., Graves, A., Harley, T., Lillicrap, T. P., Silver, D., & Kavukcuoglu, K. (2016). Asynchronous Methods for Deep Reinforcement Learning. *33rd International Conference on Machine Learning, ICML 2016*, *4*, 2850–2869. https://doi.org/10.48550/arxiv.1602.01783

Mohamed, A. A. S., Berzoy, A., de Almeida, F. G. N., & Mohammed, O. (2017). Modeling and Assessment Analysis of Various Compensation Topologies in Bidirectional IWPT System for EV Applications. *IEEE Transactions on Industry Applications*, *53*(5), 4973–4984. https://doi.org/10.1109/TIA.2017.2700281

Naimushin, A. N., Spinelli, C. B., Soelberg, S. D., Mann, T., Stevens, R. C., Chinowsky, T., Kauffman, P., Yee, S., & Furlong, C. E. (2005). Airborne analyte detection with an aircraft-adapted surface plasmon resonance sensor system. *Sensors and Actuators B: Chemical*,

104(2), 237–248. https://doi.org/10.1016/J.SNB.2004.05.020

Najafabadi, M. M., Villanustre, F., Khoshgoftaar, T. M., Seliya, N., Wald, R., & Muharemagic, E. (2015). Deep learning applications and challenges in big data analytics. *Journal of Big Data*, *2*(1), 1–21. https://doi.org/10.1186/S40537-014-0007-7/METRICS

Nex, F., Armenakis, C., Cramer, M., Cucci, D. A., Gerke, M., Honkavaara, E., Kukko, A., Persello, C., & Skaloud, J. (2022). UAV in the advent of the twenties: Where we stand and what is next. *ISPRS Journal of Photogrammetry and Remote Sensing*, *184*, 215–242. https://doi.org/10.1016/J.ISPRSJPRS.2021.12.006

Nguyen, M. T., Nguyen, C. v., Truong, L. H., Le, A. M., Quyen, T. v., Masaracchia, A., & Teague, K. A. (2020a). Electromagnetic field based WPT technologies for UAVs: A comprehensive survey. *Electronics (Switzerland)*, *9*(3). https://doi.org/10.3390/ELECTRONICS9030461

Nguyen, M. T., Nguyen, C. v., Truong, L. H., Le, A. M., Quyen, T. v., Masaracchia, A., & Teague, K. A. (2020b). Electromagnetic Field Based WPT Technologies for UAVs: A Comprehensive Survey. *Electronics 2020, Vol. 9, Page 461*, *9*(3), 461. https://doi.org/10.3390/ELECTRONICS9030461

Ning, Z., Dong, P., Wang, X., Rodrigues, J. J. P. C., & Xia, F. (2019). Deep Reinforcement Learning for Vehicular Edge Computing. *ACM Transactions on Intelligent Systems and Technology (TIST)*, *10*(6). https://doi.org/10.1145/3317572

Nonami, K., Kendoul, F., Suzuki, S., Wang, W., & Nakazawa, D. (n.d.). *Autonomous Flying Robots: Unmanned Aerial Vehicles and Micro Aerial Vehicles*.

Ouyang, J., Che, Y., Xu, J., & Wu, K. (2018). Throughput Maximization for Laser-Powered UAV Wireless Communication Systems. *2018 IEEE International Conference on*

Communications Workshops, ICC Workshops 2018 - Proceedings, 1–6. https://doi.org/10.48550/arxiv.1803.00690

Pereira, E., Bencatel, R., Correia, J., Félix, L., Gonçalves, G., Morgado, J., & Sousa, J. (2009). Unmanned Air Vehicles for Coastal and Environmental Research. In *Source: Journal of Coastal Research: Vol. II* (Issue 56). https://www.jstor.org/stable/25738051

Prithvi Krishna, C., Bharatiraja, C., & Lucian, M.-P. (2021). A Review on UAV Wireless Charging: Fundamentals, Applications, Charging Techniques and Standards. In *IEEE Access* (Vol. 9, pp. 69235–69266). Institute of Electrical and Electronics Engineers Inc. https://doi.org/10.1109/ACCESS.2021.3077041

Reed, M. A., & Jr., W. R. S. (2013). Optimized coils for electromagnetic induction systems. *Https://Doi.Org/10.1117/12.2017955*, *8709*, 61–71. https://doi.org/10.1117/12.2017955

Rejeb, A., Rejeb, K., Simske, S., & Treiblmaier, H. (2021). Humanitarian Drones: A Review and Research Agenda. *Internet of Things*, *16*, 100434. https://doi.org/10.1016/J.IOT.2021.100434

Ren, J. SJ., & Xu, L. (2015). *On Vectorization of Deep Convolutional Neural Networks for Vision Tasks*. http://arxiv.org/abs/1501.07338

Rengarajan, D., Vaidya, G., Sarvesh, A., Kalathil, D., & Shakkottai, S. (2022). *Reinforcement Learning with Sparse Rewards using Guidance from Offline Demonstration*. https://doi.org/10.48550/arxiv.2202.04628

Sánchez, J. A. H., Casilimas, K., & Rendon, O. M. C. (2022). Deep Reinforcement Learning for Resource Management on Network Slicing: A Survey. *Sensors (Basel, Switzerland)*, *22*(8), 3031. https://doi.org/10.3390/S22083031

Sanguesa, J. A., Torres-Sanz, V., Garrido, P., Martinez, F. J., & Marquez-Barja, J. M. (2021). A

Review on Electric Vehicles: Technologies and Challenges. *Smart Cities 2021, Vol. 4, Pages 372-404*, *4*(1), 372–404. https://doi.org/10.3390/SMARTCITIES4010022

Saripalli, S., & Sukhatme, G. S. (2006). Landing on a Moving Target Using an Autonomous Helicopter. *Springer Tracts in Advanced Robotics*, *24*, 277–286. https://doi.org/10.1007/10991459_27

Schmidhuber, J. (2014). *Deep Learning in Neural Networks: An Overview*. https://doi.org/10.1016/j.neunet.2014.09.003

Sengupta. (2013). *Smart RF lensing: efficient, dynamic and mobile wireless power transfer*.

Shakhatreh, H., Sawalmeh, A. H., Al-Fuqaha, A., Dou, Z., Almaita, E., Khalil, I., Othman, N. S., Khreishah, A., & Guizani, M. (2019). Unmanned Aerial Vehicles (UAVs): A Survey on Civil Applications and Key Research Challenges. *IEEE Access*, *7*, 48572–48634. https://doi.org/10.1109/ACCESS.2019.2909530

Shinohara, N. (2014a). History, Present and Future of WPT. *Wireless Power Transfer via Radiowaves*, 1–20. https://doi.org/10.1002/9781118863008.CH1

Shinohara, N. (2014b). Theory of WPT. *Wireless Power Transfer via Radiowaves*, 21–52. https://doi.org/10.1002/9781118863008.CH2

Siddiqi, M. A., Iwendi, C., Jaroslava, K., Anumbe, N., Siddiqi, M. A., Iwendi, C., Jaroslava, K., & Anumbe, N. (2022). Analysis on security-related concerns of unmanned aerial vehicle: attacks, limitations, and recommendations. *Mathematical Biosciences and Engineering 2022 3:2641*, *19*(3), 2641–2670. https://doi.org/10.3934/MBE.2022121

Simic, M., Bil, C., & Vojisavljevic, V. (2015). Investigation in Wireless Power Transmission for UAV Charging. *Procedia Computer Science*, *60*(1), 1846–1855. https://doi.org/10.1016/J.PROCS.2015.08.295

Simonyan, K., & Zisserman, A. (2014). *Very Deep Convolutional Networks for Large-Scale Image Recognition*. http://arxiv.org/abs/1409.1556

Stolaroff, J. K., Samaras, C., O'Neill, E. R., Lubers, A., Mitchell, A. S., & Ceperley, D. (2018). Energy use and life cycle greenhouse gas emissions of drones for commercial package delivery. *Nature Communications 2018 9:1*, *9*(1), 1–13. https://doi.org/10.1038/s41467-017-02411-5

Sulaiman, M., Liu, H., bin Alhaj, M., & Abudayyeh, O. (2023). *UAV Applications in the AEC/FM Industry: A Review*. 249–259. https://doi.org/10.1007/978-981-19-0968-9_20

Sun, H., Zhang, W., Yu, R., & Zhang, Y. (2021). Motion Planning for Mobile Robots - Focusing on Deep Reinforcement Learning: A Systematic Review. In *IEEE Access* (Vol. 9, pp. 69061–69081). Institute of Electrical and Electronics Engineers Inc. https://doi.org/10.1109/ACCESS.2021.3076530

System of transmission of electrical energy. (1897).

Szegedy, C., Toshev, A., & Erhan, D. (n.d.). *Deep Neural Networks for Object Detection*.

Tahir, A., Böling, J., Haghbayan, M. H., Toivonen, H. T., & Plosila, J. (2019). Swarms of Unmanned Aerial Vehicles — A Survey. *Journal of Industrial Information Integration*, *16*, 100106. https://doi.org/10.1016/J.JII.2019.100106

Tang, D., Hu, T., Shen, L., Zhang, D., Kong, W., & Low, K. H. (2016). Ground Stereo Vision-Based Navigation for Autonomous Take-off and Landing of UAVs: A Chan-Vese Model Approach: *Https://Doi.Org/10.5772/62027*, *13*(2). https://doi.org/10.5772/62027

Tang, Q., Wang, K., Song, Y., Li, F., & Park, J. H. (2020). Waiting Time Minimized Charging and Discharging Strategy Based on Mobile Edge Computing Supported by Software-Defined Network. *IEEE Internet of Things Journal*, *7*(7), 6088–6101.

https://doi.org/10.1109/JIOT.2019.2957124

Toh, T. (n.d.). *Electromagnetic theory for electromagnetic compatibility engineers*. 369.

Tompson, J., Goroshin, R., Jain, A., LeCun, Y., & Bregler, C. (2014). *Efficient Object Localization Using Convolutional Networks*. http://arxiv.org/abs/1411.4280

Toshiyuki, F., Hiroyuki, K., Hiroshi, U., & Yasuyoshi, K. (2019). A real-car experiment of a dynamic wireless power transfer system based on parallel-series resonant topology. *World Electric Vehicle Journal*, *10*(3). https://doi.org/10.3390/wevj10030049

Tovarnov, M. S., & Bykov, N. v. (2022). *Reinforcement learning reward function in unmanned aerial vehicle control tasks*. https://doi.org/10.48550/arxiv.2203.10519

Townsend, A., Jiya, I. N., Martinson, C., Bessarabov, D., & Gouws, R. (2020). A comprehensive review of energy sources for unmanned aerial vehicles, their shortfalls and opportunities for improvements. *Heliyon*, *6*(11). https://doi.org/10.1016/J.HELIYON.2020.E05285

Tullu, A., Byun, Y., Kim, J. N., & Kang, B. S. (2018). Parameter optimization to avoid propeller-induced structural resonance of quadrotor type Unmanned Aerial Vehicle. *Composite Structures*, *193*, 63–72. https://doi.org/10.1016/J.COMPSTRUCT.2018.03.014

Ucgun, H., Yuzgec, U., & Bayilmis, C. (2021). A review on applications of rotary-wing unmanned aerial vehicle charging stations: *Https://Doi.Org/10.1177/17298814211015863*, *18*(3). https://doi.org/10.1177/17298814211015863

US645576A - System of transmission of electrical energy. - Google Patents. (n.d.). Retrieved June 12, 2022, from https://patents.google.com/patent/US645576A/en

van Huynh, D., Do-Duy, T., Nguyen, L. D., Le, M. T., Vo, N. S., & Duong, T. Q. (2022). Real-Time Optimized Path Planning and Energy Consumption for Data Collection in Unmanned Ariel Vehicles-Aided Intelligent Wireless Sensing. *IEEE Transactions on Industrial*

Informatics, *18*(4), 2753–2761. https://doi.org/10.1109/TII.2021.3114358

van Seijen, H., Fatemi, M., Romoff, J., Laroche, R., Barnes, T., & Tsang, J. (2017). Hybrid Reward Architecture for Reinforcement Learning. *Advances in Neural Information Processing Systems*, *2017-December*, 5393–5403. https://doi.org/10.48550/arxiv.1706.04208

Walter, W. (1976). On the functional equation of bellman in the theory of dynamic programming. *Aequationes Mathematicae 1976 14:1*, *14*(1), 247–248. https://doi.org/10.1007/BF01836230

Wang, C., Xu, W., Zhang, C., Wang, M., & Wang, X. (2022). Microwave wireless power transmission technology index system and test evaluation methods. *Eurasip Journal on Advances in Signal Processing*, *2022*(1), 1–11. https://doi.org/10.1186/S13634-022-00846-7/TABLES/1

Wei, Z., Zhu, M., Zhang, N., Wang, L., Zou, Y., Meng, Z., Wu, H., & Feng, Z. (2022). UAV Assisted Data Collection for Internet of Things: A Survey. *IEEE Internet of Things Journal*, 1–1. https://doi.org/10.1109/JIOT.2022.3176903

WiTricity - The wireless power transfer. (2007). *IEEE Vehicular Technology Magazine*, *2*(2), 38–44. https://doi.org/10.1109/MVT.2007.913285

Woolf, B. P. (2009). Machine Learning. *Building Intelligent Interactive Tutors*, 221–297. https://doi.org/10.1016/B978-0-12-373594-2.00007-1

Xia, D., Cheng, L., & Yao, Y. (2017). A Robust Inner and Outer Loop Control Method for Trajectory Tracking of a Quadrotor. *Sensors 2017, Vol. 17, Page 2147*, *17*(9), 2147. https://doi.org/10.3390/S17092147

Xu, J., Zeng, Y., & Zhang, R. (2018a). UAV-enabled wireless power transfer: Trajectory design

and energy optimization. *IEEE Transactions on Wireless Communications*, *17*(8), 5092–5106. https://doi.org/10.1109/TWC.2018.2838134

Xu, J., Zeng, Y., & Zhang, R. (2018b). UAV-enabled wireless power transfer: Trajectory design and energy optimization. *IEEE Transactions on Wireless Communications*, *17*(8), 5092–5106. https://doi.org/10.1109/TWC.2018.2838134

Yaacoub, J. P., Noura, H., Salman, O., & Chehab, A. (2020). Security analysis of drones systems: Attacks, limitations, and recommendations. *Internet of Things*, *11*, 100218. https://doi.org/10.1016/J.IOT.2020.100218

Yan, Y., Shi, W., & Zhang, X. (2020). Design of UAV wireless power transmission system based on coupling coil structure optimization. *Eurasip Journal on Wireless Communications and Networking*, *2020*(1), 1–13. https://doi.org/10.1186/S13638-020-01679-4/FIGURES/18

Yang, J., Zhou, G., Yu, X., & Zhu, W. (2011). Design and implementation of power supply of high-power diode laser of LiDAR onboard UAV. *2011 International Symposium on Image and Data Fusion, ISIDF 2011*. https://doi.org/10.1109/ISIDF.2011.6024309

Yang, T., Li, G., Li, J., Zhang, Y., Zhang, X., Zhang, Z., & Li, Z. (2016). A Ground-Based Near Infrared Camera Array System for UAV Auto-Landing in GPS-Denied Environment. *Sensors 2016, Vol. 16, Page 1393*, *16*(9), 1393. https://doi.org/10.3390/S16091393

Yang, T., Zhang, S., Wang, Y., & Liu, J. (2021). *Optimized Deployment of Unmanned Aerial Vehicles for Wildfire Detection and Monitoring*. https://arxiv.org/abs/2112.03010v1

Yang, X., & Pei, X. (2022). Hybrid system for powering unmanned aerial vehicles: Demonstration and study cases. *Hybrid Technologies for Power Generation*, 439–473. https://doi.org/10.1016/B978-0-12-823793-9.00014-0

Yuan, Y., Wen, C., Qiu, Y., & Sun, X. (2021). Three State Estimation Fusion Methods Based on the Characteristic Function Filtering. *Sensors 2021, Vol. 21, Page 1440*, *21*(4), 1440. https://doi.org/10.3390/S21041440

Zeng, J., Ju, R., Qin, L., Hu, Y., Yin, Q., & Hu, C. (2019). Navigation in Unknown Dynamic Environments Based on Deep Reinforcement Learning. *Sensors (Basel, Switzerland)*, *19*(18). https://doi.org/10.3390/S19183837

Zhang, B., Song, Z., Zhao, F., & Liu, C. (2022). Overview of Propulsion Systems for Unmanned Aerial Vehicles. *Energies 2022, Vol. 15, Page 455*, *15*(2), 455. https://doi.org/10.3390/EN15020455

Zhang, G., Yue, X. G., Yang, J., Chen, J. X., Zhao, Z. Q., & Xie, X. L. (2013). Electromagnetic induction heating application in mining safety detection. *Advanced Materials Research*, *722*, 528–531. https://doi.org/10.4028/WWW.SCIENTIFIC.NET/AMR.722.528

Zhang, H., Shlezinger, N., Guidi, F., Dardari, D., Imani, M. F., & Eldar, Y. C. (2021). Near-field Wireless Power Transfer for 6G Internet-of-Everything Mobile Networks: Opportunities and Challenges. *IEEE Communications Magazine*, *60*(3), 12–18. https://doi.org/10.48550/arxiv.2108.07576

Zhao, X., Zhao, J., Zheng, X., Wang, X., OuYang, C., Shao, X., -, al, Li, R., Xiong, Y., Zhang -, T., Chan, C. W., & Kam, T. Y. (2020). A procedure for power consumption estimation of multi-rotor unmanned aerial vehicle. *Journal of Physics: Conference Series*, *1509*(1), 012015. https://doi.org/10.1088/1742-6596/1509/1/012015

Zhou, Z., Wang, H., & Lou, P. (2010). *Sensor Integration and Data Fusion Theory*. 160–188. https://doi.org/10.4018/978-1-60566-864-2.CH007

Zhu, Z., Chu, Z., & Li, X. (2022). Backscatter technology and intelligent reflecting technology

surface technology in the Internet of Things. *Intelligent Sensing and Communications for Internet of Everything*, 77–135. https://doi.org/10.1016/B978-0-32-385655-3.00007-2